USE OF BINARY SURFACTANT FORMULATIONS IN LOW IFT FOAM AND SURFACTANT FLOOD

Sorrawit Tantipalakul

A Thesis Submitted in Partial Fulfilment of the Requirements

for the Degree of Master of Science

The Petroleum and Petrochemical College, Chulalongkorn University

in Academic Partnership with

The University of Michigan, The University of Oklahoma,

Case Western Reserve University, and Institut Français du Pétrole

2018

Thesis Title: Use of Binary Surfactant Formulations in Low IFT Foam and Surfactant Flood

By: Sorrawit Tantipalakul

Program: Petroleum Technology

Thesis Advisors: Asst. Prof. Uthaiporn Suriyapraphadilok

Dr. Ampira Charoensaeng

Assoc. Prof. Bor-Jier Shiau

Accepted by The Petroleum and Petrochemical College, Chulalongkorn University, in partial fulfilment of the requirements for the Degree of Master of Science.

.... College Dean

(Prof. Suwabun Chirachanchai)

Thesis Committee:

....
(Asst. Prof. Uthaiporn Suriyapraphadilok)

....
(Dr. Ampira Charoensaeng)

....
(Assoc. Prof. Bor-Jier Shiau)

....
(Assoc. Prof. Boonyarach Kitiyanan)

....
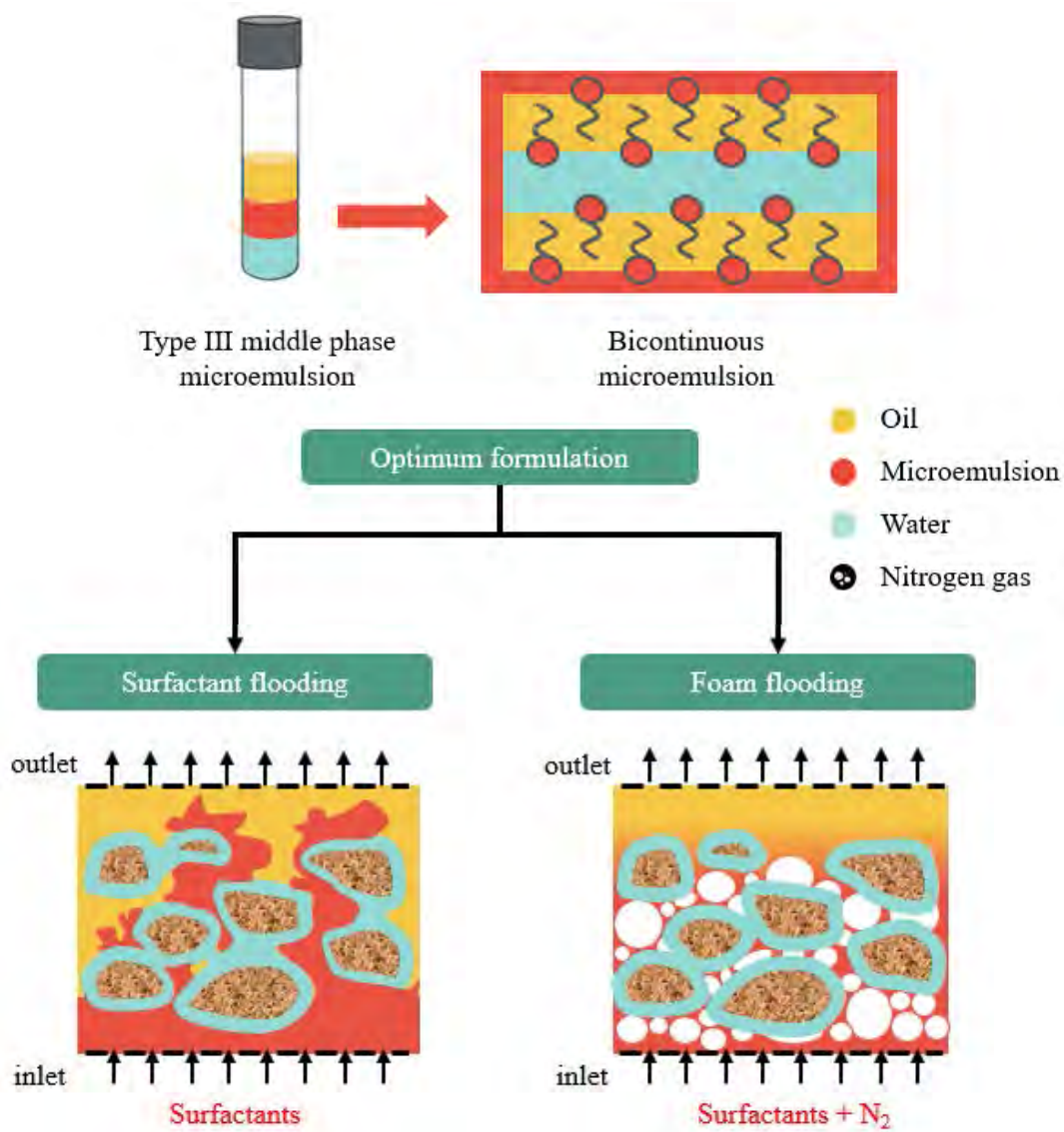(Dr. Sirinthip Kittisrisawai)

ABSTRACT

Viscous fingering and early breakthrough are the main problems observed during the water flooding. These problems could be overcome by using foam flooding by coinjection of surfactant solution and nitrogen gas as a mobility control in a porous media to help improve the sweep efficiency. To gain the maximum benefits of foam flooding, ultra-low interfacial tension foam was studied to obtain a foaming system with high sweep efficiency and at the same time high oil solubilization to help mobilize the oil phase from reservoir rock. In this work, mixed surfactant systems between sodium dioctylsulfosuccinate (AOT) and internal olefin sulfonate (IOS) with three different carbon chain lengths were tested through phase behavior studies and interfacial tension measurements without adding alcohol. The optimal type III middle phase microemulsion with ultra-low interfacial tension in the order of 10^{-3} mN/m could be obtained from the mixed systems of 1:1 surfactant/cosurfactant ratio (AOT:IOS) with a wide range of optimum salinity. Surfactant and foam floodings were conducted by a sand pack glass column at atmospheric pressure and ambient temperature. High oil recovery (>10% OOIP) at the optimum salinity was obtained in both surfactant flooding which Type III microemulsion played a key role in oil solubilization and better sweep efficiency by foam flooding.

บทคัดย่อ

สรวิศ ตันติปาลกุล : การอัดฉีดด้วยโฟมและสารลดแรงตึงที่สภาวะค่าแรงตึงผิวระหว่าง
น้ำมันและน้ำต่ำที่สุดโดยใช้สารลดแรงตึงผิวผสม (Use of Binary Surfactant Formulations in
Low IFT Foam and Surfactant Flood) อ. ที่ปรึกษา : ผศ.ดร.อุทัยพร สุริยประภาดิลก รศ.ดร.
บอร์ เจียร์ เชาว์ และ ดร.อัมพิรา เจริญแสง 112 หน้า.

ปัญหาหลักที่พบในขณะอัดฉีดน้ำเพื่อผลิตน้ำมัน (water flooding) คือ การที่น้ำทะลุผ่าน
ชั้นหินโดยปราศจากการผลิตน้ำมัน (viscous fingering) และ การแยกตัวของน้ำจากการกระบวน
ผลิตน้ำมันที่เร็วเกินไป (early breakthrough) การฉีดอัดโฟมสามารถแก้ปัญหาเหล่านี้ได้ โดยที่โฟม
เกิดจากการอัดฉีดสารลดแรงตึงผิวพร้อมกับก๊าซไนโตรเจนเพื่อเพิ่มความสามารถในการควบคุมการ
เคลื่อนที่ในตัวกลางที่มีรูพรุนเพื่อเพิ่มประสิทธิภาพในการกวาดน้ำมัน (sweep efficiency) การอัด
ฉีดโฟมให้ได้ประสิทธิภาพสูงที่สุดจะต้องศึกษาโฟมที่สภาวะค่าแรงตึงผิวระหว่างน้ำมันและน้ำต่ำที่สุด
นอกจากจะมีประสิทธิภาพในการกวาดน้ำมันที่สูงแล้วยังมีความสามารถในการละลายเข้ากับน้ำที่สูง
อีกด้วยจึงช่วยให้น้ำมันเคลื่อนที่ออกจากชั้นหินได้ง่ายขึ้น ในงานวิจัยนี้จะทำการศึกษาพฤติกรรมวัฏ
ภาค (phase behavior) และวัดแรงตึงผิวระหว่างน้ำมันและน้ำของสารลดแรงตึงผิวผสมระหว่างได
ออกทิลซัลโฟซักซิเนต (AOT) และอินเทอนอลโอเลฟินซัลโฟเนต (IOS) ที่มีความยาวของสายโซ่
คาร์บอนแตกต่างกัน 3 แบบ ไมโครอิมัลชันชนิดที่ 3 ที่เกิดขึ้นในแต่ละระบบจะทำการวัดแรงตึงผิว
ระหว่างน้ำมันและน้ำโดยปราศจากการเติมแอลกอฮอล์ เพื่อเลือกของผสมที่มีค่าแรงตึงผิวระหว่าง
น้ำมันและน้ำที่ต่ำที่สุดไปใช้ในกระบวนการผลิตน้ำมันขั้นตติยภูมิ พบว่าสารลดแรงตึงผิวผสมที่
อัตราส่วน 1:1 โดยปริมาตรสามารถเกิดไมโครอิมัลชันชนิดที่ 3 ในความเข้มข้นของเกลือที่เหมาะสม
ได้ในช่วงกว้างและมีค่าแรงตึงผิวระหว่างน้ำมันและน้ำที่ต่ำถึง 10^{-3} มิลลินิวตันต่อเมตร สารลดแรงที่
เหมาะสมนี้จะอัดฉีดเป็นสารละลายและโฟมเข้าไปในคอลัมน์ทรายที่อุณหภูมิห้องและความดัน
บรรยากาศเพื่อศึกษาความสามารถในการผลิตน้ำมัน พบว่าสามารถผลิตน้ำมันได้มากกว่าร้อยละ 10
จากปริมาณน้ำมันเริ่มต้นที่ความเข้มข้นของเกลือที่เหมาะสมเนื่องมาจากไมโครอิมัลชันชนิดที่ 3 มี
ความสำคัญในกระบวนการละลายเข้ากับน้ำมัน อีกทั้งการฉีดอัดโฟมยังช่วยเพิ่มประสิทธิภาพในการ
กวาดน้ำมันอีกด้วย

GRAPHICAL ABSTRACT

Type III middle phase
microemulsion

Bicontinuous
microemulsion

Optimum formulation

Oil

Microemulsion

Water

Nitrogen gas

Surfactant flooding

Foam flooding

outlet

inlet

Surfactants

outlet

inlet

Surfactants + N_2

ACKNOWLEDGEMENTS

TABLE OF CONTENTS

LIST OF TABLES

LIST OF FIGURES

FIGURE   **PAGE**

FIGURE   **PAGE**

FIGURE **PAGE**

CHAPTER I
INTRODUCTION

Underneath oil can be recovered lower than 50 % through a conventional oil recovery. Therefore, enhanced oil recovery is proposed for higher recovery efficiency. Foam flooding is a well-known technique in enhance oil recovery to solve the viscous fingering and early breakthrough problems. However, oil solubilization is one of the important factors to obtain high oil recovery and this condition can be obtained by a surfactant formulation that gives ultra-low interfacial tension. Hence, combining ultra-low interfacial tension property of an appropriate surfactant formulation and the high sweep efficiency of the foam technique can help improve the oil recovery.

Surfactant formulations with ultra-low interfacial tension can be obtained through a phase behavior study. Microemulsion at optimum condition is illustrated by various correlations such as Winsor R ratio, hydrophilic-lipophilic balance (HLB) concept and hydrophilic-lipophilic deviation (HLD) concept. R ratio indicates the absorbed surfactant interaction with surrounding oil and water. HLB number is used to identify the emulsification of surfactants in oil and aqueous phase. However, the R ratio parameters are not practical for property prediction while the HLB equation does not include equilibrium and conditions of formulation. These limitations can be neutralized by the HLD equations because parameters are uncomplicated and the estimation is based on equilibrium conditions. HLD equation does not only explain hydrophobicity and hydrophilicity of surfactant (C_c) in the microemulsion at optimum condition but also estimates proper surfactant/cosurfactant ratio. Precision of the calculated correlation is compared with attained results from phase behavior experiment and oil-water interfacial tension measurement.

The presence of oil and brine in the reservoir is a challenge condition and appropriate surfactant formulation must be designed for a specific system. High salinity brine can create two phase aqueous micellar solution phenomena and leads to an increase of interfacial tension. Furthermore, the increase of salinity affects the reduction of foam properties such as foam ability and foam stability. Moreover, the foam stability becomes lower in the presence of oil. Therefore, efficiency of enhanced oil recovery can be dramatically decreased.

Cosurfactants combining with the conventional surfactants can deal with these challenges. In this work, mixed surfactant systems between sodium dioctylsulfosuccinate (AOT) and internal olefin sulfonate (IOS) with three different carbon chain lengths were studied. AOT is an extended surfactant with two tails while IOS contains a long hydrophobic tail. A mixture of a surfactant with two hydrophobic groups and a surfactant with one hydrophobic group could yield a system with ultra-low interfacial tension (Rosen *et al.*, 2005). Hence, ultra-low interfacial foam was anticipated from the mixture of AOT and IOS.

The purpose of this work was to determine the capability to recover oil in place via ultra-low interfacial tension formulation. Firstly, the mixed surfactant was verified by the HLD equation to obtain the optimum surfactant formulations for both surfactant and foam flooding. Secondly, the phase behavior experiments were investigated via salinity scan and then compared the experimental optimum salinity which form Type III middle phase microemulsion with predicted optimum salinity from HLD equation. After that, foam stability were examined in both preliminary screening in the silica sand pack column at atmospheric pressure and ambient temperature of 25±2ºC to anticipate the foam properties flow through the porous media. Finally, surfactant and foam flooding using optimum formulation with minimum interfacial tension were investigated and the quantity of additional oil recovery for both surfactant and foam flooding were compared and discussed.

CHAPTER II
THEORETICAL BACKGROUND AND LITERATURE REVIEW

2.1 Oil Recovery Processes

Oil recovery processes are classified into 3 stages which are primary, secondary and tertiary recovery. In primary recovery, the oil naturally flows by underneath pressure due to gravity force. Over a period of production times not only produced oil is diminished, the pressure also decreases in production wells. Wettability of reservoir is a significant problem due to the alteration of composition caused by lessen crude oil. When the reservoir pressure is not enough to recover the oil, pressure can be restored by water injection. Therefore, the secondary recovery or water flooding has been proposed to solve this problem. Only 30-35% of Original oil in place (OOIP) can be recovered by combining both primary and secondary recovery. Thus, remaining oil is the main challenge to be consider (Bera *et al.*, 2015).

Tertiary recovery, or enhanced oil recovery, is categorized into three main techniques as shown in Figure 2.1 which are thermal methods, chemical flooding and injection of gas. Polymers, Foams, Surfactants and Alkali solutions are examples of chemical flooding. Thermal methods consist of hot water, electromagnetic, cyclic vapor, continuous vapor and in-situ combustion. Viscosity and trapped oil mobility are modified by this method. Furthermore, particular techniques can be integrated such as steam-assisted gravity drainage (SAGD) or water-alternating-with-gas process (WAG) (Gurgel *et al.*, 2008).
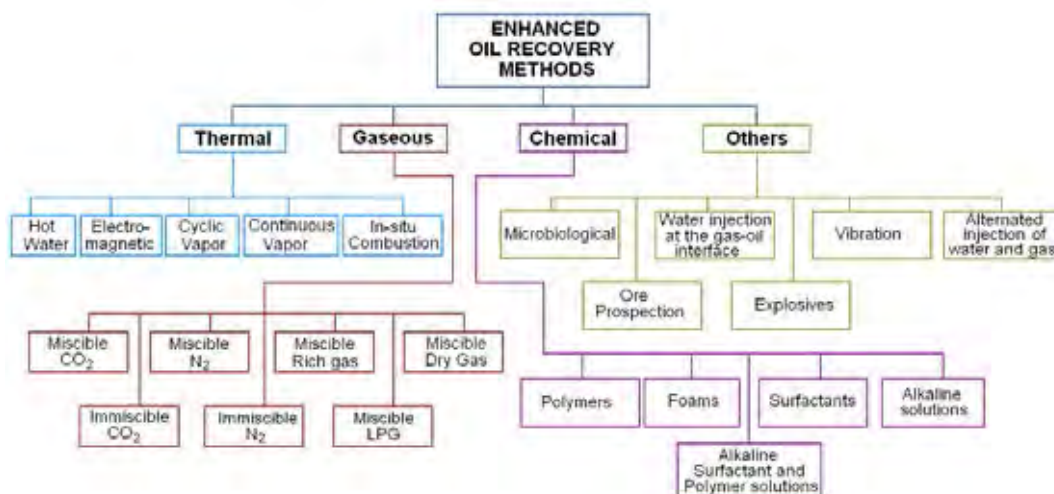
Figure 2.1 EOR processes categorizations (Gurgel *et al.*, 2008).

2.1.1 Microemulsion Flooding

Injections of polymer, surfactant, microemulsion or alkaline solutions can be used to improve the interaction between chemical slugs and oil in reservoir in chemical flooding. Surfactant flooding is proposed to deduct oil/water interfacial tension thus improvement of oil recovery. Low viscosity of injected fluid against the oil is concerned in recovery efficiency. Consequently, microemulsion was introduced instead of a single surfactant. Specific properties, higher viscosity and low interfacial tension, are appropriate to be injected fluid. The superb displacement efficiency are indicated by lowest surfactant loss from adsorption, minimization of oil/brine interfacial tension.

2.1.1.1 Microemulsion Flooding Mechanism

Surfactants, cosurfactant, cosolvent or optional additives combining with water are employed to flood the trapped oil in reservoir. Microemulsion is generated by injecting surfactant solution to reduce the interfacial tension. Trapped oil can be mobilized from the rock due to higher oil mobility. Microemulsion flooding will be injected after water flooding is done. Nevertheless, microemulsion flooding can be performed without water flooding if oil mobility is very low. Figure 2.2 indicates two-dimensional schematic diagram of microemulsion flooding. A 0.5-1.5 Pore volume surfactant slug is injected after water flooding.

Oil-water bank is formed in front of the microemulsion slug because of ultralow interfacial tension and increasing oil mobility. Microemulsion oil-water bank is driven by thickened fresh water through the production well. Polymer solution is added to water to increase viscosity in the thickened fresh water. Before adding surfactant slug, pH or salinity of brine is regulated by a preflush solution to improve both microscopic displacement and sweep efficiency. Adsorbent is added in the preflush solution to adsorb on the rock thus the surfactant loss in surfactant slug due to adsorption will be decreased. (Bera *et al.*, 2015).
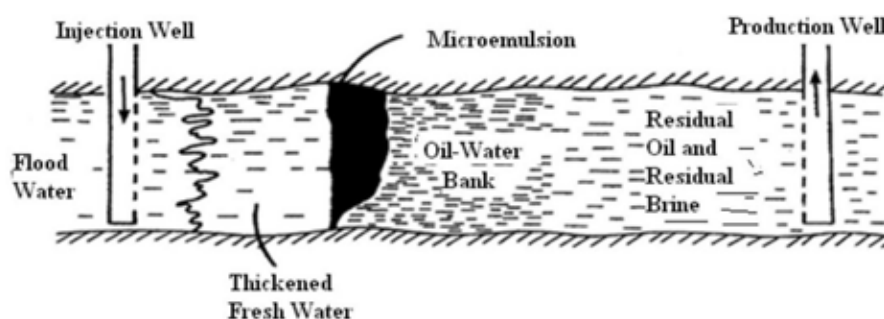
Figure 2.2 2D schematic of microemulsion flooding (Bera *et al.*, 2015).

2.1.2 Foam Flooding

Gas flooding has been proposed in EOR processes. However, there are some drawbacks of gas flooding such as lower viscosity than residue oil in reservoir, and viscous fingering. Surfactants are co-injected with gases to generate foam which can solve these drawbacks. The large amount of gases are stored in the porous media thus gas mobility is decreased. Therefore, Foam flooding can improve the sweep efficiency or increase oil displacement after water flooding. In addition, the performance of foam flooding is determined by foam stability. When oil is introduced in the system, the interaction between oil and foam is the main challenge (Simjoo *et al.*, 2013). Various laboratory experiments and practical applications show the good oil recovery performance by foam flooding. (Farzaneh *et al.*, 2013).

2.1.2.1 Foam Flooding Mechanism

Foam is generated by combination between surfactant and gases into wellbore. It initially penetrates into higher permeability layers due to its high apparent viscosity. Therefore, water channels are obstructed and turn away to lower permeability layers. Sealed water channels can handle the viscous fingering. Consequently, injected foam typically increases oil displacement efficiency (Chen *et al.*, 2015).

2.2 Surfactant Selection in EOR Process

The surfactant selection is concerned for identifying trapped oil recovery from reservoirs (Bera *et al.*, 2015). Unique application in EOR process requires appropriate surfactant selection using laboratory experiment (Sheng, 2013). High (2-10 %wt) and low (0.1-0.2 %wt) surfactant concentrations are suitable for different conditions. Ultralow interfacial tension is attained by low surfactant concentration. However, this concentration must be defined as obvious critical micelle concentration (CMC). CMC is the first concentration at which the micelle is formed.

2.2.1 Surfactant Classifications

Surfactants are divided into four groups due to the head group charge; anionic, cationic, nonionic and zwitterionic. Negative head charge represents anionic surfactants that is normally used in oil recovery process. Moreover, they can merge with sodium carbonate to deduct adsorption in both sandstone and carbonate reservoirs. Positive head charge indicates cationic surfactants. Sand and clay are negative charge surfaces, which are simply adsorbed by cationic surfactants. Therefore, cationic surfactants are not widespread injected in sandstone reservoirs. Even though, nonionic surfactant cannot form ionic bonds, hydrogen bond when combining with water can be formed. Rich oxygen parts at the end molecules and other organic parts exhibit the polarity. Ultralow interfacial tension and high solubilization are also achieved from nonionic surfactants. Combination of positive and negative head charges are zwitterionic surfactants (Bera *et al.*, 2015).

Recently, the zwitterionic surfactants are conducted in the oil and gas applications; however, there are only few researches of these surfactants in enhanced oil recovery (Negin *et al.*, 2016)

2.2.2 Surfactant Adsorption

Surfactant loss and flow plugging due to adsorption during enhanced oil recovery are the main undesired problems. Surfactant adsorption is considered as adsorbate partitioning in the interface between porous media and surfactant slug. The compatibility of surfactant charges with porous media causing the adsorption (Gogoi, 2011). The alteration of surfactant concentration is measured in both static and dynamic adsorption by pieces reservoir rock and dynamic flooding in porous media, respectively. For static adsorption, the exact surfactant concentration (0-4000 mg/L) is added to pieces of reservoir rock until equilibrium following by measuring the surfactant concentration after reaching the equilibrium. For dynamic adsorption, outlet surfactant concentration from porous media is determined by UV spectrophotometric analysis and can be calculated by Equations 2.1 and 2.2 (Yuan *et al.*, 2015)

$$\Gamma_i = \frac{V_i (C_0 - C_i)}{m} \tag{2.1}$$

$$\Gamma_n = \sum_{i=1}^{n} \Gamma_i \tag{2.2}$$

Where Γ_i is dynamic adsorption at i time (mg/g)

Γ_n is aggregate adsorption at n time (mg/g)

C_0 is inlet surfactant concentration (mg/L)

C_i is the outlet surfactant concentration (mg/L)

V_i is the outlet surfactant volume (L)

m is the reservoir rock weight (g)

Yuan *et al.* (2015) found that the dynamic adsorption of AOS+AEC and AES+AI surfactant formulations was lower than the static adsorption because of these three reasons. Firstly, not only reservoir rocks had negative charge but surfactant solution also had anionic charge thus introducing electrostatic repulsion. Secondly, powerful barrier was occurred by the adsorption of big head surfactant on reservoir rock surface. Finally, the adsorption decreased with higher temperature because of exothermic process.

Gogoi (2011) studied equilibrium adsorption in Nahorkatiya reservoir rocks by injecting alkaline/surfactant solution, which are sodium lignosulfonate (SL) mixed with NaOH. Sulfonate adsorption increased in presence of monovalent from brine in the reservoir because monovalent sodium behaved like counter ions. When the surfactant solution pass through reservoir rock sample, surfactant was adsorbed first and followed by desorption. Desorption process can improve the oil recovery by reducing IFT between oil and water phase.

2.3 Phase behavior and optimum formulation studies.

The important property that determine the ability of oil displacement by surfactant flooding is phase behavior of the surfactant/brine/oil systems. Surfactant flooding requires both phase behavior knowledge for appropriate designing and laboratory experiment for predicting the phase behavior in reservoir condition. Moreover, the physical properties that are related in phase behavior are viscosity and interfacial tension.

Oil recovery performance is interpreted by the phase behavior that is an essential factor in microemulsion flooding. The improved correlations between microemulsion and interfacial tension (IFT) are typically used to scrutinize formulation of surfactant to reach the minimum IFT in phase behavior experiments. Laboratory studies for phase behavior have been introduced to analyze the boundary of phase behavior. Minimum interfacial tension is desirable for stability of microemulsion systems. Nowadays, the specific oilfield applications are evaluated and forecasted by phase behavior. Therefore, performance of oil recovery is optimized with suitable phase behavior (Bera *et al.*, 2015).

Zhao *et al.* (2008) compared conventional surfactants with various kinds of internal olefin sulfonate (IOS). Proper co-surfactants, co-solvent and alkali combined with IOS which generated ultralow IFT were proposed and phase behavior were displayed. According to laboratory testing, surfactant formulations are optimized by phase behavior experiment followed by core flooding experiments. High carbon IOS is more suitable for surfactant flooding than conventional surfactant. Co-solvent was added to improve solubility and accelerate equilibration. The presence of alkali can reduce optimum salinity from soap by saponification.

2.3.1 Winsor-Type Systems

Oil, brine and surfactants are combined to attain microemulsions. There are three main types of Winsor or microemulsions as displayed in Figure 2.3. Winsor Type I is a water microemulsion in equilibrium with an oil excess phase. Surfactants and cosurfactants spherical micelles are spread out in water and loaded with oil. Winsor Type II is an oil microemulsion in equilibrium with a water excess phase. Micelles are spread out in oil and loaded with water. Winsor type III is a microemulsion in equilibrium with both water and oil excess phases. Micelles are contained in bicontinuous or middle phase microemulsion (García-Sánchez *et al.*, 2001). Low interfacial tension ($\leq 10^{-3}$) with equal volume of brine and oil in the middle phase at an optimum salinity represents the highest oil recovery capability. Furthermore, high capillary number due to low interfacial tension displaces trapped crude oil. Therefore, the middle phase or Winsor type III is maintained to achieve the maximum oil recovery in surfactant flooding (Hsieh *et al.*, 1977)
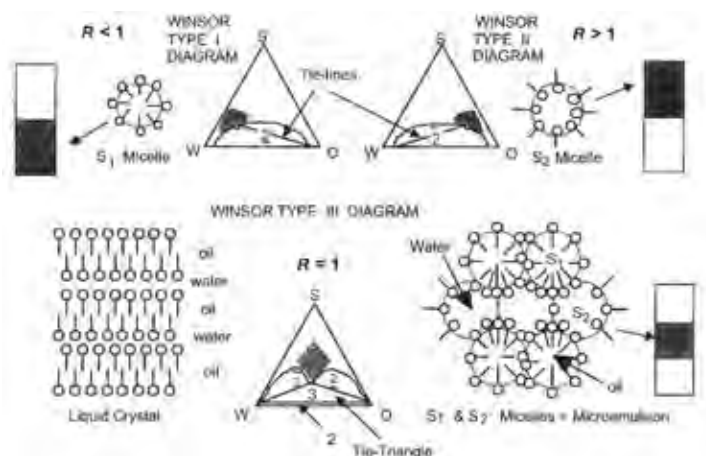
Figure 2.3 Phase behavior types in SOW system. Abundant Surfactant phase is indicated by black shading (Salager *et al.*, 2005).

2.3.1.1 Winsor R Ratio

R ratio was introduced as an upgrade on limited and imprecise hydrophilic-lipophilic balance in 1950s. Furthermore, each type of Winsor or microemulsion can be identified by the R ratio. This ratio illustrates the absorbed surfactant interaction with surrounding oil and water (Salager *et al.*, 2013). The relationship can be written as Equation 2.3.

$$R = \frac{A_{co}}{A_{cw}}$$ (2.3)

Where A_{co} = absorbed surfactant interaction with oil phase per unit area of interface

A_{cw} = absorbed surfactant interaction with water phase per unit area of interface.
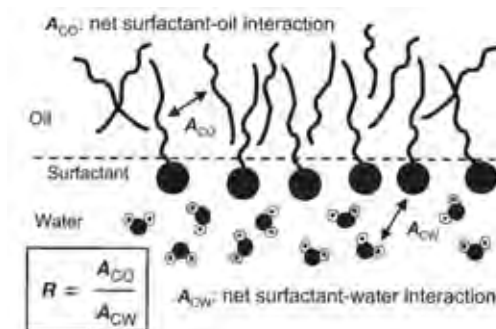
Figure 2.4 Interactions between surfactant, oil and water (Salager *et al.*, 2005).

Winsor type III that contains equal volume of oil and water in the middle phase indicates R=1. The transition of phase behavior can be observed by varying one of these parameters which are alcohol concentration and type, salinity, oil type, water/oil ratio, temperature and surfactant structure. Figure 2.5 presents the transformation of Winsor type I→III→II when increasing salinity because of the deduction in interaction between surfactant and water or the A_{cw} term in Equation 2.3. Consequently, R increases. In contrary, R decreases when increasing ACN or n-alkane chain length. Therefore, Winsor II→III→I is illustrated.

The formulation scan was introduced in series of test tubes with a single scanned variable such as salinity. The surfactant, water and oil are constant in the system. Minimum interfacial tension and maximum solubilization are achieved when R=1. Consequently, this formulation is called optimum formulation (Salager *et al.*, 2005)
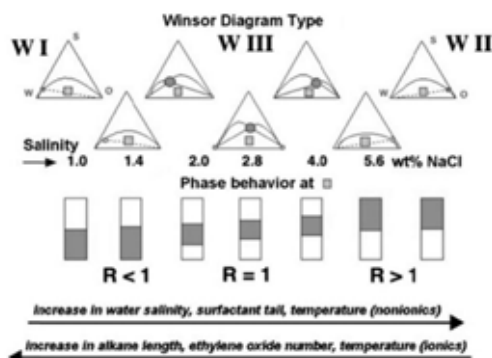
Figure 2.5 Phase behavior in test tube by salinity scan (Salager *et al.*, 2013).

Although Winsor-type systems quite well explain the phenomena in surfactant-oil-water phase behavior, they cannot evaluate quantities that is important for practical applications. Numerical explanation is used as a preliminary prediction of the minimum interfacial tension or optimum formulation. The correlation of various formulation variables is suggested for EOR researches (Salager *et al.*, 2000).

2.3.2 Numerical Expression for Optimum Formulation

Salager *et al.* (1979) described the different phenomena of optimum formulation by scanning variables which are IFT, solubilization ratio of oil/water in the middle phase and surfactant partition coefficient. In addition, some variables are scanned to observe the transition of phase behavior in anionic surfactants such as salinity, high molecular weight alcohol, ACN and Temperature. Moreover, the correlation of these variables can be written as Equation 2.4

$$\ln(S) + C_C - K(EACN) - f(A) - \alpha_T (\Delta T) = 0 \qquad (2.4)$$

The correlation for logarithm of the optimum salinity and EACN is linear. f(A) values in high molecular weight alcohol rely on alcohol type and concentration. Hydrophilic/lipophilic of surfactant is expressed by the Cc value. Temperature deviation from ambient is also linear.

2.3.2.1 Surfactant Affinity Difference (SAD)

Salager *et al.* (2000) described the numerical expression that is related to formulation variables in the three-phase behavior. These correlations in Equation 2.5 are the standard chemical potentials difference of the surfactant in oil and water phase or surfactant affinity difference (SAD). Transferred free energy ($\Delta G_{oil \rightarrow water}$) of surfactant molecule from water to oil phase is also related to the expressions.

$$SAD = \mu_w{}^* - \mu_o{}^* = \Delta G_{oil \rightarrow water} = -RTlnK_p \qquad (2.5)$$

Where $\mu_w{}^*$ and $\mu_o{}^*$ are chemical potential of the surfactant in the water and oil phase, respectively. K_p is the partition coefficient of the surfactant between water and oil. According to the experiment, Equation 2.6 can be extended by the SAD equation for ionic and nonionic surfactant that shown in Equation 2.7

Ionic surfactant

$$\frac{SAD}{RT} = \ln(S) + \sigma - K \times ACN - f(A) - a_T \Delta T + CONST \qquad (2.6)$$

Nonionic surfactant

$$\frac{SAD}{RT} = \alpha - EON + bS - k \times ACN - \varphi(A) + c_T \Delta T + CONST \qquad (2.7)$$

At SAD = 0, affinity of surfactant for water phase precisely equilibrates to affinity for oil phase which is called optimum formulation as the same as R=1 in Winsor type. Equation 2.6 and 2.7 illustrate compensating and coherent effects of SAD with diverse formulation variables.

Hydrophilic-lipophilic deviation or HLD was introduced by Salager *et al.* (2005) which is the dimensionless of SAD value (SAD/RT).

2.3.2.2 *Hydrophilic Lipophilic Deviation (HLD) Concept*

HLD describes the free energy deviation of microemulsion system with shifting surfactant molecules in oil to surfactant solution or aqueous phase. Positive, Negative and Zero HLD values indicate Type II, Type I and Type III of microemulsion systems, respectively. HLD equation divides into two equation which are for ionic and nonionic surfactants. Anionic surfactants are widely used in EOR application. The ionic surfactant HLD equation is written in Equation 2.8

$$HLD = \ln(S) + C_C - K(EACN) - f(A) - \alpha_T(\Delta T) \qquad (2.8)$$

Where   S = salinity of aqueous phase (g/100mL)

C_c = characteristic curvature of surfactants represent hydrophobicity

K = slope of plotting logarithm optimum salinity with EACN (0.1 to 0.2)

EACN = equivalent alkane carbon number of the oil

f(A) = alcohol constant depends on concentration and type

α_T = Temperature constant (0.01 K^{-1} for anionic surfactant)

ΔT = Temperature difference between reservoir and reference (T_{ref} = 25°C)

Cc, K and α_T are surfactant dependent parameters

An optimum formulation is obtained by adjusting HLD parameters such as C_c, K, and α_T. Negative HLD values refer to higher soluble surfactant in water than oil (Type I). In contrary, positive HLD values account for water in oil which is produced by the formations of hydrophobic surfactant (Type II). In addition, HLD is equal to zero when ultralow IFT is reached and the middle phase microemulsion is formed. Optimum salinity (S*) is defined as the salinity at HLD=0 (Type III) as indicated in Equation 2.9

$$\ln(S^*) = K(EACN) - C_C + f(A) + \alpha_T(\Delta T) \qquad (2.9)$$

However, HLD equation cannot be used to analyze the volume of oil or water dissolved in the middle phase.

(Budhathoki *et al.*, 2016) evaluated Sodium alkyl sulfate and sodium alkyl ethoxy sulfate surfactants (Steol Cs 460) in high salinity condition as surfactant formulations. Ultra-low interfacial tension and miscible clear aqueous phase were obtained without adding alcohols. The binary mixture with the lowest IFT or the optimum formulation was tested in a sand pack bed. 60% of trapped oil was displaced by surfactant injection. In addition, the residual oil saturation decreased from 25% to 10%. Moreover, surfactant/co-surfactant ratio of optimum formulation was correctly predicted by HLD equation.

Jin *et al.* (2015)predicted solubilization ratio curves and phase volume via HLD-NAC model of 3 systems including single surfactant, surfactant mixture and surfactant mixtures with co-solvent. A Net-Average Curvature equation was correlated with the curvature of the microemulsion. Experimental results were matched to the predicted values with only one fitting parameter that is the length constant (L). Fitted parameter is proportional to surfactant tail length size. Longer tail surfactant is suitable for higher salinity microemulsion region. Adding alcohols as a co-solvent is negligible by assuming alcohols completely portioned on interphase. Parameters of HLD equation are important to obtain high accuracy HLD values for examples, temperature constant, characteristic curvature and K-value.

K and C_c value in HLD equation can be determined experimentally by obtaining an optimal formulation that gives a middle phase microemulsion (HLD = 0) at a reference temperature $(T = T_{ref} = 25°C)$ without alcohol adding f(A)=0. For a single ionic surfactant system, Equation 2.10 is then simplified to

$$\ln(S^*) = K(EACN) - C_C \qquad (2.10)$$

A plot of ln(S*) versus EACN generates a straight line. K is obtained from the slope of the straight line. C_c value is determined by the y-axis intercept.

Witthayapanyanon *et al.* (2008) performed the minimum interfacial tension and phase volume experiment to measure the optimum salinity or S*. The K and C_C values of 0.7 M AMA surfactant and EACN of limeonene were attained by plotting the ln(S*) versus EACN with various kind of oils at 25°C without adding additive. The slope and y-intercept can be obtained from the plot and were assigned to K and C_c value, respectively. EACN of limonene is 5.7 which is close to the EACN of hexane.
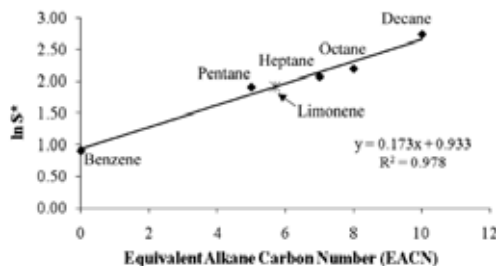
Figure 2.6 K, C_C values of AMA and EACN of limeonene determination (Witthayapanyanon *et al.*, 2008).

For multiple surfactants system using linear mixing rules.

$$\ln(S_{mix}*) = K_{mix}(EACN) - C_{C\,mix} \qquad (2.11)$$

$$\ln S_{mix}* = \sum x_i \ln S_i * \qquad (2.12)$$

$$K_{mix} = \sum x_i K_i \qquad (2.13)$$

$$C_{C_{mix}} = \sum x_i C_{ci} \qquad (2.14)$$

Where X_i is the mole fraction of surfactant i in a surfactant mixture.

For a binary mixture, Equations 2.12, 2.13 and 2.14 can be simplified by substituting with $x_2 = 1 - x_1$ as shown in Equation 2.15

$$\ln(S_{mix}*) = ((C_{C_1} - C_{C_2}) + (K_2 - K_1)(EACN))x_2 + \ln S_1 * \qquad (2.15)$$

A straight line is generated by plotting $\ln S_{mix}*$ versus x_2

Slope of the straight line $\quad : ((C_{C_1} - C_{C_2}) + (K_2 - K_1)(EACN)) \qquad (2.16)$

Y-axis intercept $\quad\quad\quad : \ln S_1 * = K_1(EACN) - C_{c_1} \qquad (2.17)$

Witthayapanyanon *et al.* (2008) studied microemulsion formulation of combining AMA and four extended surfactants as surfactant mixture systems with limonene oil by varying the mixture ratios to determine C_c value by plotting $\ln(S^*)$ vesus x_2. Surfactant Mixtures have different slopes refer to hydrophilic-lipophilic nature changing. Adding PO and EO groups affected both hydrophilicity (K value) and hydrophobicity (C_c value) of surfactants.
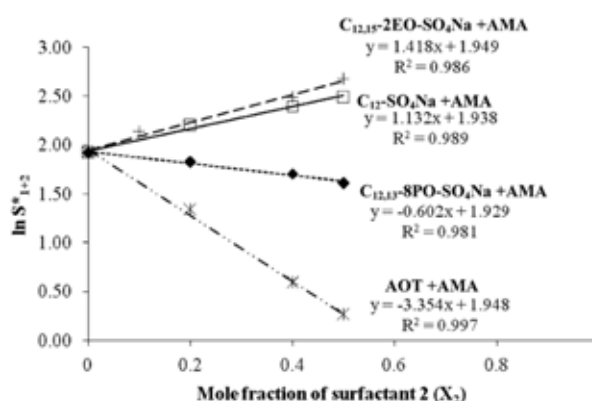
Figure 2.7 C_c determination of blended surfactants (Witthayapanyanon *et al.*, 2008).

In case of adding long chain alcohol as a cosolvent, The alcohol term or f(A) in optimum formulation Equation 2.9 must be considered. Salager *et al.* (1979) observed optimum salinity from middle phase formation as shown in Figure 2.8. Various alcohol concentrations were plotted with optimum salinity and ACN. It was observed that the straight line depended on the concentration and type of alcohol. Increasing alcohol concentration shifted the straight line to the right or downward. f(A) or alcohol function induced the vertical shift. The f(A) value of 3 g/cm^3 sec-butanol is equal to -0.16 in high salinity.
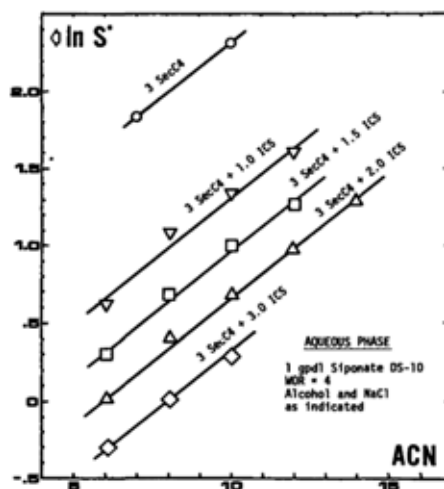
Figure 2.8 Plotting between ln S* and ACN with various alcohol concentrations using Siponate DS-10 as surfactant (Salager *et al.*, 1979).

Figure 2.9. represents the plot of f(A) versus alcohol concentration. Long chain alcohol is considered as a function of f(A) which depended on concentration and type of alcohol.
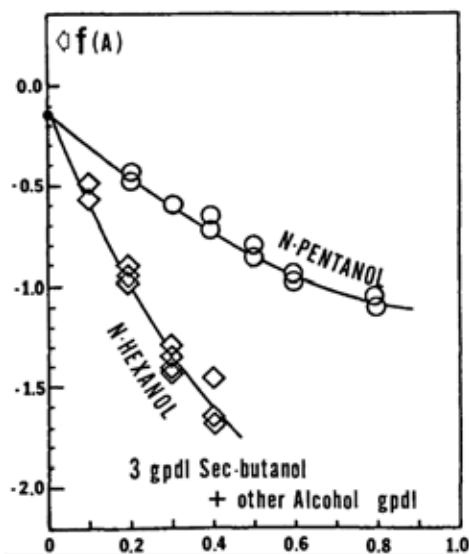
Figure 2.9 f(A) determination of 3gpdl sec-butanol with n-pentanol and n-hexanol (Salager *et al.*, 1979).

Anton *et al.* (1997) analyzed the effect of alcohol with salinity-EACN scan by varying alcohol concentration with the same surfactant. Alkyl amine salt and quaternary ammonium species were the surfactants in the system. 3%vol sec-butanol was introduced as a reference. A total 3%vol was fixed in the system by adding sec-butanol and another alcohol. Plotting ln S versus EACN created an optimum formulation line as shown in Figure 2.10. The parallel shifted line occurred when increasing n-pentanol concentration. The vertical shift compared to reference line was called f(A). Moreover, the relationship between f(A) and n-pentanol concentration was linear. f(A) for 1%vol n-pentanol in alkyl amine salt and quaternary surfactants are 0.7 ± 0.1 and 1.1 ± 0.1, respectively.
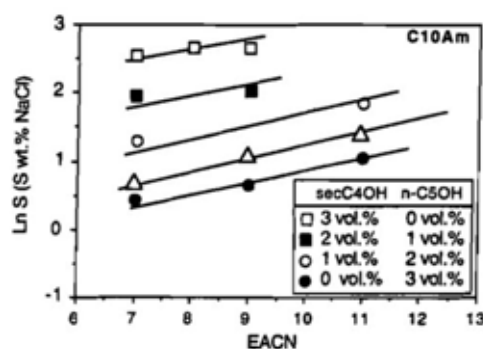
Figure 2.10 Salinity-EACN scan by plotting ln S versus EACN with various alcohol concentration in alkyl amine salt (Anton *et al.*, 1997).

Alcohols contribute to some physicochemical formulations at the interface such as lipophilicity and adsorption. Firstly, some alcohols combining with a surfactant can increase the lipophilicity at the interface. Secondly, adsorption at the interface is hindered by alcohol. Consequently, interfacial tension of surfactant decreases because the surfactant molecules are pulled by alcohol at the interface. This effect interrupted a liquid crystal formation; hence, alcohol is usually added in ionic surfactant system for seeking microemulsion. In addition, higher chain length of alcohol increases the oil side interaction by increasing hydrophobicity from OH groups leading to higher oil solubilization. This mechanism is called lipophilic linking where occurred at alcohol-oil interface.

Graciaa *et al.* (1993) studied the effect of alcohol chain length in microemulsion system by mixing nonionic surfactant mixed with various kind of alcohol (C_2 to C_{16}). Oil side interaction depended on the amount of interface adsorption and alcohol chain length. Gas chromatography was used to analyze alcohol in the microemulsion. Alcohol concentration is attained by the amount of adsorbed alcohol at the interface using a pseudo-phase model. C_6 to C_{10} alcohols can increase the solubilization by additional oil side interaction while higher solubilization of above C_{10} is achieved by lipophilic linking effect at oil phase boundary. Moreover, the solubility parameter variation of n-alcohol is calculated. As a result, solubilization is proportional to alcohol chain length. The effect of increasing in solubilization by mixing different alcohol chain lengths effect is stronger in linear than branching alkane oil phase.

2.4 Experimental Studies of Surfactant Flooding

After the surfactant formulation have been accomplished, the experimental studies are performed to verify the additional oil recovery in porous media to simulate the actual reservoir rocks. There are several methods for setting up the experiment due to hypothesis or scope of study. The typically well-known experiments are core flooding or sand pack column. The core is defined as the pieces of reservoir rocks that is achieved by an exploration process. Diverse rocks, silica sand, quartz sand and clay are the packing materials in the sand pack column to imitate as reservoir rocks. The difference between these experiments is operating pressure range. Low operating pressure is more favorable for a sand pack column than the core flooding.

Zhao *et al.* (2008) studied the behavior of surfactant flooding passing through the reservoir rock of two core flooding tests. First core experiment was used to screen the ability of high chain length surfactant of IOS C_{20-24} with high paraffin crude oil. Second core experiment was used to test the oil recovery in higher viscosity crude oil. Both experiments used the same surfactant solution from phase behavior experiments and same core preparation. Berea sandstone core was originally flooded with 3% NaCl brine for some pore volume. After that, the core was saturated with oil and flooded with brine. Finally, surfactant was flooded by injection of a surfactant-polymer slug.

As a result, both two core experiments recovered nearly 100% of the remaining oil with low pressure gradient. Consequently, the surfactant solution possibly flowed along the reservoir rock with low pressure.

Budhathoki *et al.* (2016) determined the oil recovery efficiency of appropriate surfactant formulation without adding polymer or alcohol at 52°C. The minimum interfacial tension system was attained by a mixed surfactant formulation, which are C_{10}-(PO_4)-$(EO)_1$-SO_4Na and Steol Cs460. The sand pack column was filled with Ottawa sand using a wet packing method until sand was saturated with brine. After that, reservoir oil was inversely injected to guarantee the uniformly saturated oil. If the water cut less than 1%, oil injection was changed to brine injection until the oil cut was less than 1%. Finally, the surfactant formulation was injected at 0.3 mL/min. Trapped oil displacement efficiency of surfactant flooding was 60% and the remaining oil is decreased from 25% to 10%.

Chen *et al.* (2015) investigated surfactant flooding with adding middle-carbon alcohol to recover heavy oil. The sand pack flooding experiments were performed to observe the mechanisms of heavy oil recovery. The sand pack column was filled with quartz sand using wet packing method to assure uniform wettability. Permeability and porosity was calculated when initially injected with 0.5% NaCl. Oil was then injected until no water remaining. Next, reservoir fluid was injected until no oil production followed by 0.5 pore volume of AOS surfactant slug. Extended water flooding was finally injected until no oil production. Adding middle carbon alcohol can additionally recover more oil at 3%-6% original oil in place. AOS surfactant with n-hexanol performed the highest oil recovery of 43.13% in surfactant flooding as compared to other middle carbon alcohols

2.5 Foam

Foam is an unbalance dispersion between large amount of gas bubbles and small volume of liquid filling with surfactant. Figure 2.11 illustrates a foam system schematic. A Thin liquid film between two interfaces isolates the gas phase. Lamella is the dotted square region containing interfaces and the thin liquid film. The connection in the middle of three thin liquid films is called Plateau border that is indicated by dotted circle region. The mixtures of surfactant, gas and water are the composition of foam.
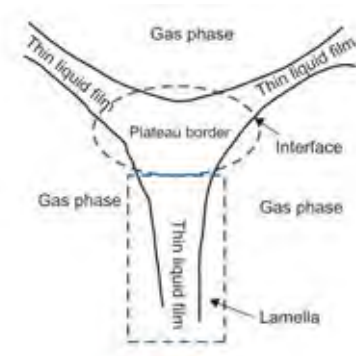
Figure 2.11 foam system schematic (Sheng, 2013).

When oil is introduced in the system, a symmetric film between gas phase and oil droplets is defined as pseudoemulsion film. The thin liquid film is surrounded by an oil droplet on one side of oil and the other side with a gas phase as displayed in Figure 2.12. (Manlowe *et al.*, 1990).
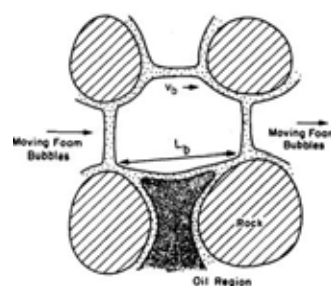
Figure 2.12 Pseudoemulsion film schematic. (Manlowe *et al.*, 1990).

Bubble size and foam quality are used to characterize the foam. The gas percentage or fraction in foam is defined as foam quality which typically ranges between 75% and 90%. Bubble size and spreading of sizes (0.01-0.1 µm to mm) depend on the foam quality. Lower foam quality and unstable foam are indicated by bigger bubble sizes. (Sheng, 2013)

2.5.1 <u>Foam Generation and Decay in Porous Media</u>

Snap off, lamella division and leave behind are the three primary mechanisms of foam in porous media. Firstly, snap off happens when gases enter in porous media or formation rocks, new gas bubbles are created and bring them to discrete form. Huge section of flow field is affected by the repeated snap off mechanism. Thus, it is commonly confided as outstanding foam formation mechanism. Lamellae forming and expansion of discrete gas region are the flow characteristics of a gas phase which is induced by the snap off mechanism. New gas bubbles are hidden in porous media thus gas permeability decreases by obstruction gas route. Figure 2.13 represents the snap off mechanism schematic.
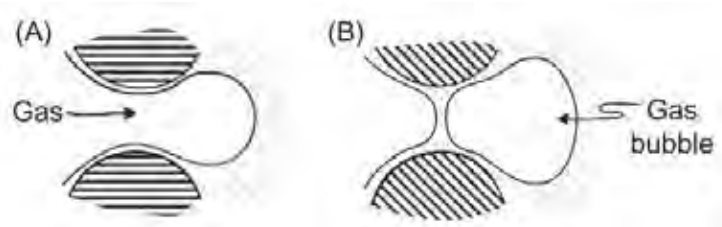
Figure 2.13 Snap off mechanism schematic indicates (A) Entering of gas (B) Forming New bubble. (Sheng, 2013).

Secondly, Lamella division happens when individual lamella reaches a separate region thus it is distributed into many lamellae as shown in Figure 2.14. The discrete bubbles are generated and obstruct the gas route. This phenomenon occurs repeatedly as the same as snap off mechanism. Both lamella division and snap off mechanisms are considered in the case of high gas flow velocities.
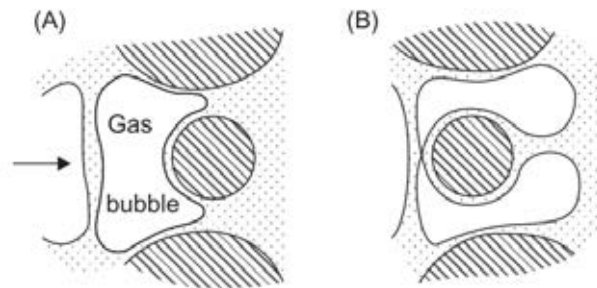
Figure 2.14 Lamella division mechanism schematic indicates (A) Lamella enter separate region (B) Forming separated gas bubble or lamellae. (Sheng, 2013).

Thirdly, when two gas menisci penetrate the closed liquid-filled pore bodies, the leave-behind mechanism is created as shown in Figure 2.15. Various amount of lamellae are generated from this mechanism to obstruct the gas routes because they decrease relative gas permeability by forming dead-end routes and also hindering flow routes. Leave-behind mechanism must be considered in a system with low gas velocities and creating feeble forms. This mechanism cannot occur repeatedly so large decreasing gas permeability is not obtained from this mechanism.
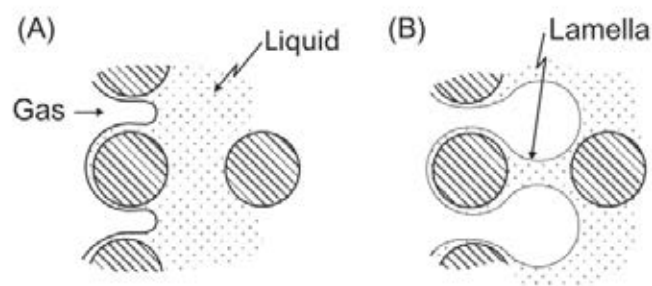
Figure 2.15 Leave behind mechanism schematic indicates (A) Gas intrusion (B) Forming lens (Sheng, 2013).

Decay of foam can be described by two mechanisms, which are the yield from the occupying of large single bubble on the pore body instead of two divided bubbles. Capillary suction coalescence is a rapid physical process. Lamella are quickly expanded across large pore bodies leading to shift gather lamella. A second mechanism is gas diffusion coalescence, which is the slow diffusion process. Two different arc bubbles are close together. Gas spreads from a higher arc or a smaller bubble to a lower arc or a bigger bubble by passing through intrusion lamella. Then, the smaller bubbles collapse together with normal lamella (Farzaneh *et al.*, 2013)

2.5.2 Foam Stability

Foams are thermodynamically unstable leading to a self-collapse process. Authentic resistance of lamella to abate interfacial area in a kinetic sense is called foam stability. In addition, foam stability is varied with the surfactant concentration, lipophilicity, bubble size and water-air interface diffusion rate. Haft-life or average lifetime is a method to measure the foam stability. Increasing elasticity of the interface by adding solid particles can obstruct the film collapse and foam coalescence for foam stability improvement (Bera *et al.*, 2013).

Bulk foam stability is typically measured by the static foam tests. However, the bulk foam behavior is moderately different in porous media because of the different foam generation and decay mechanisms. These experiments are considered as a preliminary screening of various formulations before using in porous media. (Singh *et al.*, 2015). Dynamic foam test in porous media is introduced to investigate the foam behavior in porous media. Foam can essentially obstruct the formulation of higher permeability to reroute the steam flow direction and increases oil recovery in porous media. The mobility reduction factor (MRF) represents the foam stability in porous media. The ratio between the mobility in foam flooding (mff) to mobility in water flooding (wbf) are used to calculate the mobility reduction factor as shown in Equation 2.15. Pressure drop between inlet and outlet of sand pack are obtained during water flooding and foam flooding, respectively as demonstrated by ΔP_{mff} and ΔP_{wbf}, respectively (Sun *et al.*, 2016).

$$MRF = \frac{(\Delta P/q)_{mff}}{(\Delta P/q)_{wbf}} \tag{2.15}$$

Where ΔP_{mff} is the differential pressure during foam flooding

ΔP_{wbf} is the differential pressure during water flooding

q is the injection rate (mL/min)

MRF is the mobility reduction factor

Manlowe *et al.* (1990) found that foam stability in porous media depends on stability of pseudoemulsion films. Transparent micromodel illustrates that lamellae is collapsed by pseodoemulsion film rupture.

Bera *et al.* (2013) studied the foam properties of SDS, CTAB, three ethoxylated alchols which are nonionic surfactant and mixed surfactant. High foaming was generated by an ordinary shaking method. SDS has the highest foam stability due to the highest volume of foam. Surface tension dramatically abated when increasing surfactant concentration. Adsorption of nonionic surfactant decreased with higher CMC. For mixed surfactant systems, the foamability was higher than a single surfactant. Moreover, combination of nonionic with anionic/cationic surfactants indicated high foamability. Various kinds of salt in brine represented low foam stability.

Sun *et al.* (2016) investigated the mobility controlling of foaming agent in sand pack with absence and presence crude oil. The resistance factors (MRF) dramatically increased up to 32 after 0.55 PV of foam slug in absence crude oil and significant greater than presence of crude oil. The results shown that the existing of crude oil demonstrated the foam decay or low foam stability. In addition, foam was easy to collapse in high oil saturation because of the separation of gas and liquid.

Wei *et al.* (2017) studied the foam performance in porous media wth different pressure (5 MPa, 10 MPa and 20 MPa). The mobility reduction factor (MRF) was drastically increased from 5 MPa to 20 MPa corresponding to high foam stability under high pressure because the regeneration mechanism of foam in porous media was improved at elevated pressures.

2.6 Experimental Studies of Foam Flooding

Poor sweep efficiency in reservoir rocks is one of the causes of low additional oil recovery from an oil reservoir. Moreover, high gas mobility permits high amount of injected gas flow through the reservoir rocks without additional oil recovery. These drawbacks can be resolved by introducing foam. Higher viscosity of injected gas can be accomplished by foam. Therefore, bubble gas phase divided by thin liquid films are formed to reduce gas mobility and gravity segregation. Nonwetting gas, which accumulated in high a permeability zone is transferred to a lower permeability formation for additional oil recovery. Adding cosolvent, alkaline and polymer are several ways to enhance oil recovery.

Chen *et al.* (2015) investigated the foam flooding in a sand pack column by adding middle carbon alcohols to the main surfactants, AOS. The foam flooding can achieve 10% additional oil recovery than the surfactant flooding. In the presence of alcohols, an additional 3-6% of original oil in place can be recovered because of the improvement in emulsification properties of the main surfactant by alcohols. Furthermore, sweep efficiency was improved due to the high foam stability and foam ability in the presence of alcohol. Moreover, the diffusion of alcohol to an oil phase can reduce the oil viscosity, resulting in the improved oil recovery. AOS surfactant with isoamyl alcohol performed the highest of 54.88% oil recovery in foam flooding among all middle carbon alcohols.

Osama *et al.* (2015) conducted a series of core flooding experiment to determine the additional oil recovery from foam flooding and foam stability in porous media. Surfactant solutions consisted of both nonionic (Triton X-100, Triton X-405, Zonyl FSO, Noigen N-10 and Noigen N-20) and anionic (Hitenol H-10, Hitenol H-20) in 4% brine. Oil phase and injected gas were Light Saudi crude and carbon dioxide gas, respectively. Pressure differential and oil recovery were measured to evaluate the gas mobility control and oil recovery enhancement. Hitenol H-10 surfactant formulation exhibited high pressure differential and high oil recovery; thus, a system with higher foam stability in porous media gave higher additional oil recovery.

Osei-Bonsu *et al.* (2017) compared oil recovery enhancement in two 2D porous media models using a 3D printer with four different surfactants that are Cobobetaine, SDS, Triton X100 and CocoSDS. Surfactant formulation was initially coinjected with gas into a foam generator. The foam was then transferred to a model using a plastic tube with 85% foam quality. First the model was saturated with water to determine the water displacement efficiency with foam. Second the model was saturated with oil to evaluate oil displacement efficiency with the same foam formulation. The existing water had been displaced after 1.15 PV foam injection for all four surfactants. For oil displacement experiments, the performance to recover oil can be ranked as flows: Triton X100 > CocoSDS > SDS > Cocobetaine. Stability of foam is indicated by needed pore volume for displacing oil.

Hua *et al.* (2015) compared two methods of oil recovery by a sand pack experiment between air and foam flooding. Liao He oil, $NaHCO_3$, air and HS-403 or alkyl benzene sulfonate surfactant were the oil phase, formation water, injected gas and foaming agent, respectively. For air flooding, the oil recovery was gently increased with higher PV until the air breakthrough at 0.23 PV with 35.8% oil recovery. After that, oil recovery was steadily declined until constant at 38.45% oil recovery. It is worth nothing that oil can be recovered before the air breakthrough and after that the oil recovery was constant. For foam flooding, oil recovery was increased when injected more air until the air breakthrough at 0.47 PV with 73.35% oil recovery and finally reaching 74.61%. In conclusion, the foam flooding can recover 36.1% more remaining oil than the air flooding. Higher gas viscosity and reducing gas permeability from introducing foam gave a lower gas mobility leading to a higher oil recovery.

MOTIVATION

Enhanced oil recovery was used to recover more oil after primary and secondary oil recovery are not economical. The flooding experiments are preliminary evaluated before developing to use in a practical field. Surfactant flooding is chosen since it has great potential to lower the interfacial tension between oil and displacing fluid. Moreover, foam is a mobility control agent that helps increase sweep efficiency. Therefore, the combination between low interfacial tension and efficient foam properties is investigated in this study.

HYPOTHESIS

Minimum interfacial tension between oil and aqueous phase is the main property to achieve high oil recovery in a surfactant flooding. This property is attained at optimum salinity or middle phase microemulsion. HLD equation is the tool for predicting the optimum formulation for surfactant flooding. The optimum salinity is achieved when the HLD is equal to zero. Therefore, the optimum formulation should be the best condition for surfactant flooding because surfactant can equally solubilize in oil and water. However, early breakthrough in the reservoir formation has been commonly observed in the surfactant flooding technique. Foam flooding can help slow down the penetration of surfactant through the formation and decrease the channeling effect. It is hypothesized that by combining the advantages of both surfactant and foam flooding by formulating a low interfacial tension foam can maximize oil recovery efficiency. The effect of alkyl chain length of both surfactant itself and the oil phase will be studied.

OBJECTIVES

      1.   To study phase behavior of mixed surfactant systems with various oils using different alkyl chain length cosurfactants.

      2.   To determine the optimum formation with efficient foam properties.

      3.   To study the oil recovery efficiency of foam flooding and surfactant flooding using surfactant formulation with minimum interfacial tension and other conditions.

SCOPE OF RESEARCH

To accomplish the objectives of this study, the following scope of work is proposed:

      1.   Sodium dioctylsulfosuccinate (AOT) was selected as the main surfactant solution and it was combined with internal olefin sulfonate (IOS) with different carbon chain lengths; $C_{15\text{-}18}$, $C_{19\text{-}23}$ and $C_{24\text{-}28}$.

      2.   Individual surfactant was prepared at temperature higher than the Krafft point.

      3.   Phase behavior experiment was conducted at ambient temperature of $25\pm2°C$.

      4.   HLD parameters were obtained from literatures.

      5.   Minimum interfacial tension was attained at optimum salinity, which HLD=0.

      6.   The porous media experiments were performed in a silica sand pack glass column at atmospheric pressure and ambient temperature of $25\pm2°C$.

      7.   Foam was generated in a sand pack column using co-injection method.

      8.   Brine flooding was used as a reference oil recovery method to compare the oil recovery performance with the foam and surfactant flooding.

      9.   Oil recovery efficiency was compared between surfactant and foam flooding at various conditions.

CHAPTER III
METHODOLOGY

3.1 Materials and Equipments

3.1.1 Materials

1. Sodium dioctylsulfosuccinate (AOT) (purity 97%) purchased from Sigma-Aldrich.

2. Internal olefin sulfonate C_{15-18} (ENORDET 0332), C_{19-23} (ENORDET 0342), and C_{24-28} (ENORDET 0352) were complimentarily obtained from Shell Technology Centre Houston.

3. N_2 (purity 99.99%) purchased from Praxair (Thailand) Co., Ltd.

4. Heptane and Hexadecane (purity 99% AR grade) purchased from Merck.

5. Crude oil was supplied by PTTEP from Southern of Thailand.

6. Sodium Chloride (purity 99 % AR grade) purchased from V.S.Chem House.

7. Silica Sand Mesh no.50-100 purchased from Herosign Marketing Co., Ltd.

3.1.2 Equipments

1. Glass column ID 2.5 cm x L 15 cm with a flow adapter (Kimble)

2. Syringe pump (NE-300)

3. Digital pressure gauge for gas and liquid (SSI technologies, Inc) with accuracy of ±1.0% full scale

4. Differential pressure transmitter (OMEGA, PX409 series) with 0.08% BSL linearity, hysteresis and repeatability combined

5. Mass flow controller (Aalborg, GFCS-010057)

6. Sieves (Cole-Palmer)

7. Spinning drop tensiometer (Dataphysics, SVT1)

3.2 Methodology

3.2.1 Salinity Scan Using HLD Equation

To investigate the optimum salinity in Winsor type III or HLD=0, a salinity scan was performed by mixing the surfactant solution with various salt concentration and interacting with alkane as an oil phase. The experimental procedure is illustrated in Figure 3.1

$$HLD = \ln(S) + C_C - K(EACN) - f(A) - \alpha_T(\Delta T)$$

HLD = 0

Surfactant : cosurfactant = 1:1
No alcohol ; f(A) = 0
Ambient temperature (25±2°C)

K and Cc from the literatures

$$\ln(S_{mix}{}^*) = K_{mix}(EACN) - C_{Cmix}$$

Predicted optimum

Salinity scan

| 2.5 mL of brine NaCl Varying conc. | 2.5 mL of Surfactants Surfactant : Cosurfactant 1:1 **At const conc.** | 5 mL of alkane Heptane Hexadencane |

Winsor type III (Microemulsion)

Optimum Salinity With Lowest IFT

Calculated HLD

Figure 3.1 Optimum formulation investigation procedure.

3.2.2 Equilibrium Interfacial Tension Measurement

The equilibrium IFT measurements were conducted using a spinning drop tensiometer (Dataphysics, SVT1). Only the samples that formed middle phase microemulsion were chosen to measure the equilibrium IFT measurement. Firstly, the excess aqueous phase was collected from the lower portion of the equilibrated sample and filled into a capillary tube. Then, the excess oil phase was drained from the upper portion in the same vial and carefully injected approximately 1-5 µL into the capillary tube. The tube was spun by increasing rpm until the the length of the oil droplet expanded to approximately four times of its width and equilibrium was reached. The data was recorded every 5 minutes for ensuring the constant IFT value.

3.2.3 Preliminary Foam Stability Test

A 5 mL surfactant solution was mixed with salt solution at the optimum salinity in vial. A 5 µL oil droplet was added into the vial, followed by hand-shaken and left at room temperature. The foam height was recorded versus the time until foam collapse. Foam stability was indicated by half-life of foaming agent.

3.2.4 Surfactant and Foam Enhanced Oil Recovery in A Sand Pack Column

A sand pack was employed to simulate as reservoir rocks by firstly saturated with brine, followed by the saturation with oil. Then brine flooding was performed as the secondary oil recovery. In the step of tertiary oil recovery, either surfactant or foam floodings was conducted and the amount of additional oil recovery was determined. Figure 3.2 shows a schematic of the sand pack column.
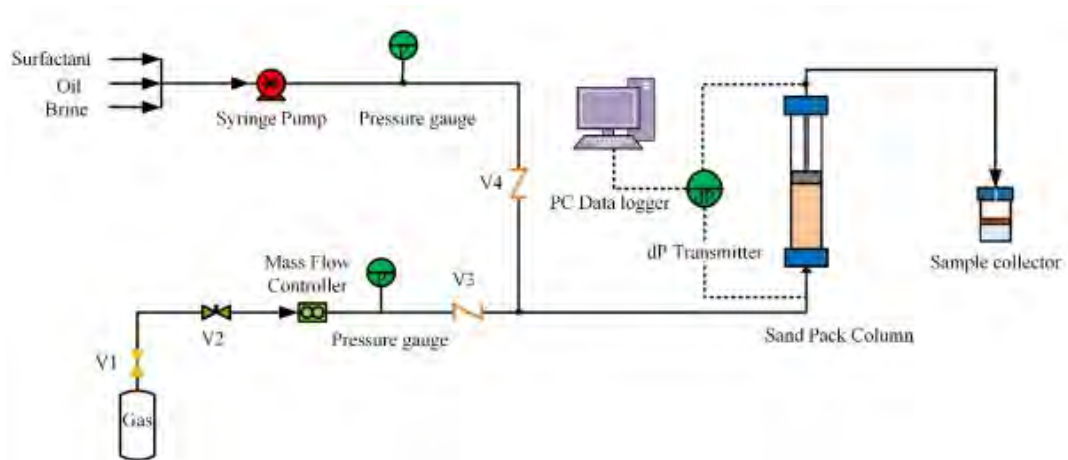
Figure 3.2 The flow chart of experimental set up.

3.2.4.1 Sand Pack Preparation

Silica sand from Herosign Margeting.Co.,Ltd was screened by a sieve shaker to obtain a homogenous sand pack of 200-300 μm. A glass chromatography of 1-inch diameter and 6-inch long with adjustable adapter was used in this study. A dry packing was performed to pack the sand by pouring sand about 60 gram at a time and the column was gently beaten to ensure a uniform packing. All sand packing tests were performed on a fixed height of 3-inch sand bed and the amount of sand in the column was 60±2 grams.

3.2.4.2 Sand Pack Saturation Procedure

The reservoir condition was simulated by saturating the sand pack with 3gNaCl/100mL solution at a flow rate of 0.5 cm^3/min until no more bubble was produced (about 3-4 pore volume). The fraction of brine left in the column is called initial brine saturation (S_{wi}).

Pore Volume and Porosity Calculation

The pore volume, porosity and permeability were measured in this step. The total injected brine volume and outlet volume were measured and the pore volume and porosity were calculated by Equations 3.1 and 3.2, respectively.

$$\text{Pore volume (PV)} = \text{Total injected volume} - \text{Total outlet volume} \qquad (3.1)$$

$$\text{Porosity}(\varphi) = \frac{\text{Pore volume}}{\text{Bulk Volume}} \qquad (3.2)$$

where the bulk volume includes void and solid material volume.

Permeability Measurement

Permeability (k) was determined by Darcy's law as shown in Equation 3.3

$$\frac{\Delta P}{L} = \frac{q\mu}{kA} \qquad (3.3)$$

where q is the flow rate (cm^3/s); μ is the water viscosity (cP); A crossectional area of the sand pack (cm^2); k is the permeability (D); ΔP is the pressure drop along the sand pack (atm) and L is the length of the sand pack (cm).

Pressure drops at different flow rates were measured. A and μ, which are the constant values, were plotted with q versus $\Delta P/L$. Then, a straight line that passes the origin point was obtained. The permeability of the sand pack was then determined from the slope of the plot.

After that, an oil was injected at a rate of 0.5 cm^3/min until no more brine was produced. Initial oil saturation (S_{oi}) was calculated by measuring the volume of brine displaced by oil saturation, also called Oil in Place (OOIP).

$$\text{OOIP} = \text{Volume of brine displaced by oil} \qquad (3.4)$$

$$S_{wi} = \frac{PV - OOIP}{PV} \qquad (3.5)$$

$$S_{oi} = \frac{OOIP}{PV} \tag{3.6}$$

Where OOIP is the original oil in place; S_{wi} is the initial brine saturation; S_{oi} is the initial oil saturation; and PV is pore volume. In this study, the pore volume of 3-in sand packs was 16.8 ± 0.6 cm^3 and connated water (%S_{wc}) was 46.0 ± 11.3 %

3.2.4.3 Brine Flooding

The secondary oil recovery or brine flooding was performed by using salt solution (NaCl) at the optimal salinity determined from the microemulsion phase study as the injected fluid. Oil was displaced by brine until it reached the residual oil saturation (S_{or1}) when the recovered oil volume was less than 1% of the collected sample volume. Brine volume used was recorded as pore volume (PV).

$$S_{or1} = \frac{OOIP - V_1}{OOIP} \tag{3.7}$$

Where S_{or1} is residual oil saturation after brine flooding; V_1 is the collected oil volume after brine flooding and OOIP is the original oil in place.

3.2.4.4 Chemical Flooding

Two types of chemical floodings were performed and compared as follows:

a) <u>Surfactant Flooding</u>

Different carbon chain lengths of Internal olefin sulfonate (IOS) and appropriate cosurfactant with 1:1 ratio were prepared in a salt solution (NaCl). The surfactant concentration was kept constant above the critical micelle concentration or CMC. The surfactant slug was injected after brine flooding to recover the remaining oil as additional oil recovery in Equation 3.8.

b) Foam Flooding

Surfactant solution was co-injected with N_2 through the sand pack column and foam was generated in-situ and propagated in the sand pack. The foam quality was 90% which is the fraction or percentage of the gas in a total fluid volume. Additional oil recovery after brine flooding was calculated by Equation 3.9. After that, the efficiency to displace the oil was compared between the foam flooding and surfactant flooding.

$$S_{or2} = \frac{OOIP - V_1 - V_2}{OOIP} \tag{3.8}$$

$$\text{Additional oil recovery (\%)} = \frac{S_{or1} - S_{or2}}{S_{or1}} \times 100 \tag{3.9}$$

Where S_{or1} is the residual oil saturation after brine flooding: S_{or2} is the residual oil saturation after chemical flooding and OOIP is the original oil in place. The experimental procedure of the surfactant and foam floodings in sand pack column is shown in Figure 3.3

3.2.4.5 Sand Pack Post Flushing

The salt solution (NaCl) with the same concentration in brine flooding step was injected at a rate of 0.5 cm^3/min until no more oil was produced. Post flushing was conducted to ensure the amount of oil recovery after chemical flooding.

```
┌─────────────────────────────────────────────────────┐
│    Pack silica sand in column (3 inches of height)    │
└─────────────────────────────────────────────────────┘
                           │
                           ▼
┌─────────────────────────────────────────────────────┐
│   Saturate sand pack with oil until no more bubble    │
│  measure pore volume (PV), porosity (∅), permeability (k) │
│              (100% OOIP and $S_{oi}$)                 │
└─────────────────────────────────────────────────────┘
                           │
                           ▼
┌─────────────────────────────────────────────────────┐
│       Water flooding: Inject water  until             │
│  no more oil produced and measure oil saturation ($S_{or1}$) │
└─────────────────────────────────────────────────────┘
          │                              │
          ▼                              ▼
┌────────────────────┐        ┌────────────────────┐
│ Foam flooding: Co-inject │  │  Surfactant flooding: │
│ surfactant solution and air │ │ Inject surfactant solution │
└────────────────────┘        └────────────────────┘
          │                              │
          └──────────────┬───────────────┘
                         ▼
┌─────────────────────────────────────────────────────┐
│ Measure oil saturation ($S_{or2}$) and determine additional oil │
└─────────────────────────────────────────────────────┘
                         │
                         ▼
┌─────────────────────────────────────────────────────┐
│           Comparing the efficiency of                 │
│         displacing oil between foam                   │
│        flooding and surfactant flooding               │
└─────────────────────────────────────────────────────┘
```

Figure 3.3 The surfactant and foam flooding in sand pack column procedure.

3.2.5 <u>Study Procedure</u>

Minimum interfacial tension or optimum formulation was achieved from microemulsion phase behavior experiment. A 5 ml an aqueous phase and 5 ml of an oil phase was added in a vial, followed by hand-shake and left at room temperature to allow equilibrium. The aqueous phase consisted of AOT as the primary surfactants and IOS as the co-surfactant at various salinity. The oil phase was an alkane oil, i.e. heptane and hexadecane as a representative of light and heavy oil, respectively. For crude oil systems, the salinity scan was performed in 5 mL pipette for more obvious phase behavior observation. A 2.5 ml an aqueous phase and 2.5 ml of crude oil was mixed and hand-shaken in a vial Then the mixture was poured into a bottom-flame-seal measuring pipette. The top of pipette was wrapped with parafilm and left in the oven at 60°C for equilibrium more than 30 days.

The formation of a middle phase microemulsion was observed when a clear blue middle phase in alkanes or opaque phase under the flashlight in crude oil were formed and divided the aqueous and oil phases into equal volume. The vials and pipettes with middle phase microemulsion were further tested by measuring the equilibrium interfacial tension.

The optimum condition was defined as the salinity that gave the minimum equilibrium interfacial tension and was selected to perform a preliminary foam stability test and flooding experiment in a silica sand pack glass column at atmospheric pressure and ambient temperature of 25±2 °C. The amount of additional oil recovery after the secondary oil recovery or brine flooding was determined. The percentage of additional oil recovery was compared between the surfactant and foam floodings at the same optimum formulation. All study procedures were summarized in Figure 3.4.

3.2.5.1 Predicted Optimum Salinity

The objective of this step was to calculate the optimum salinity by an HLD equation. The HLD equation is a tool for predicting the optimum salinity thus the range of salinity scan becomes narrower. All parameters were obtained from literature both AOT and IOS surfactant.

3.2.5.2 Salinity Scan

The objective of this step was to observe the middle phase microemulsion with the lowest interfacial tension. Salt concentrations were varied by mixing 1:1 mole ratio of the primary surfactant with different carbon chain lengths IOS surfactants; C_{15-18}, C_{19-23} and C_{24-28}. Alkane and crude oil were introduced as an oil phase to form middle phase microemulsion. The mixtures were left at room temperature and the middle phase microemulsion was observed without surfactant retention.

3.2.5.3 Equilibrium IFT Measurement

The objective of this step was to ensure the optimum salinity with minimum IFT among the Type III middle phase microemulsion from salinity scan. The optimum salinity and appropriated solution were selected to inject into the sand pack column in brine flooding and enhanced oil recovery steps.

3.2.5.4 Preliminary Foam Stability Test

The objective of this step was to observe the foamability and foam stability of optimum formulation in the presence of alkanes before investigate the oil recovery efficiency of foam flooding in the sand pack column.

3.2.5.5 Effect of Surfactant Slug Size

The objective of this step was to study the additional oil recovery in both surfactant and foam flooding of different amount of surfactant slug injection. $AOT:C_{15-18}$ with heptane at optimum salinity from phase behavior experiment were tested in this experiment. 1 PV of surfactant slug was compared to 3 PV of surfactant slug with absence and presence of N_2.

3.2.5.6 Effect of Salinity

The objective of this step was to compare the ability to displace the trapped oil in the sand pack after brine flooding using different salinity. AOT:IOS C_{15-18} with heptane were chosen to investigate this effect in both optimum salinity and dilute condition. Surfactant solution was prepared by salt concentration with 10 times dilution from the respective optimum salinity.

3.2.5.7 Oil Recovery at The Optimum Salinity

The objective of this step was to compare oil recovery efficiency of surfactant and foam flooding. The mixed surfactants with different carbon chain lengths IOS surfactants; C_{15-18}, C_{19-23} and C_{24-28} was injected in the sand pack column in the absence and presence of N_2 for surfactant and foam flooding, respectively. Injection rate, foam quality, concentration and other conditions were fixed for all experiments.

3.2.5.8 Effect of Shut In

The objective of this step was to investigate the effect of different operating conditions after 1 PV of surfactant slug injection. Shutting in was employed to compare the oil recovery efficiency with conventional operation. AOT:IOS C_{24-28} with hexadecane was used in this experiment due to slow coalescence rate from phase behavior experiment.
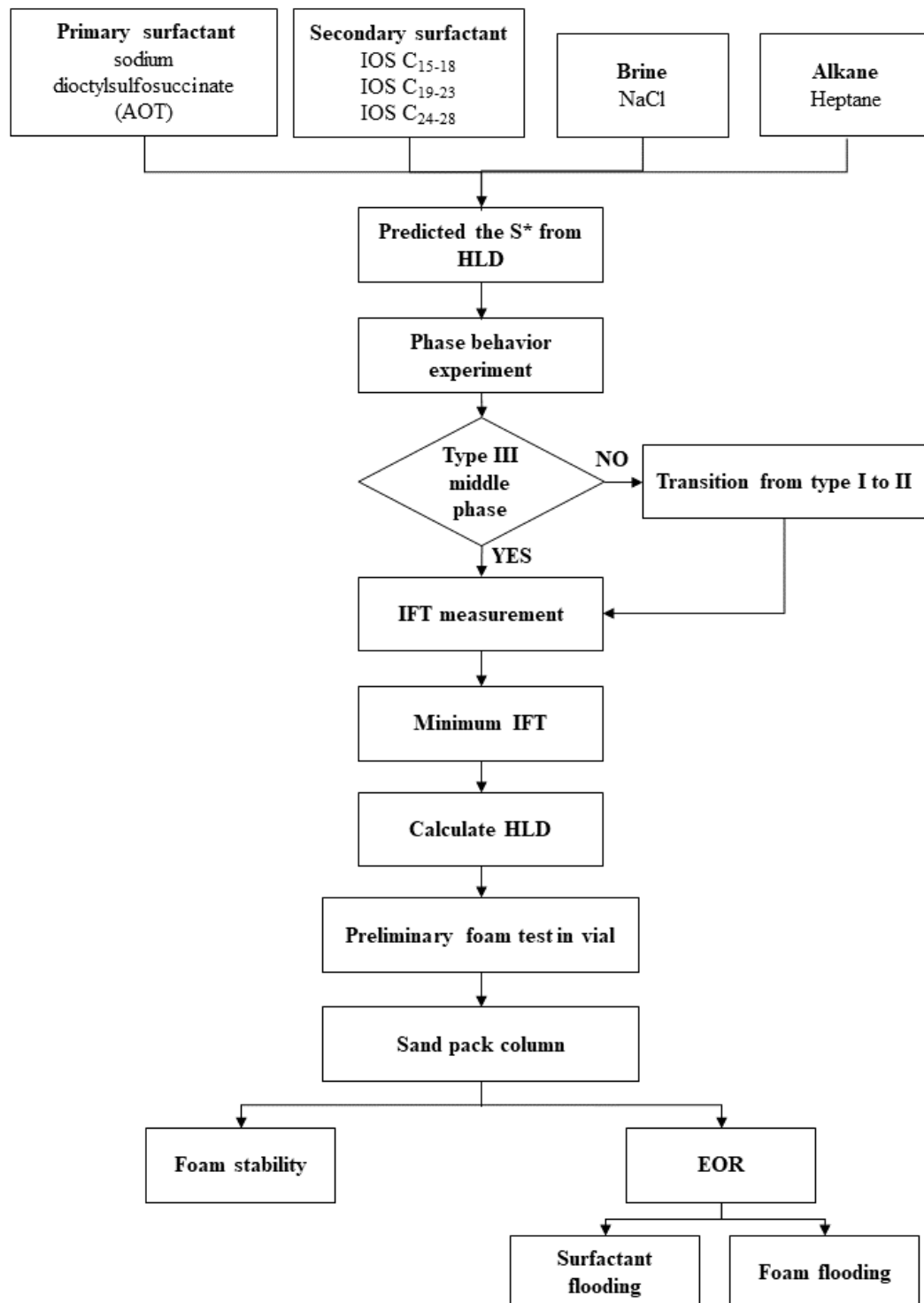
Figure 3.4 Summary of study procedure.

CHAPTER IV
RESULTS AND DISCUSSION

4.1 Phase Behavior Experiments

In surfactant flooding, an appropriate surfactant selection is important factor for effective oil recovery from the reservoirs. Phase behavior experiments are commonly considered as preliminary screening before conducting prolonged sand pack tests. Alkanes such as heptane and hexadecane were conducted as an oil phase due to lucidity of interfaces in the presence of huge molecule of surfactant. Crude oil was introduced as another oil phase for more practical use in petroleum industries. Salinity scan were performed to measure coalescence rate and equilibrium interfacial tension.

4.1.1 Predicted Optimum Salinity

The optimum salinity of the binary surfactants system without adding alcohol at room temperature was evaluated by an HLD equation. K and Cc values of sodium dioctylsulfosuccinate (AOT) are 0.17 and 2.42 (Witthayapanyanon *et al.*, 2008). In addition, K and Cc values of three different carbon chain lengths IOS surfactants; C_{15-18}, C_{19-23} and C_{24-28} are confidential due to Shell's proprietary. The optimum salinity of the mixed surfactant system from the HLD calculation was shown in Table 4.1. It is indicated that the optimum salinity decreased with longer carbon chain length of IOS due to higher hydrophobicity (Levitt *et al.*, 2009).

Table 4.1 Predicted optimum salinity by HLD equation

Mixed surfactant	Alkane (Oil phase)	Predicted $S*_{mix}$ (g NaCl/100mL)
1:1 AOT:IOS C_{15-18}	Heptane	2.1
1:1 AOT:IOS C_{19-23}	Heptane	1.6
1:1 AOT:IOS C_{24-28}	Heptane	1.2
1:1 AOT:IOS C_{15-18}	Hexadecane	6.6
1:1 AOT:IOS C_{19-23}	Hexadecane	5.8
1:1 AOT:IOS C_{24-28}	Hexadecane	4.4

4.1.2 <u>Salinity Scan</u>

The mixed surfactant solution was conducted with a fixed 0.03 M of total surfactant concentration and the salinity scans were performed. The salinity scans in Figures 4.1 to 4.3 shown the mixture of AOT with three different carbon chain lengths IOS surfactants; C_{15-18}, C_{19-23} and C_{24-28} at 1:1 volume ratio in heptane, hexadecane and crude oil as an oil phase, respectively. The property of crude oil used in this work is tabulated in Table 4.2. It is noticed that increasing salinity shifted the microemulsion from Type I to III to II because of higher hydrophobicity of the system (Budhathoki *et al.*, 2016). For heptane, the middle phase or Type III microemulsions was observed in AOT:IOS C_{15-18} and AOT:IOS C_{19-23} as the surfactant formulation when the salinity was in the ranges of 1.2-1.9 (see Figure 4.1a) and 0.7–0.9 gNaCl/100 mL (see Figure 4.1b), respectively. However, type III microemulsion could not be generated in the system of AOT:IOS C_{24-28} in heptane as an oil phase (see Figure 4.1c) because of the unbalancing between the high hydrophobicity of the long carbon chain length surfactant and the low hydrophobicity of the short chain alkane.

Table 4.2 The property of PTTEP crude oil

Properties	Values
API gravity	43.0
Density at 60°C	0.7980 g/cm^3
Kinematic Viscosity at 60°C	4.316 cSt (mm^2/s)
Total Acid Number	0.10 mgKOH/g

In Figure 4.2, Type III microemulsion of AOT:IOS C_{15-18}, AOT:IOS C_{19-23} and AOT:IOS C_{24-28} with hexadecane as an oil phase was observed when the salinity was in the ranges of 5.4-6.4, 1.8-2.5 and 0.9-1.2 gNaCl/100 mL, respectively. Increasing carbon chain length of alkane represents higher hydrophobicity of an oil phase. AOT:IOS C_{15-18} with lower hydrophobicity consumed long coalescence time to achieve the middle phase microemulsion.

A microemulsion phase study of crude oil as an oil phase was performed using AOT:IOS C_{15-18}, AOT:IOS C_{19-23} and AOT:IOS C_{24-28} as surfactant formulations. Type III microemulsion was observed in all three surfactant formulation when the salinity was in the ranges of 6-6.5, 4.3-5.0 and 3.3-4.0 gNaCl/100 mL, respectively as seen in Figure 4.3. The optimal saliny observed in crude oil correlated with the results in the system of hexadecane as an oil phase because the crude oil mostly consists of long chain hydrocarbons. Therefore, the hydrophobicity of oil phase might balance with the hydrophilicity of all three surfactant formulations.

(a)

(b)

(c)
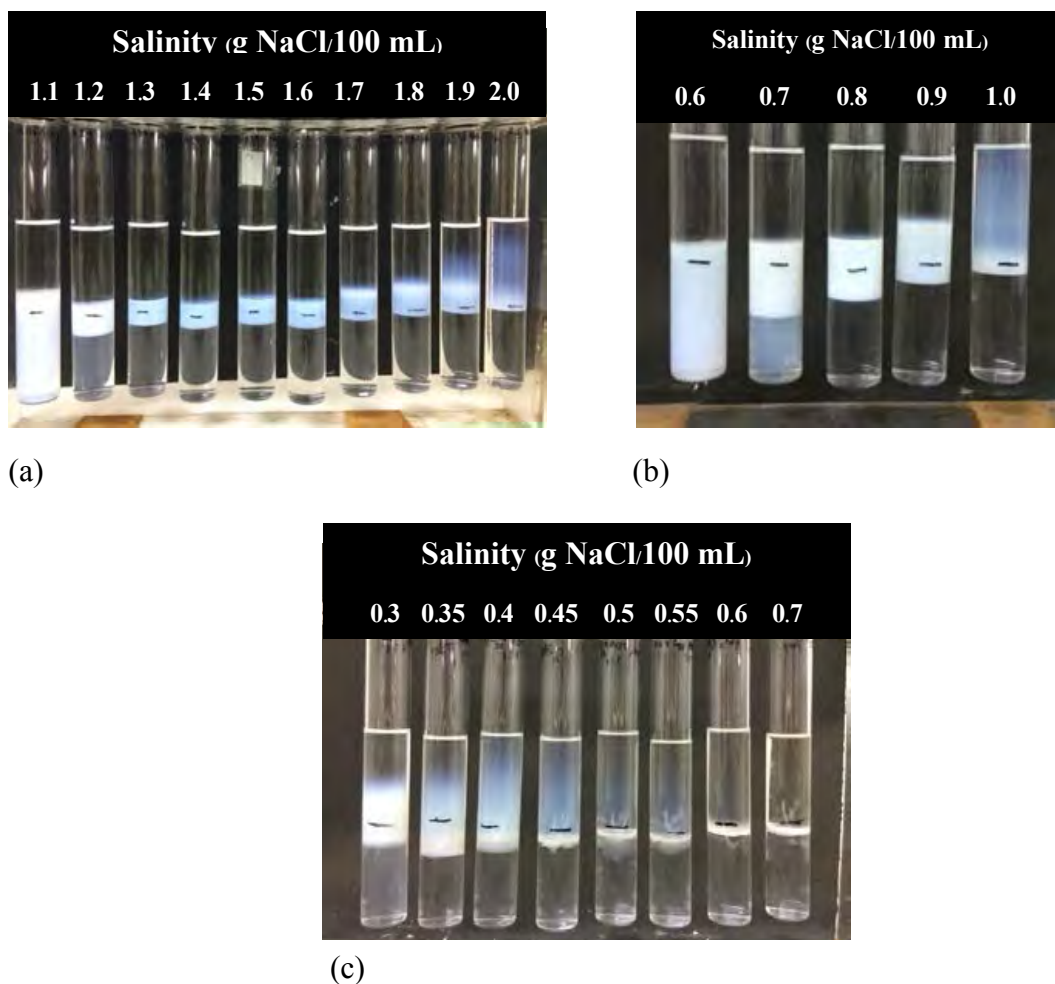
Figure 4.1 Phase behavior of 1:1 volume ratio of **(a)** AOT:IOS C_{15-18} **(b)** AOT:IOS C_{19-23} and **(c)** AOT:IOS C_{24-28} using heptane as an oil phase.

Salinity (gNaCl/100mL)

5.0 5.2 5.4 5.6 5.8 6.0 6.2 6.4

(a)

Salinity (g NaCl/100 mL)

1.8 1.9 2.0 2.1 2.3 2.5 2.7

(b)

Salinity (gNaCl/100mL)

0.8 0.9 1.0 1.1 1.2 1.3

(c)
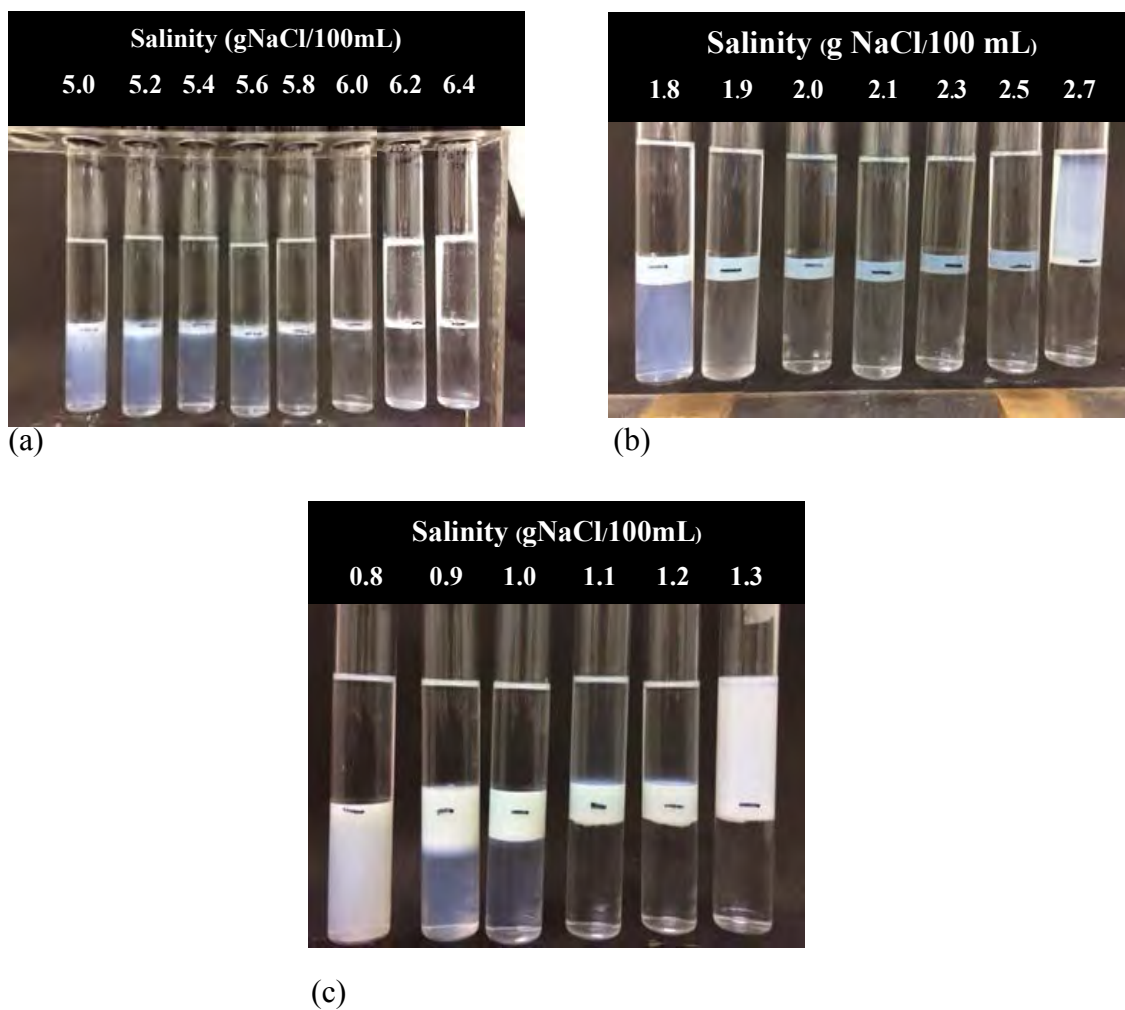
Figure 4.2 Phase behavior of 1:1 volume ratio of (a) AOT:IOS $C_{15\text{-}18}$ (b) AOT:IOS $C_{19\text{-}23}$ and (c) AOT:IOS $C_{24\text{-}28}$ using hexadecane as an oil phase.

As seen in Figures 4.1(a), 4.1(b), 4.2(a) and 4.2(b), both AOT:$C_{15\text{-}18}$ and AOT:$C_{19\text{-}23}$ generated Type III microemulsion in both heptane and hexadecane. It was observed that the middle phase region in heptane as an oil phase was thicker than the systems of hexadecane as an oil phase. This may indicate that the surfactant molecules had stronger interaction with shorter hydrophobic tail of the oil phase. Consequently, more surfactants solubilize in the oil phase.
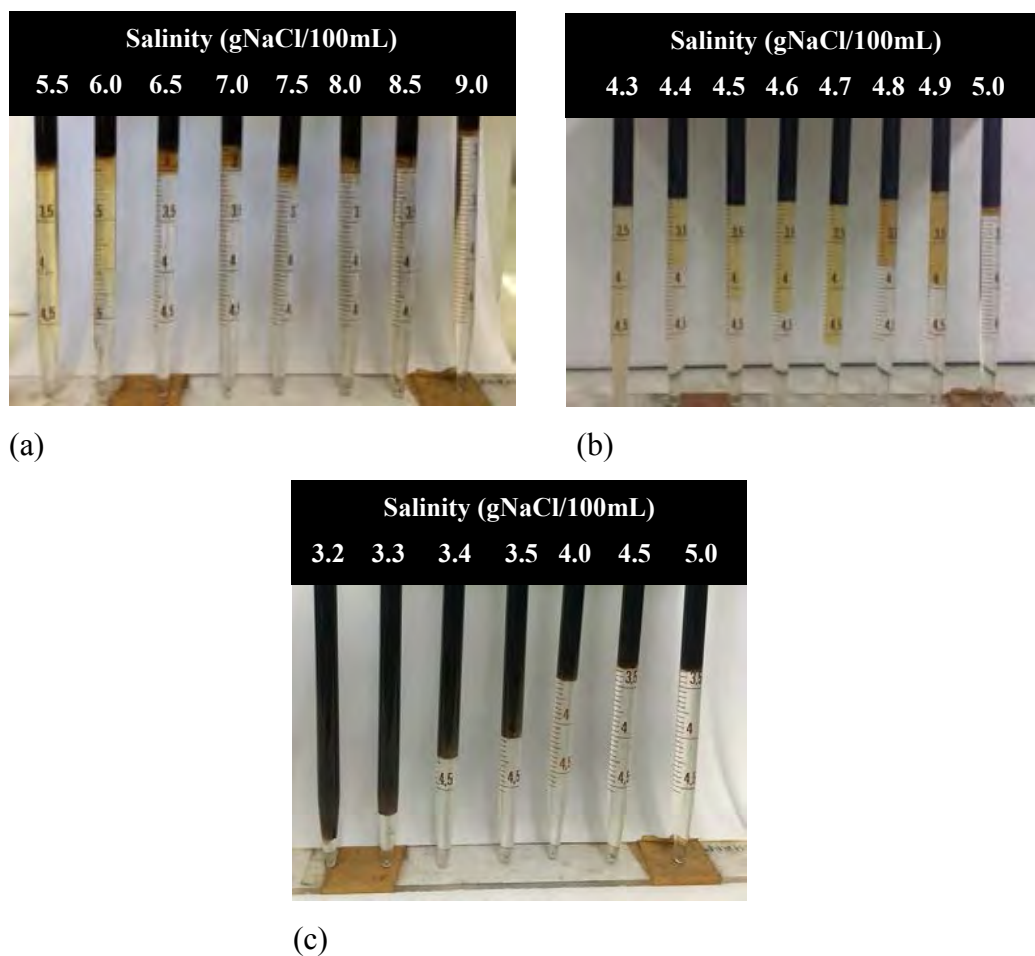
Figure 4.3 Phase behavior of 1:1 volume ratio of (a) AOT:IOS $C_{15\text{-}18}$ (b) AOT:IOS $C_{19\text{-}23}$ and (c) AOT:IOS $C_{24\text{-}28}$ using crude oil as an oil phase.

Type III middle phase microemulsion of crude oil system was observed from the opaque and thicker phase in both AOT:IOS $C_{15\text{-}18}$ (see Figure 4.3a) and AOT:IOS $C_{19\text{-}23}$ (see Figure 4.3b). The opaque phase was clearly seen when observed under the flashlight in all formulation, especially in AOT:IOS $C_{24\text{-}28}$ (see Figure 4.3c), confirming the formation of Type III middle phase. The opaque and thicker phase was the result from variety of oil components such as benzene, alkenes, alkanes and others. The crude oil was viscous and cannot flow at room temperature. Consequently, the sand pack column with ambient temperature and atmospheric pressure was not appropriate with the crude oil systems. The oil recovery efficiency was not investigated in this study.

4.1.3 Equlibrium Interfacial Tension Measurement

Table 4.3 IFT values and coalescence rate of various salinity in each surfactant solution

Surfactant solution	Alkane (Oil phase)	Salinity (g NaCl/100mL)	IFT values (mN/m)	Coalescence time
1:1 AOT:IOS C$_{15-18}$	Heptane	1.3	0.00473	3hr 55min
		1.4	0.00349	1hr 8min
		1.5	0.00362	21hr22min
		1.6	0.00159	23 min
		1.7	0.00351	5hr 15min
1:1 AOT:IOS C$_{19-23}$	Heptane	0.7	0.00499	> 24 hr
		0.8	0.00129	4hr 28min
		0.9	0.00569	> 24 hr
1:1 AOT:IOS C$_{24-28}$	Heptane	-	-	-
1:1 AOT:IOS C$_{15-18}$	Hexadecane	5.4	0.07827	> 24 hr
		5.6	0.01581	> 24 hr
		5.8	0.00937	> 24 hr
		6.0	0.01343	> 24 hr
		6.2	0.00590	> 24 hr
		6.4	0.00810	> 24 hr
1:1 AOT:IOS C$_{19-23}$	Hexadecane	1.8	-	> 24 hr
		1.9	0.01265	> 24 hr
		2.0	0.01315	> 24 hr
		2.1	0.00471	6hr 38min
		2.3	0.00201	6hr 30min
		2.5	0.00507	12hr40min
		2.7	-	> 24 hr

Table 4.3 IFT values and coalescence rate of various salinity in each surfactant solution (continued)

Surfactant solution	Alkane (Oil phase)	Salinity (g NaCl/100mL)	IFT values (mN/m)	Coalescence time
1:1 AOT:IOS C_{24-28}	Hexadecane	0.9	0.00773	23hr 36min
		1.0	0.00759	> 24 hr
		1.1	0.00537	23hr 13 min
		1.2	0.00150	9hr 50min
		1.3	0.00691	> 24 hr

Moreover, the optimum salinity was verified by the lowest coalescence rate and the lowest interfacial tension (10^{-3} mN/m) from IFT measurements as shown in Table 4.3. AOT:C_{15-18} reached equilibrium with the shortest time when compared with other surfactants in the systems of heptane as an oil phase. The experimental optimum salinity was selected by the lowest coalescence rate and minimum interfacial tension.

Table 4.4 Comparison between experimental and predicted optimum salinity

Mixed surfactant	Alkane (Oil phase)	Minimum IFT (mN/m)	Predicted S^*_{mix} (g NaCl/100mL)	Experimental S^*_{mix} (g NaCl/100mL)
1:1 AOT:IOS C_{15-18}	Heptane	0.00159	2.1	1.6
1:1 AOT:IOS C_{19-23}	Heptane	0.00129	1.6	0.8
1:1 AOT:IOS C_{24-28}	Heptane	-	1.2	-

Table 4.4   Comparison between experimental and predicted optimum salinity (continued)

Mixed surfactant	Alkane (Oil phase)	Minimum IFT (mN/m)	Predicted S^*_{mix} (g NaCl/100mL)	Experimental S^*_{mix} (g NaCl/100mL)
1:1 AOT:IOS C_{15-18}	Hexadecane	0.00937	6.6	6.2
1:1 AOT:IOS C_{19-23}	Hexadecane	0.00201	5.8	2.3
1:1 AOT:IOS C_{24-28}	Hexadecane	0.00150	4.4	1.2

It is observed from Table 4.4 that the optimum salinity from the experiment was lower than the predicted HLD equation because of a synergism in the mixed surfactant system. Sodium dioctylsulfosuccinate (AOT) is considered as an unconventional surfactant with twin-tails C_8 sulfosuccinate. Furthermore, the internal olefin sulfonates are muticomponent mixtures with various species of sulfonates.

Table 4.5 IFT values of various salinity in each surfactant solution with crude oil

Surfactant solution	Oil phase	Salinity (g NaCl/100mL)	IFT values (mN/m)
1:1 AOT:IOS C_{15-18}	Crude oil	6.5	0.10671
		7.0	0.13750
		7.5	0.16453
		8.0	0.17117
		8.5	0.11104

Table 4.5 IFT values of various salinity in each surfactant solution with crude oil (continued)

Surfactant solution	Oil phase	Salinity (g NaCl/100mL)	IFT values (mN/m)
1:1 AOT:IOS C_{19-23}	Crude oil	4.3	0.01469
		4.4	0.00871
		4.5	0.01258
		4.6	0.01340
		4.7	0.01501
		4.8	0.01623
		4.9	0.01623
		5.0	0.01756
1:1 AOT:IOS C_{24-28}	Crude oil	3.1	0.00343
		3.2	0.00265
		3.3	0.01000
		3.4	0.00784
		3.5	0.01073
		4.0	0.04215
		4.5	0.02296
		5.0	0.07226

Table 4.6 Summary of the optimum salinity in crude oil systems

Mixed surfactant	Oil phase	Minimum IFT value (mN/m)	Optimum salinity (g NaCl/100mL)
1:1 AOT:IOS C_{15-18}		0.10671	6.5
1:1 AOT:IOS C_{19-23}	Crude oil	0.00871	4.4
1:1 AOT:IOS C_{24-28}		0.00265	3.2

The lowest interfacial tension of crude oil systems can reach 10^{-3} mN/m as indicated in Table 4.6. It is illustrated that the IFT value decreased with longer carbon chain length of IOS. The results related with the alkane systems (as see Table 4.4). The larger degree of hydrophobicity from surfactant tend to reduce the IFT due to high surface activity (Bera *et al.*, 2016).

4.1.4 Preliminary Foam Stability Test

The optimum formulation from phase behavior experiments and equilibrium interfacial tension measurement was prepared in vials for testing. The initial screening of foam stability was conducted in presence of both heptane and hexadecane. Half-life is defined as the time taken when half of the liquid was drained from the foam (Duan *et al.*, 2014) as see Table 4.7.

Table 4.7 The half-life time of surfactant solution at optimum salinity in presence of alkanes

Mixed surfactant	Alkane (Oil phase)	Optimum salinity (g NaCl/100mL)	Half-life (min)
1:1 AOT:IOS C_{15-18}	Heptane	1.6	67±35.6
1:1 AOT:IOS C_{19-23}	Heptane	0.8	51.3±46

Table 4.7 The half-life time of surfactant solution at optimum salinity in presence of alkanes (continued)

Mixed surfactant	Alkane (Oil phase)	Optimum salinity (g NaCl/100mL)	Half-life (min)
1:1 AOT:IOS C_{15-18}	Hexadecane	6.2	Surfactant precipitation
1:1 AOT:IOS C_{19-23}	Hexadecane	2.3	8.2±2.8
1:1 AOT:IOS C_{24-28}	Hexadecane	1.2	9.8±1.3

The foam properties of mixed surfactant systems were investigated in the presence of alkanes with different carbon chain lengths, namely heptane and hexadecane. The total surfactant concentration was fixed at 0.03 M. The result showed that half-life in the presence of heptane was approximately five times greater than that in presence of hexadecane. This study contradicted with the observation reported by Simjoo *et al.* (2013) since in their study the shorter carbon chain length of the alkane gave the low foam stability due to the higher tendency of oil solubilization in micelles causing reduction of repulsive forces between micelles. Hence, the foam was faster destabilized in short chain alkane. However, our result was supported by the observation of Meling *et al.* (1990) and Aveyard *et al.* (1994). Furthermore, foam properties by varying alkyl chain length of surfactant was investigated by Wang *et al.* (2017) and Sansen *et al.* (2015). They showed that foamability and foam stability decreased with longer alkyl chain length or higher hydrophobicity of the surfactants in both alpha olefin sulfonates (AOS) and internal olefin sulfonates (IOS). It was illustrated that surfactants with long alkyl chain length represent lower water solubilization due to stronger tail-tail interaction, resulting in low foamability and weak air-water interaction at the interface. This observation was quite well agreed with the results in the presence of heptane but not obvious in presence of hexadecane because the high deviation of half-life by preliminary screening in the vial test.

In addition, the foam stability in porous media will be further investigated by the mobility reduction factor (MRF) in section 4.2.3.

4.2 Sand Pack Oil Recovery Experiments

4.2.1 Effect of Surfactant Slug Size

This experiment was conducted with AOT:IOS C_{15-18} and heptane. The sand pack column was preflushed with 3% NaCl brine solution. A 40.0-56.4 %S_{oi} (initial oil saturation) was measured after displacing the injected brine with heptane as an oil phase. The column was brine flooded with the respective optimum salinity condition at the initial stage, then injected surfactant solution with absence and presence of N_2 for surfactant and foam flooding, respectively. The injection volume was compared between 1 PV and 3 PV. Finally, the column was post-flushed with the brine solution at the respective optimum salinity until no more oil was further recovered.
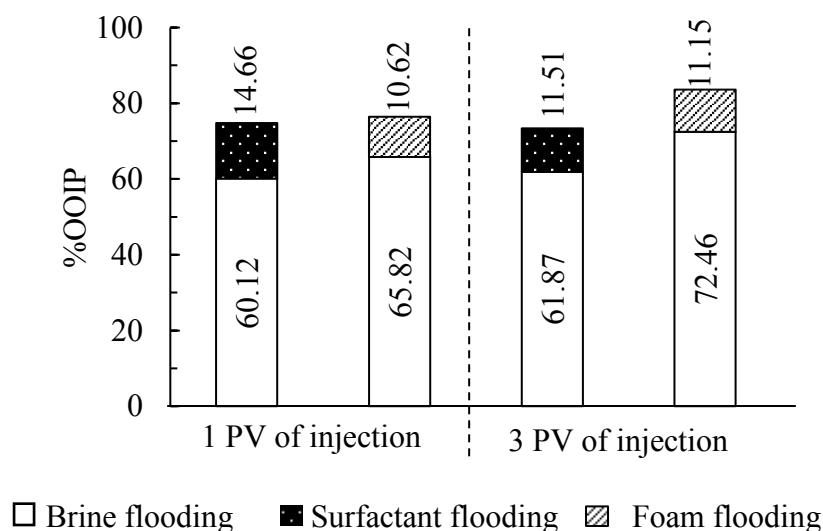
Figure 4.4 Summary total oil recovery of AOT and IOS C_{15-18} with heptane for different surfactant slug size in surfactant and foam flooding.
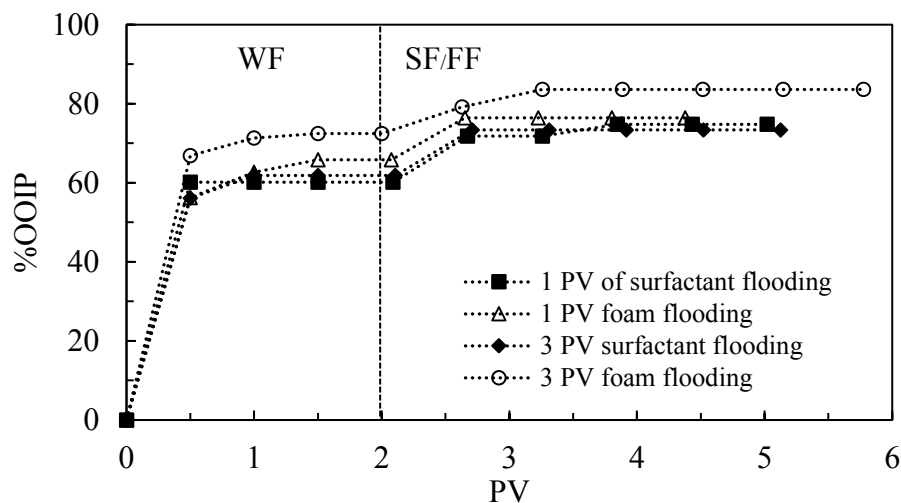
Figure 4.5 Accumulative oil recovery of AOT and IOS C_{15-18} with heptane for different surfactant slug size in surfactant and foam flooding.

The results in Figure 4.5 showed that the additional oil recovery after injecting 1 PV or 3 PV in both surfactant and foam flooding were comparable. Hence, 1 PV of surfactant or foam slug was sufficient to inject the costly surfactant solution and achieving similar maximum oil recovery (>70%). Consequently, Injecting 1 PV of surfactant slug reduced the surfactant usage for more economical surfactant or foam flooding. The result was in good agreement with the work from Zhang *et al.* (2014). They investigated the enhanced oil recovery by varying foam injection rate. The final oil recovery by injecting 0.4 PV foam was slightly higher than injecting 0.3 PV foam, thus they suggested that the proper amount of foam injection was 0.3 PV to minimize the surfactant cost.

4.2.2 Effect of Salinity

The purpose of this study was to investigate the effect of salinity to the amount of additional oil recovery. Since an optimal salinity, where Type III microemulsion was formed, has been suggested to ensure maximum solubilization between the water-oil interfaces performed by the surfactant. From the phase equilibria experiment, the optimum salinity of AOT:IOS C_{15-18} in heptane was 1.6 g NaCl/100mL. To investigate the effect of salinity, the brine solution was diluted 10 times or one order of magnitude from the optimum salinity. Therefore, the surfactant and foam flooding with 0.16 and 1.6 g NaCl/100mL was investigated and the amount of oil recovery was compared.
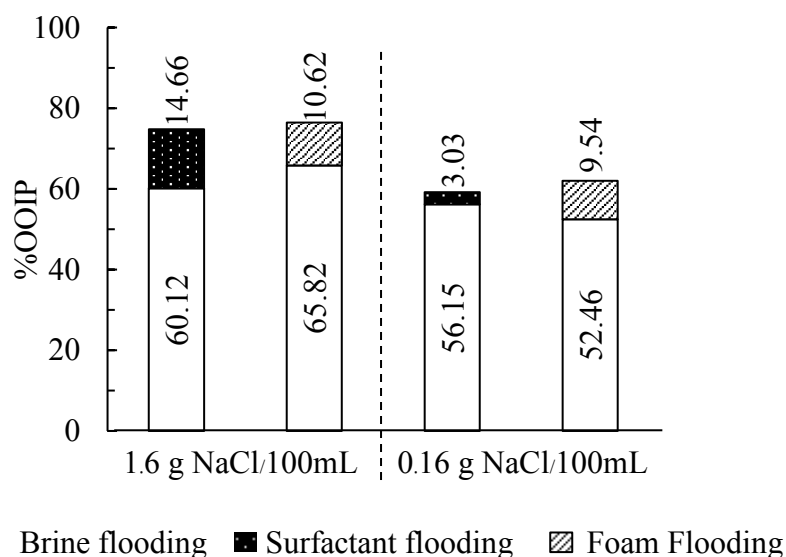
Figure 4.6 Summary total oil recovery of AOT and IOS C_{15-18} with heptane at optimum salinity and dilute condition by surfactant and foam flooding.

According to Figure 4.6, it is indicated that surfactant flooding with the optimum salinity (HLD=0) can additionally recover more oil than the system with lower salinity (HLD<0) because type III microemulsion behavior played a key role in oil solubilization. Bera *et al.* (2014) employed phase behavior experiments and found that the optimum salinity when NaCl was used to formulate brine. They conducted microemulsion flooding in a sand pack column with three different salinity; lower than the optimum salinity, at optimum salinity and at higher than optimum salinity. The additional oil recovery by microemulsion flooding was observed to be highest at the optimum salinity. If the IFT between oil and water was low enough, trapped oil attached to the water-wet sand was emulsified and could be push forward. This means that more oil could be solubilized, resulting in an improvement of both vertical and sectional sweep efficiency.

In the foam systems, there was no difference in the additional oil recovery between optimum salinity (HLD=0) and lower salinity (HLD<0) in foam flooding because foam helped increase sweep efficiency whether microemulsion was formed or not (see Figure 4.6). Although foam was generally collapse with increasing salinity because of weakening in electrostatic double layer forces or lowering the water solubilization of surfactant, some anionic surfactants represented good foaming properties at various salinity conditions (Farzaneh *et al.*, 2013). Liu *et al.* (2005) used Chaser CD 1045 in CO_2 foam which is a type of anionic surfactant. When CD concentration was high enough, the foam was stable and insensitive to salinity because of low foam collapse by gravity drainage.

Comparing the surfactant flooding and foam flooding at the optimal salinity, the surfactant flooding could recover more oil (14.66 % OOIP v.s. 10.62 % OOIP in surfactant and foam flooding, respectively). However, in system of lower salinity (HLD<0), foam flooding can recover more oil than the surfactant flooding (3.03 % OOIP v.s. 9.54 % OOIP in surfactant and foam flooding, respectively). Hence, foam flooding can generally gave high oil recovery in both conditions at both optimum salinity and low salinity conditions.

4.2.3 <u>Oil Recovery at Optimum Salinity</u>

The surfactant and foam flooding were conducted to estimate the oil recovery in the silica sand pack column. The binary mixtures between AOT with three different carbon chain length IOS surfactants; C_{15-18}, C_{19-23} and C_{24-28} at 1:1 volume ratio were used to evaluate the amount of tertiary oil recovery after the brine flooding has been exhausted. Heptane or hexadecane was used as an oil phase. In addition, The oil recovery efficiency was evaluated and compared between surfactant and foam flooding. In all experiment, a dry packing was used as the sand packing method. The sand pack column was preflushed with 3% NaCl solution to measure pore volume, porosity and permeability. The brine concentration in the preflush step was kept constant at 3% NaCl in all runs to ensure the same sand condition of all experiments. The oil phase was then injected in the sandpack column until the first drop of oil appeared on the exit side of the sandpack column and the total amount of oil was called the original oil in place (OOIP). The initial oil saturation ($\%S_{oi}$) was calculated as the ratio of OOIP and the total pore volume. The average sandpack properties are shown in Table 4.8.

Table 4.8 Silica sand pack properties

Property (Unit)	Average Value
Column diameter (cm)	2.5
Sand height (inch)	3
Type of sand	Silica sand
Particle size (μm)	200-300
Pore volume (mL)	16.8±0.6
Porosity (%)	41.4±1.3
Permeability (mD)	640±93
Initial Oil Saturation ($\%S_{oi}$)	54.0±11.3
%OOIP by brine flooding	58.6±10.0

In the secondary oil recovery, the brine solution at optimum salinity, i.e. the optimal brine concentration to form Type III middle phase microemulsion as determined from the phase behavior and IFT measurements, was flooded into the sand pack. The amount of oil recovery was determined by the volume of oil in the effluents collected in the fractional sample collector. The effluent was collected every 0.5 PV untill the termination of brine flooding. If oil was displaced less than 1% of each 0.5 PV in the sample collector, the injection of salt solution was stopped and the secondary oil recovery was considered exhausted. Typically 2 PV of brine flooding was performed in all runs except AOT:IOS C_{15-18} with hexadecane system when 5 PV of brine flooding was performed until the oil recovery by brine flooding was exhausted. The optimum salinity from the microemulsion phase study of the AOT:IOS C_{15-18} with hexadecane system was 6.2 gNaCl/100mL, which was the highest salinity obtained from all SOW systems in this study. Mohammad Salehi *et al.* (2017) observed that when increasing the salinity of brine used in the brine flooding step, oil recovery increased due to lowering IFT and increasing water viscosity. Reducing IFT increased water-oil interaction by increasing the capillary number of the displacing fluid and overcome the high capillary force of the oil-reservoir rock. Hence, it is not uncommon to observe a higher oil recovery when using higher brine concentration in the brine flooding step. However, high brine concentration may cause another effect and could limit the use of the proposed surfactant system. It was observed that precipitation occurred in the system of AOT:IOS C_{15-18} when the optimum salinity of 6.2 gNaCl/100mL was prepared without an oil phase (see Figure 4.7). Sand pack experiments could not be done at this high brine concentration. Therefore, the optimum salinity was shifted by lowering the salinity until no surfactant precipitation as seen in Figure 4.8. The results shown that the mixtures with 5.4 gNaCl/100mL was clear and no surfactant retention which was suitable for injecting in the sand pack experiments. To run the sand pack experiments of this specific system, salinity was then dropped to 5.4 gNaCl/100mL. Although this condition did not give the lowest IFT, the SOW system still formed middle phase microemulsion as shown in Figure 4.2a. The oil recovery in sand pack column of this formulation was conducted in Appendix C.
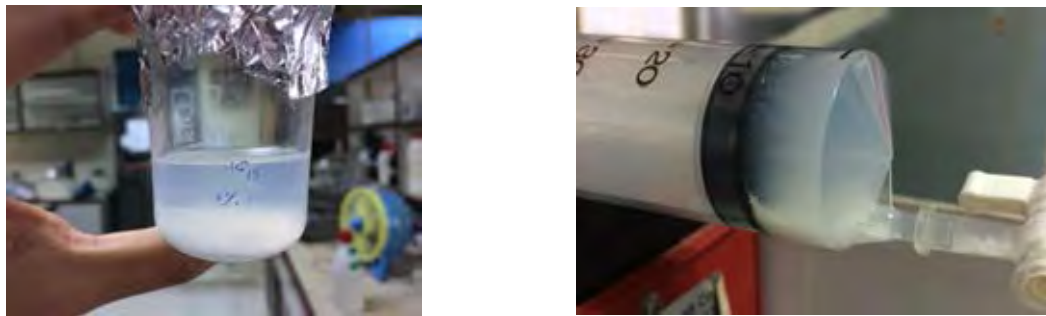
(a)   (b)

Figure 4.7 The surfactant precipitation with 6.2 gNaCl/100mL (a) Solution in beaker (b) Solution in the syringe.
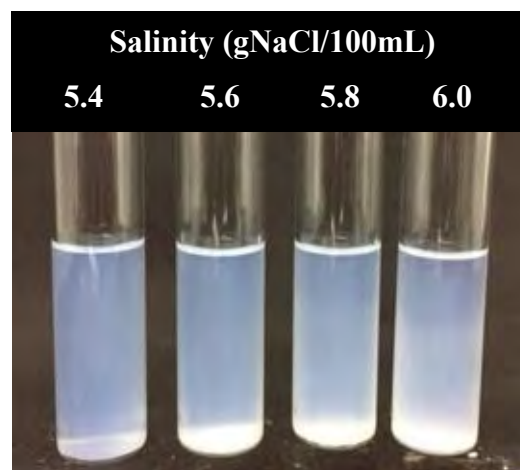
Figure 4.8 The precipitation testing mixtures between 1:1 AOT:IOS C_{15-18} and various salinity.

Approximately 53.2-65.4 %OOIP were recovered by 2 PV of brine flooding as observed in Figure 4.9. Due to water-wet property or high hydrophilicity of the silica sand, the high oil volume was displaced from the column by brine flooding, corresponding to high average porosity (~41%) and permeability (~640 mD) of silica sand.

High oil recovery from brine flooding was also observed in the work of Torabi *et al.* (2010) with an oil recovery of 48-52 %OOIP in a sand pack experiment and in the study of Hosseini-Nasab *et al.* (2017) with an oil recovery of 43 %OOIP. The fluctuation of displaced oil by brine flooding may be misleading in a comparison of the efficiency of chemical/method of enhanced oil recovery. The more oil was recovered in the water flooding step, the less amount of oil left in the sand pack and resulted in less amount of oil recovered in the enhanced oil recovery step. The incremental oil recovery by surfactant and foam flooding were investigated as explained in the next section**.**
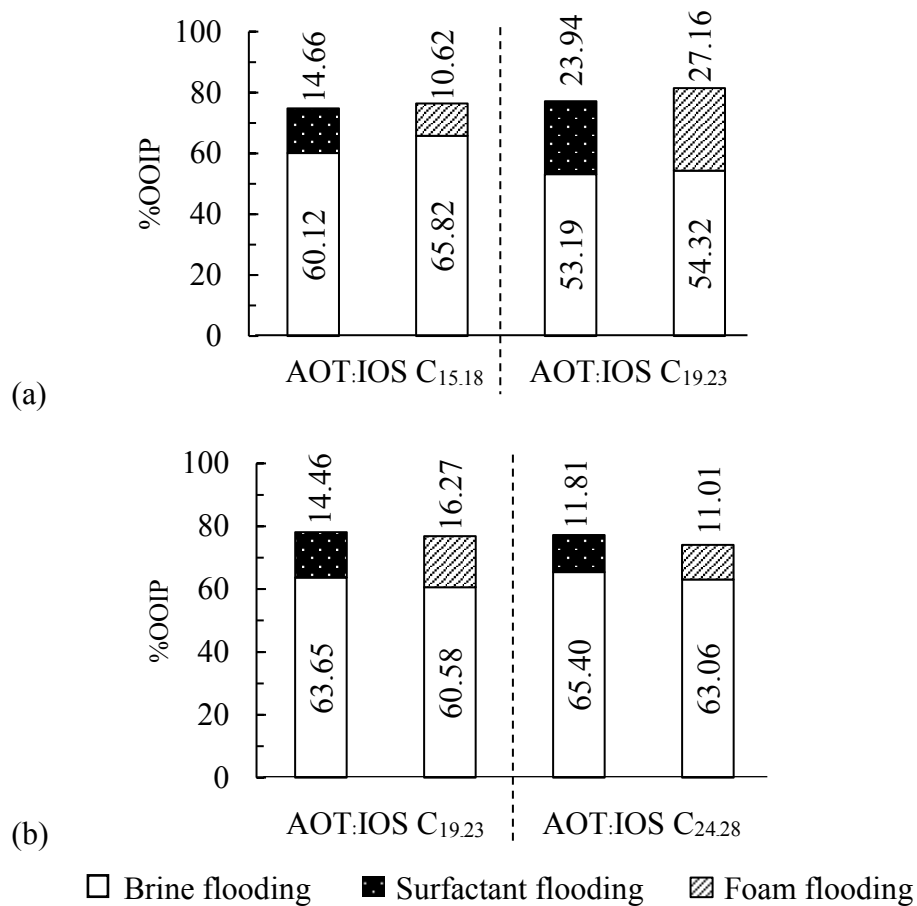
Figure 4.9 Summary total oil recovery of AOT and IOS with different carbon chain length at optimum salinity by surfactant and foam flooding in (a) heptane and (b) hexadecane as an oil phase.

4.2.3.1 Tertiary oil recovery using heptane as an oil phase
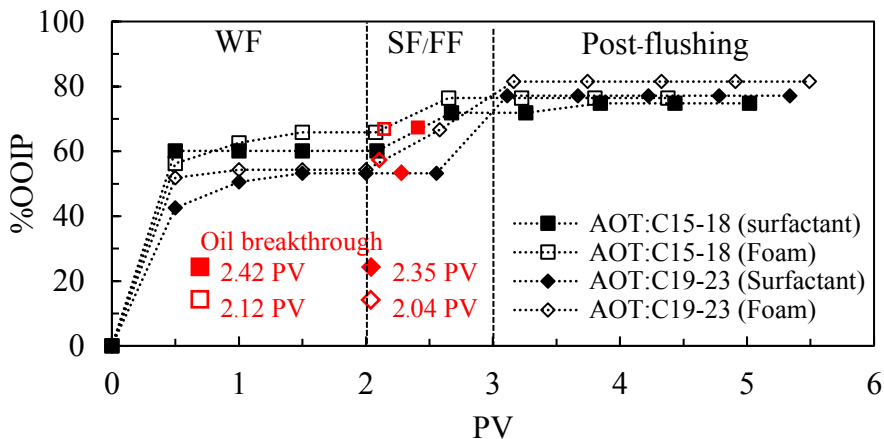
Figure 4.10 Accumulative oil recovery by surfactant and foam flooding in heptane.
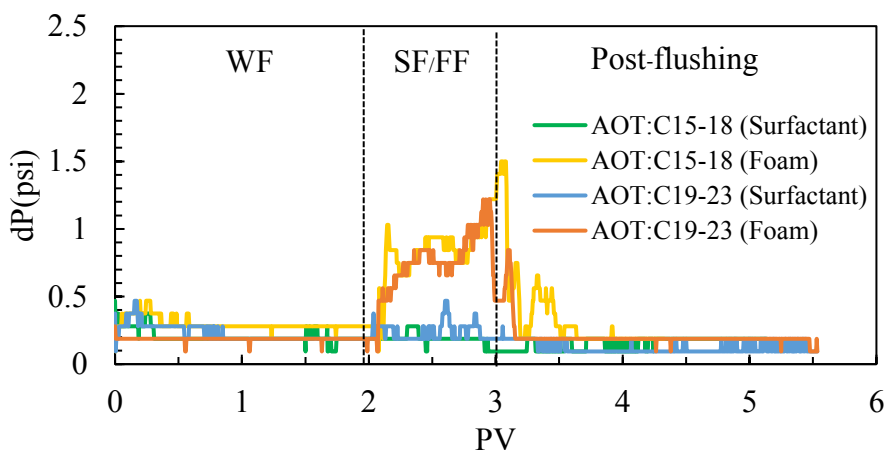
Figure 4.11 Variation of pressure drop across the sand pack column at different flooding conditions using an optimum formulation in AOT:C$_{15-18}$ and AOT:C$_{19-23}$ when heptane was used as an oil phase.

Heptane was used as an oil phase in this experiment. The tertiary oil recovery was performed after the brine flooding had been exhausted. At this surfactant flooding step, 1 PV of a surfactant slug was introduced into the sand pack column, following by brine flooding. Oil breakthrough occured at around 2.4 PV or after 0.4 PV of injected surfactant slug in both AOT:IOS C$_{15-18}$ and AOT:C$_{19-23}$ as shown in Figure 4.10.

Comparing the same surfactant formulation, the oil breakthrough in foam flooding occured a little earlier than that of the surfactant flooding in both surfactant formulations. In post flushing step, the recovered oil was slightly increased and finally exhausted. The trapped oil was additionally displaced after flooding with surfactant solution in both forms of surfactant and foam slugs because of the ability to alter the surface activities by lowering the oil/water interfacial tension.

In surfactant flooding, approximately 14.7-23.9 %OOIP was additionally recovered by a surfactant slug as indicated using solid symbols in Figure 4.9, giving a total oil recovery of 74.8-77.1 %OOIP when combining the secondary and tertiary oil recovery processes. It is noted that the differential pressure during 1 PV surfactant slug was fairly constant around 0.2-0.3 psi in the runs with surfactant flooding for the entire experiment from the brine flooding, surfactant flooding and post-flushing in both AOT:IOS C_{15-18} and AOT:IOS C_{19-23}.

For foam flooding, approximately 10.6-27.2 %OOIP of trapped oil was additionally displaced after flooding by foam for 1 PV. The total oil recovery of 76.4-81.5 %OOIP was observed after combining the secondary and tertialry oil recovery. Foam was generated as evidenced from the high fluctuation of differential pressure in the sandpack column as shown in Figure 4.11. Foam stability in porous media was observed by the mobility reduction factor (MRF). The differential pressure along 1 PV of surfactant or foam slug was divided by the average differential pressure of brine flooding step. It is remarked that the MRF of surfactant flooding was used as the baseline for comparing (see Figure 4.12).
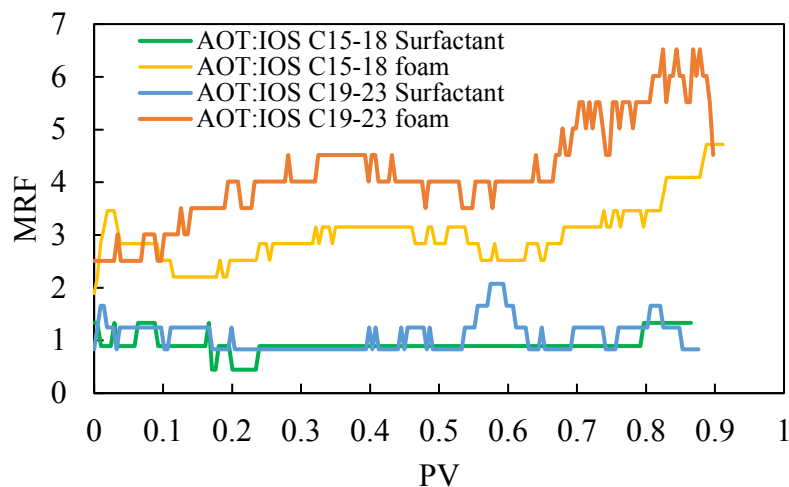
Figure 4.12 Plotting between the mobility reduction factor (MRF) versus pore volume of surfactant or foam slug injection in presence of heptane.

The resistance factor of foam flooding was twice higher than surfactant flooding in both AOT:IOS C_{15-18} and AOT:IOS C_{19-23} in heptane was used as an oil phase. The half-life from preliminary screening was 67 ± 35.6 and 51.3 ± 46 minutes for AOT:IOS C_{15-18} and AOT:IOS C_{19-23}, respectively, in the presence of heptane. The longevity of foam half-life was long enough for foam to propagate along the sand-pack column as the 1 PV injection of surfactant or foam slug took approximately 30-40 minutes until breakthrough the column. Consequently, the foam was generated along the injection due to high foam stability (>30 minutes).

The incremental oil recovery of AOT:IOS C_{19-23} was twice higher than AOT:IOS C_{15-18}, probably due to the low oil recovery during the brine flooding step. The oil breakthrough was observed at 2.1 PV or immmediately emerged after 0.1 PV of foam injection. The result emphasized the two great abilities of foam as (1) a mobility control to reduce channeling effect in reservoir by diverting injected fluid from relatively high to relatively low permeability zone, and (2) high sweep efficiency to remove more oil from the unreached zone in the reservoir. Figure 4.13 illustrated that the trapped oil bank was swept around 0.75 of foam slug.

After oil breakthrough, incremental oil can be recovered until plateau around 0.7 PV after foam injection by AOT:C_{15-18}, whereas AOT:C_{19-23} can futher displace oil untill steady in post flushing.
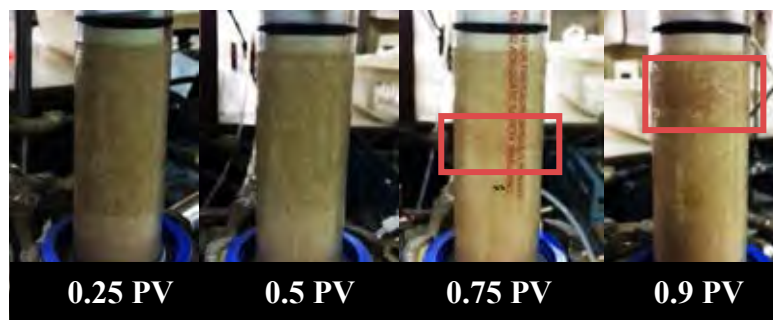
Figure 4.13 The column image in each pore volume of foam injection.

4.2.3.2 Tertiary oil recovery using hexadecane as an oil phase
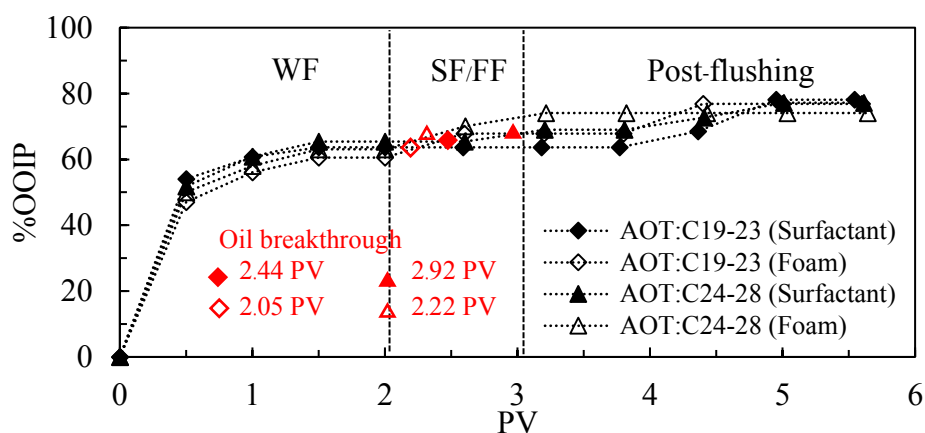
Figure 4.14 Accumulative oil recovery by surfactant and foam flooding of AOT:IOS C$_{19-23}$ and AOT:IOS C$_{24-28}$ using hexadecane as an oil phase.
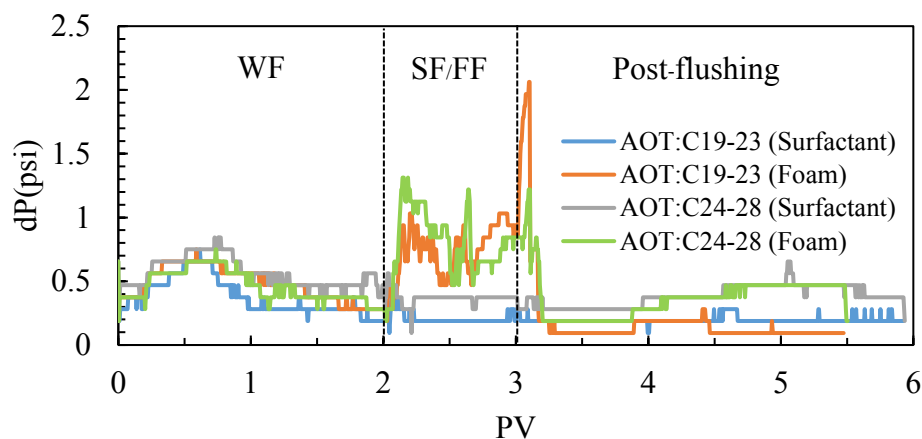
Figure 4.15 Variation of pressure drop across the sand pack column at different flooding conditions using an optimum formulation of AOT:IOS C$_{19-23}$ and AOT:IOS C$_{24-28}$ in hexadecane.

In the systems of hexadecane as an oil phase, the amount of oil recovery in term of %OOIP by surfactant and foam flooding was plotted with pore volume (PV) as presented in Figures 4.14. The trapped oil was pushed by 1 PV surfactant slug and the oil was additionally recovered at about 11.8-14.5 %OOIP, giving a total amount of recovered oil of 77.2-78.1 %OOIP in surfactant flooding of AOT:IOS C_{19-23} and AOT:IOS C_{24-28}. However, It has been found that oil began to break through when the injected volume of surfactant slug reached 0.4 PV and 0.9 PV in AOT:IOS C_{19-23} and AOT:IOS C_{24-28}, respectively, and slightly increased until no more oil was recovered in post flushing step. It was observed that more oil was recovered in the post-flushing in the surfactant flooding experiments, especially in the systems of AOT:IOS C_{19-23} and AOT:IOS C_{24-28} (see Figure 4.14 solid symbols). Since all experiments were performed at an optimal salinity of the respective surfactant formulation and the oil phase, the time to form type III microemulsion or the coalescence time plays an important role in these systems. According to Table 4.2 the systems with either long alkyl chain length surfactant or long chain hydrocarbon as an oil phase formed Type III microemulsion at long coalescene time. This observation may suggest a shut-in process after injecting 1 PV of a surfactant slug during the oil recovery process. This experiment is discussed in Section 4.2.4.

In foam flooding, the additional oil recovery after the brine flooding was 11-16.3 %OOIP as illustrated in Figure 4.9, giving a total oil recovery of 74.1-76.9 %OOIP in AOT:IOS C_{19-23} and AOT: IOS C_{24-28}. The evidence of foam generation in the porous media was confirmed by the increase in pressure drop due to the higher viscosity of foam as compared to liquid as illustrated in Figure 4.15 (Heins *et al.*, 2014). There are no significant difference in differential pressure profile between AOT:IOS C_{19-23} and AOT: IOS C_{24-28}. The half-life from preliminary screening was 8.2±2.8 and 9.8±1.3 minutes for AOT:IOS C_{19-23} and AOT:IOS C_{24-28}, respectively. The MRF was slightly difference between foam and surfactant flooding due to low foam stability (<10 minutes) in both AOT:IOS C_{19-23} and AOT:IOS C_{24-28} as shown in Figure 4.16. Hence, foam might be destabilized after injected into the column causing oil solubilization of surfactant to play a key role in oil recovery.
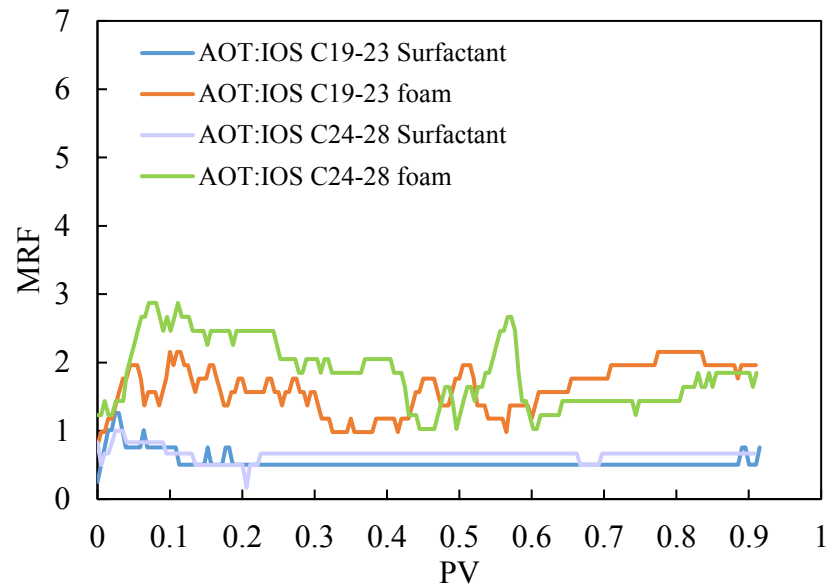
Figure 4.16 Plotting between the mobility reduction factor (MRF) versus pore volume of surfactant or foam slug injection in presence of heptane.

Comparing.between heptane and hexadecane as an oil phase, the mobility reduction factor (MRF) in the system of heptane (see Figure 4.12) was relatively higher than the system of hexadecane (see Figures 4.16) as an oil phase. This may indicate that the longer chain hydrocarbon had a higher tendency to cause foam collapse as compared to the shorter chain hydrocarbon. Furthermore, the oil breakthrough in the system of AOT:IOS C_{19-23} foam occured at 2 PV or suddenly after the coinjection of surfactant slug with N_2 while the oil breakthrough by the system of AOT:IOS C_{24-28} foam occured at 2.2 PV.

4.2.4 Effect of Shut In

From Table 4.3, it was observed that Type III middle phase microemulsion of the formulations with both heptane and hexadecane as an oil phase were generated with various coalescence times from an hour to a few days (>24 hr). This means that these surfactant formulations needed more contact time to reach the equilibrium with trapped oil in the sand pack column. Therefore, 24 hour-shut in operation was conducted after 1 PV of surfactant slug injection in both surfactant and foam floodings.
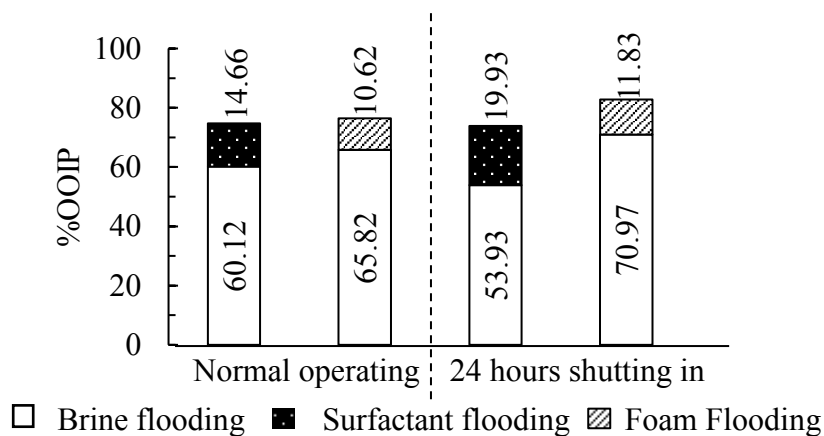
Figure 4.17 Summary total oil recovery of AOT and IOS $C_{15\text{-}18}$ with heptane for different operating condition in surfactant and foam flooding.
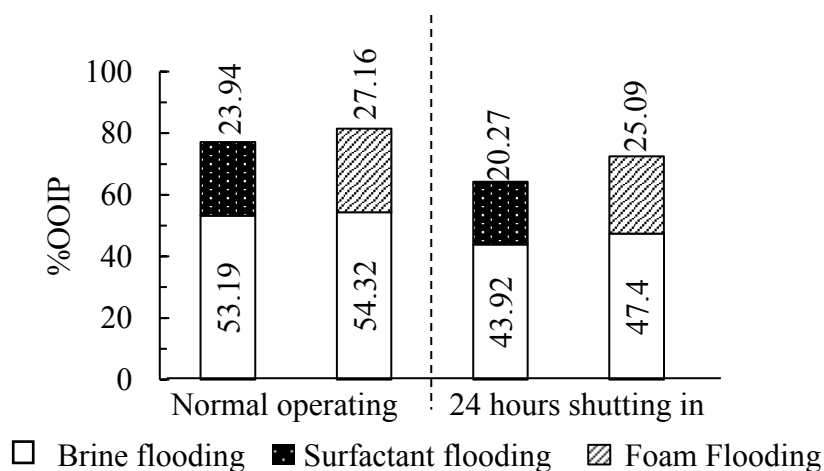
Figure 4.18 Summary total oil recovery of AOT and IOS $C_{19\text{-}23}$ with heptane for different operating condition in surfactant and foam flooding.
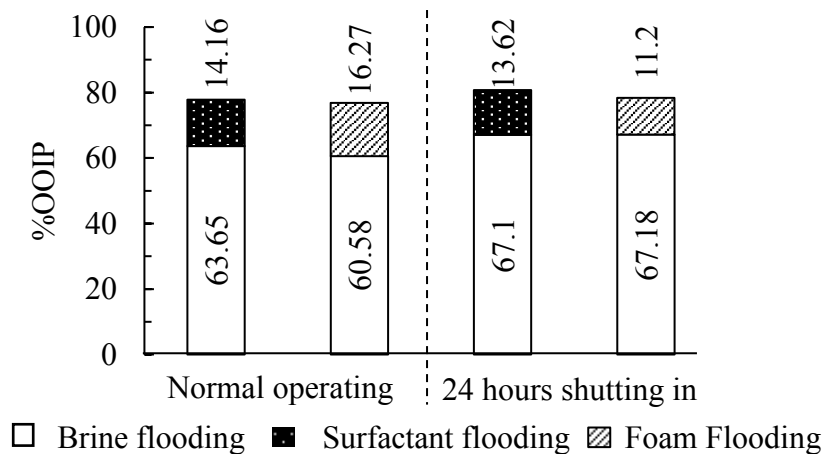
Figure 4.19 Summary total oil recovery of AOT and IOS $C_{19\text{-}23}$ with hexadecane for different operating condition in surfactant and foam flooding.
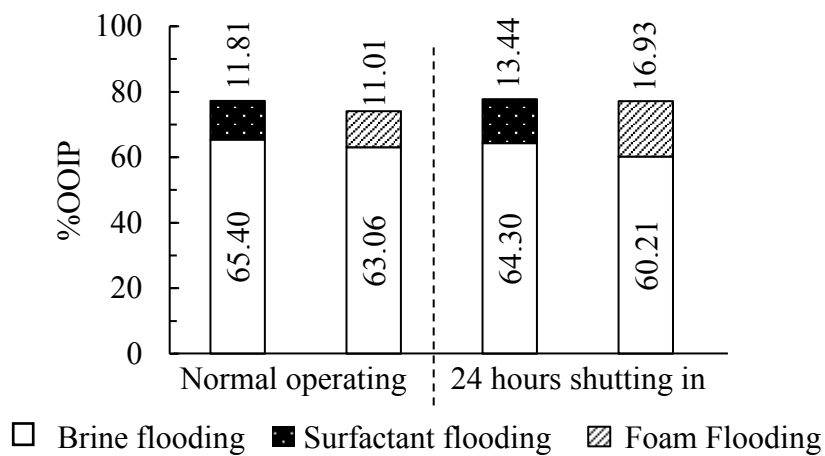
Figure 4.20 Summary total oil recovery of AOT and IOS $C_{24\text{-}28}$ with hexadecane for different operating condition in surfactant and foam flooding.

As seen in Figures 4.17 to 4.20, the shut in operations can slightly recover more oil (1 to 5 %OOIP) than normal operations except AOT:IOS C_{19-23} with both heptane and hexadecane as seen in Figure 4.18 and 4.19. It is worth noting that additional of 4-7% OOIP was recovered in the brine flooding step from the normal operation (no shut-in) as compared to the shut-in operation in the system of AOT:IOS C_{19-23}. Nevertheless, it is obviously revealed that the 24-hr shut in operation after surfactant injection can improve the additional oil recovery in both surfactant and foam flooding because it allowed sufficient time for surfactants to form the Type III microemulsion. Equilibrium between aqueous phase and oil phase in sand pack column was reached within the coalescence time, and thus the middle phase was additionally generated in sand pack during shut in. The shut in operation also helped in the foam flooding. Although foam might be collapsed during the 24-hr shut in, the surfactant solution still can form Type III microemulsion with the oil phase; hence, more oil was solubilized and recovered.

CHAPTER V
CONCLUSIONS AND RECOMMENDATIONS

5.1 Conclusions

The mixed surfactants between AOT and three different carbon chain length IOS (IOS C_{15-18}, IOS C_{19-23} and IOS C_{24-28}) was prepared at 1:1 volume ratio and 0.03 M with various salt (NaCl) concentration through phase behavior experiments. The predicted optimum salinity was higher than the experiment because of a synergism in mixed surfactant system. Type III middle phase microemulsion can be generated with a wide range of optimum salinity between 0.8-6.2 and 3.2-6.5 gNaCl/100mL for alkanes and crude oil systems, respectively. All optimum formulation can reach the low interfacial tension (10^{-3} mN/m).

The optimum formulations with lowest IFT were injected in silica sand pack column to estimate the tertiary oil recovery. Heptane and hexadecane were introduced as an oil phase. 1 PV of surfactant or foam slug was sufficient to fulfill surfactant adsorption capacity and to reach the maximum oil recovery (>70%). Surfactant flooding with optimum salinity can recover more oil than lower salinity system while foam flooding gave high oil recovery in both conditions at optimum salinity and low salinity. High oil recovery (>10%) by surfactant flooding was obtained at the optimum salinity condition which Type III microemulsion behavior played a key role in oil solubilization. High oil recovery by foam flooding emphasized two great abilities, (1) A mobility control to reduce channeling effect in reservoir (2) high sweep efficiency to remove more oil from the unreached zone. Shutting in after surfactant injection for 24 hours can improve additional oil recovery in both surfactant and foam flooding.

5.2 Recommendations

Base on what has been discovered in this study, the following recommendations were suggested:

- The predicted HLD equation should be added the terms corresponding to synergism effect of mixed anionic surfactant.

- The silica sand used in this study was the water-wet with the size of 200-300 μm. Because the sand was water-wet, it cannot trap the oil well. When brine flooding was performed, the oil was removed easily, leaving only small amount of oil left in the sand. There was only very limited amount of oil during the surfactant and foam flooding.

- Aging process should be introduced after oil saturation step to increase the contact time between oil and sand.

- Increasing oil flowrate during oil saturation step to fulfill the void inside the column and identical initial oil saturation.

- Precipitation test should be done with the mixed surfactant formulation to avoid the precipitation of surfactant in the tested region of salt concentration.

- Static foam test should be conducted to lower the deviation of half-life.

- High temperature and pressure sand pack steel column might be conducted for crude oil systems to estimate incremental oil recovery by surfactant and foam flooding with the same optimum formulation as atmospheric pressure and ambient temperature sand pack column.

REFERENCES

Anton, R.E., Garces, N. and Yajure, A. (1997) A Correlation for Three-Phase Behavior of Cation1c Surfactant-Oil-Water Systems. Journal of Dispersion Science and Technology 18(5), 539-555.

Aveyard, R., Binks, B.P., Fletcher, P.D.I., Peck, T.G. and Rutherford, C.E. (1994) Aspects of aqueous foam stability in the presence of hydrocarbon oils and solid particles. Advances in Colloid and Interface Science 48, 93-120.

Bera, A. and Belhaj, H. (2016) Ionic liquids as alternatives of surfactants in enhanced oil recovery—A state-of-the-art review. Journal of Molecular Liquids 224, 177-188.

Bera, A., Kumar, T., Ojha, K. and Mandal, A. (2014) Screening of microemulsion properties for application in enhanced oil recovery. Fuel 121, 198-207.

Bera, A. and Mandal, A. (2015) Microemulsions: a novel approach to enhanced oil recovery: a review. Journal of Petroleum Exploration and Production Technology 5(3), 255-268.

Bera, A., Ojha, K. and Mandal, A. (2013) Synergistic Effect of Mixed Surfactant Systems on Foam Behavior and Surface Tension. Journal of Surfactants and Detergents 16(4), 621-630.

Budhathoki, M., Hsu, T.-P., Lohateeraparp, P., Roberts, B.L., Shiau, B.-J. and Harwell, J.H. (2016). Design of an optimal middle phase microemulsion for ultra high saline brine using hydrophilic lipophilic deviation (HLD) method. Colloids and Surfaces A: Physicochemical and Engineering Aspects 488, 36-45.

Chen, Z. and Zhao, X. (2015). Enhancing Heavy-Oil Recovery by Using Middle Carbon Alcohol-Enhanced Waterflooding, Surfactant Flooding, and Foam Flooding. Energy & Fuels 29(4), 2153-2161.

Duan, X., Hou, J., Cheng, T., Li, S. and Ma, Y. (2014) Evaluation of oil-tolerant foam for enhanced oil recovery: Laboratory study of a system of oil-tolerant foaming agents. Journal of Petroleum Science and Engineering 122, 428-438.

Farzaneh, S.A. and Sohrabi, M. (2013) A Review of the Status of Foam Application in Enhanced Oil Recovery. Society of Petroleum Engineers.

García-Sánchez, F., Eliosa-Jiménez, G., Salas-Padrón, A., Hernández-Garduza, O. and Ápam-Martínez, D. (2001) Modeling of microemulsion phase diagrams from excess Gibbs energy models. Chemical Engineering Journal 84(3), 257-274.

Gogoi, S.B. (2011) Adsorption–Desorption of Surfactant for Enhanced Oil Recovery. Transport in Porous Media 90(2), 589-604.

Graciaa, A., Lachasise, J., Cucuphat, C., Bourrel, M. and Salager, J.L. (1993) Improving solubilization in microemulsions with additives. 2. Long chain alcohols as lipophilic linkers. Langmuir 9, 3371-3374.

Gurgel, A., Moura, M.C.P.A., Dantas, T.N.C., Barros Neto, E.L. and Dantas Neto, A.A. (2008) A review on chemical flooding methods applied in enhanced oil recovery. Brazilian Journal of Petroleum and Gas 2(2), 83-95.

Heins, R., Simjoo, M., Zitha, P.L.J. and Rossen, W.R. (2014) Oil Relative Permeability During Enhanced Oil Recovery by Foam Flooding. SPE Annual Technical Conference and Exhibition. Amsterdam, The Netherlands, Society of Petroleum Engineers.

Hosseini-Nasab, S.M. and Zitha, P.L.J. (2017) Investigation of Chemical-Foam Design as a Novel Approach toward Immiscible Foam Flooding for Enhanced Oil Recovery. Energy & Fuels 31(10), 10525-10534.

Hsieh, W.C. and Shah, D.O. (1977) The Effect of Chain Length of Oil and Alcohol As Well as Surfactant to Alcohol Ratio on the Solubilization, Phase Behavior and Interfacial Tension of Oil/Brine/Surfactant/Alcohol Systems. Society of Petroleum Engineers.

Hua, S., Liu, Y., Di, Q., Chen, Y. and Ye, F. (2015) Experimental study of air foam flow in sand pack core for enhanced oil recovery. Journal of Petroleum Science and Engineering 135, 141-145.

Jin, L., Jamili, A., Li, Z., Lu, J., Luo, H., Ben Shiau, B.J., Delshad, M. and Harwell, J.H. (2015) Physics based HLD–NAC phase behavior model for surfactant/crude oil/brine systems. Journal of Petroleum Science and Engineering 136, 68-77.

Levitt, D., Jackson, A., Heinson, C., Britton, L.N., Malik, T., Dwarakanath, V. and Pope, G.A. (2009) Identification and Evaluation of High-Performance EOR Surfactants. Society of Petroleum Engineers.

Liu, Y., Grigg, R.B. and Bai, B. (2005) Salinity, pH , and Surfactant Concentration Effects on CO2-Foam. SPE International Symposium on Oilfield Chemistry. The Woodlands, Texas, Society of Petroleum Engineers.

Manlowe, D.J. and Radke, C.J. (1990) A Pore Level Investigation of Foam Oil Interactions in Porous Media. Society of Petroleum Engineers 5(04), 495-502.

Meling, T. and Hanssen, J.E. (1990) Gas-blocking foams in porous media: effects of oil and surfactant hydrophobe carbon number. Surfactants and Macromolecules: Self-Assembly at Interfaces and in Bulk, Darmstadt, Steinkopff.

Mohammad Salehi, M., Omidvar, P. and Naeimi, F. (2017) Salinity of injection water and its impact on oil recovery absolute permeability, residual oil saturation, interfacial tension and capillary pressure. Egyptian Journal of Petroleum 26(2), 301-312.

Negin, C., Ali, S. and Xie, Q. (2016) Most common surfactants employed in chemical enhanced oil recovery. Petroleum.

Osama, A. and Azmi, B. (2015) Foamability and Foam Stability of Several Surfactants Solutions: The Role of Screening and Flooding. Journal of Petroleum & Environmental Biotechnology 06(04).

Osei-Bonsu, K., Grassia, P. and Shokri, N. (2017) Relationship between bulk foam stability, surfactant formulation and oil displacement efficiency in porous media. Fuel 203, 403-410.

Rosen, M.J., Wang, H., Shen, P. and Zhu, Y. (2005) Ultralow Interfacial Tension for Enhanced Oil Recovery at Very Low Surfactant Concentrations. Langmuir 21(9), 3749-3756.

Salager, J.-L., Antón, R.E., Sabatini, D.A., Harwell, J.H., Acosta, E.J. and Tolosa, L.I. (2005) Enhancing solubilization in microemulsions—State of the art and current trends. Journal of Surfactants and Detergents 8(1), 3-21.

Salager, J.-L., Forgiarini, A.M. and Bullón, J. (2013) How to Attain Ultralow Interfacial Tension and Three-Phase Behavior with Surfactant Formulation for Enhanced Oil Recovery: A Review. Part 1. Optimum Formulation for Simple Surfactant–Oil–Water Ternary Systems. Journal of Surfactants and Detergents 16(4), 449-472.

Salager, J.-L., Márquez, L., Peña, A.A., Rondón, M., Silva, F. and Tyrode, E. (2000) Current Phenomenological Know-How and Modeling of Emulsion Inversion. Industrial & Engineering Chemistry Research 39(8), 2665-2676.

Salager, J.L., Morgan, J.C., Schechter, R.S., Wade, W.H. and Vasquez, E. (1979) Optimum Formulation of SurfactantWaterOil Systems for Minimum Interfacial Tension or Phase Behavior. Society of Petroleum Engineers.

Sansen, V., Charoensaeng, A., Shiau, B. and Suriyapraphadilok, U. (2015) Foam stability test for surfactant in enhanced oil recovery. The Petroleum and Petrochemical College, Chulalongkorn University, Bangkok, Thailand. **M.S. Thesis**.

Sheng, J.J. (2013) Chapter 11 - Foams and Their Applications in Enhancing Oil Recovery. Enhanced Oil Recovery Field Case Studies. Boston, Gulf Professional Publishing**:** 251-280.

Simjoo, M., Rezaei, T., Andrianov, A. and Zitha, P.L.J. (2013) Foam stability in the presence of oil: Effect of surfactant concentration and oil type. Colloids and Surfaces A: Physicochemical and Engineering Aspects 438, 148-158.

Singh, R. and Mohanty, K.K. (2015) Foams With Wettability-Altering Capabilities for Oil-Wet Carbonates A Synergistic Approach. Society of Petroleum Engineers. .

Sun, L., Wei, P., Pu, W., Wang, B., Wu, Y. and Tan, T. (2016) The oil recovery enhancement by nitrogen foam in high-temperature and high-salinity environments. Journal of Petroleum Science and Engineering 147, 485-494.

Torabi, F., Jamaloei, B.Y., Zarivnyy, O., Paquin, B.A., Rumpel, N.J. and Wilton, R.R. (2010) Effect of Oil Viscosity, Permeability and Injection Rate on Performance of Waterflooding, CO2 Flooding and WAG Processes on Recovery of Heavy Oils. Society of Petroleum Engineers.

Wang, Y., Liu, X., Bai, L. and Niu, J. (2017) Influence of alkyl chain length of alpha olefin sulfonates on surface and interfacial properties. Journal of Dispersion Science and Technology 38(12), 1764-1769.

Wei, P., Pu, W., Sun, L. and Wang, B. (2017) Research on nitrogen foam for enhancing oil recovery in harsh reservoirs. Journal of Petroleum Science and Engineering 157, 27-38.

Witthayapanyanon, A., Harwell, J.H. and Sabatini, D.A. (2008) Hydrophilic-lipophilic deviation (HLD) method for characterizing conventional and extended surfactants. J Colloid Interface Sci 325(1), 259-266.

Yuan, C.D., Pu, W.F., Wang, X.C., Sun, L., Zhang, Y.C. and Cheng, S. (2015) Effects of Interfacial Tension, Emulsification, and Surfactant Concentration on Oil Recovery in Surfactant Flooding Process for High Temperature and High Salinity Reservoirs. Energy & Fuels 29(10), 6165-6176.

Zhang, S., Jiang, G.-C., Wang, L., Guo, H.-T., Tang, X.-g. and Bai, D.-G. (2014) Foam Flooding with Ultra-Low Interfacial Tension to Enhance Heavy Oil Recovery. Journal of Dispersion Science and Technology 35(3), 403-410.

Zhao, P., Jackson, A., Britton, C., Kim, D.H., Britton, L.N., Levitt, D. and Pope, G.A. (2008) Development of High-Performance Surfactants for Difficult Oils. Society of Petroleum Engineers 113432, 1-11.

APPENDICES

Appendix A Calculation of Solution Preparation

A1. Salt solution preparation

The concentration of surfactant in all experiments was 0.03 M. In phase behavior experiments and oil recovery processes, the twice concentration of salt solution and surfactant soution should be considered when combined together. The example of calculation is shown below.

Assume 1000mL of 10 gNaCl/100mL solution

$$\text{Desired NaCl weight (g)} = \frac{\text{gNaCl}}{100\text{mL solution}} \times \text{Stock volume (mL)}$$

$$\text{Desired NaCl weight (g)} = \frac{10\text{ gNaCl}}{100\text{mL solution}} \times 1000\text{mL solution}$$

$$\text{Desired NaCl weight (g)} = 100\text{ g}$$

Assume 2.5 mL of 2 gNaCl/100mL mixing with surfactant solution in salinity scan

$$\text{Stock solution volume} \times \frac{\text{gNaCl stock solution}}{100\text{mL solution}} = 2 \times \frac{\text{Desired gNaCl}}{100\text{mL solution}} \times 2.5\text{mL}$$

$$\text{Stock solution volume} \times \frac{10\text{ gNaCl}}{100\text{mL solution}} = 2 \times \frac{2\text{ gNaCl}}{100\text{mL solution}} \times 2.5\text{mL}$$

$$\text{Stock solution volume} = 1\text{ mL}$$

A2. Surfactant solution preparation

Table A1 Acrive mass and molecular weight of surfactants in this study

Surfactant	Active content (%)	Molecular weight
AOT	>97.00	444.56
IOS C_{15-18}	28.03	350.00
IOS C_{19-23}	31.30	414.90
IOS C_{24-28}	69.40	498.10

Assume 250 mL of 0.03 M AOT solution

$$\text{Surfactant weight (g)} = 2 \times \frac{0.03\,\text{mol}}{\text{L}} \times \frac{\text{g Mw}_{\text{surfactant}}}{1\,\text{mol}} \times \frac{1\,\text{L}}{1000\,\text{mL}} \times \frac{1}{\%\text{active}} \times \text{Stock Volume (mL)}$$

The desired surfactant weight for preparing stock solution in each surfactant can be calculated as following

$$\text{AOT weight (g)} = 2 \times \frac{0.03\,\text{mol}}{\text{L}} \times \frac{444.56\,\text{g}}{1\,\text{mol}} \times \frac{1\,\text{L}}{1000\,\text{mL}} \times \frac{1}{0.97} \times 250\,\text{mL} = 6.8746\,\text{g}$$

$$\text{IOS}\,C_{15-18}\text{ weight (g)} = 2 \times \frac{0.03\,\text{mol}}{\text{L}} \times \frac{350\,\text{g}}{1\,\text{mol}} \times \frac{1\,\text{L}}{1000\,\text{mL}} \times \frac{1}{0.2803} \times 250\,\text{mL} = 18.7299\,\text{g}$$

$$\text{IOS}\,C_{19-23}\text{ weight (g)} = 2 \times \frac{0.03\,\text{mol}}{\text{L}} \times \frac{414.9\,\text{g}}{1\,\text{mol}} \times \frac{1\,\text{L}}{1000\,\text{mL}} \times \frac{1}{0.313} \times 250\,\text{mL} = 19.8834\,\text{g}$$

$$\text{IOS}\,C_{24-28}\text{ weight (g)} = 2 \times \frac{0.03\,\text{mol}}{\text{L}} \times \frac{498.1\,\text{g}}{1\,\text{mol}} \times \frac{1\,\text{L}}{1000\,\text{mL}} \times \frac{1}{0.694} \times 250\,\text{mL} = 10.7659\,\text{g}$$

Appendix B Phase Behavior Results

B1. Predicted optimum salinity from HLD equation

Table B1 The parameters for calculating the predicted optimum salinity in heptane from HLD equation

Volume fraction	Volume fraction	Cc_{mix}	K_{mix}	$lnS*_{mix}$	Predicted $S*_{mix}$
AOT	C_{15-18}				
0.5	0.5	0.145	0.127	0.741	2.097
AOT	C_{19-23}				
0.5	0.5	0.515	0.142	0.479	1.614
AOT	C_{24-28}				
0.5	0.5	0.885	0.149	0.155	1.167

Table B2 The parameters for calculating the predicted optimum salinity in hexadecane from HLD equation

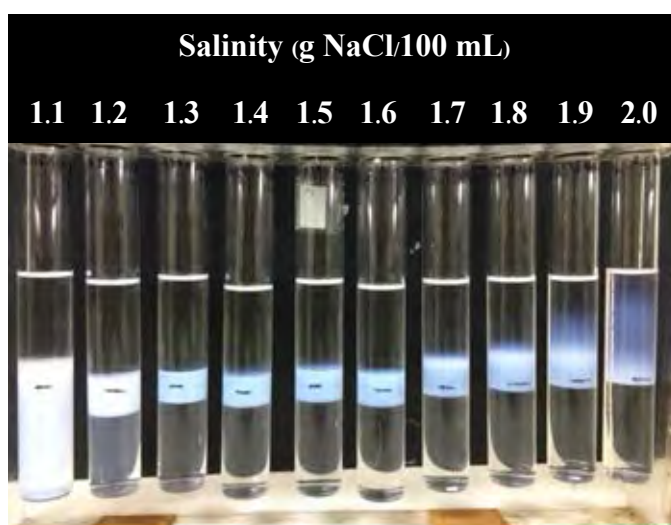| Volume fraction	Volume fraction	Cc_{mix}	K_{mix}	$lnS*_{mix}$	Predicted $S*_{mix}$
AOT	C_{15-18}				
0.5	0.5	0.145	0.1265	1.879	6.55
AOT	C_{19-23}				
0.5	0.5	0.515	0.142	1.757	5.80
AOT	C_{24-28}				
0.5	0.5	0.885	0.1485	1.491	4.44

Figure B1 Phase behavior of 1:1 volume ratio of sodium dioctylsulfosuccinate (AOT) and internal olefins sulfonate (IOS C_{15-18}) using heptane as an oil phase.
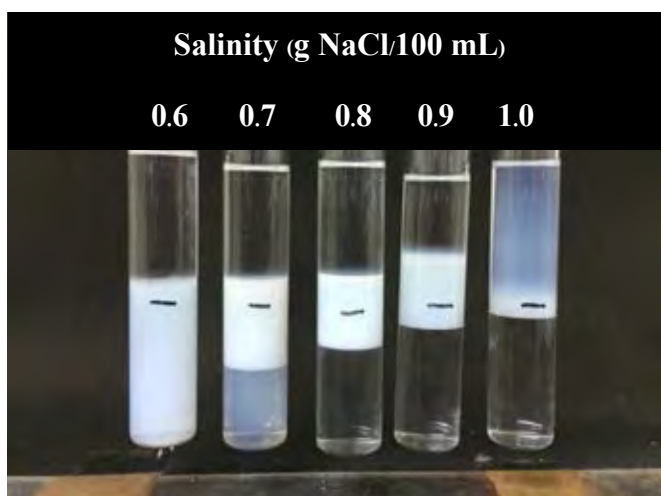

Figure B2 Phase behavior of 1:1 volume ratio of sodium dioctylsulfosuccinate (AOT) and internal olefins sulfonate (IOS C_{19-23}) using heptane as an oil phase.
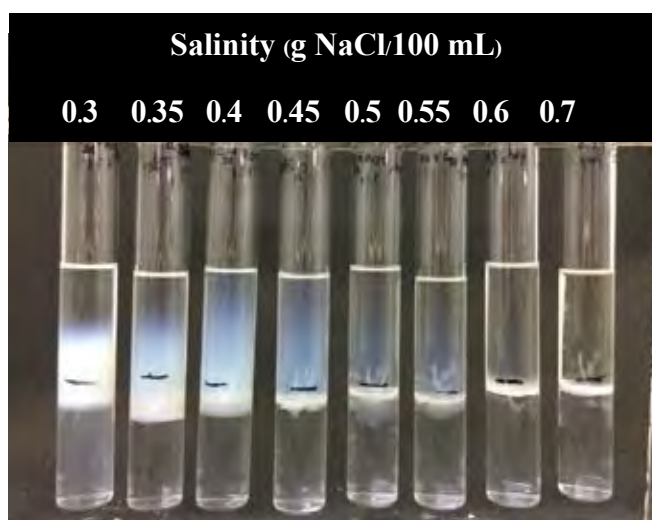
Figure B3 Phase behavior of 1:1 volume ratio of sodium dioctylsulfosuccinate (AOT) and internal olefins sulfonate (IOS C$_{24\text{-}28}$) using heptane as an oil phase.

Figure B4 Phase behavior of 1:1 volume ratio of sodium dioctylsulfosuccinate (AOT) and internal olefins sulfonate (IOS C$_{15\text{-}18}$) using hexadecane as an oil phase.
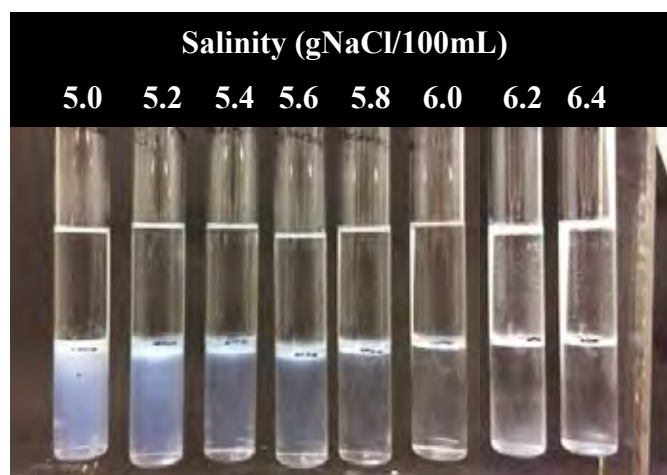
Figure B5 Phase behavior of 1:1 volume ratio of sodium dioctylsulfosuccinate (AOT) and internal olefins sulfonate (IOS C_{19-23}) using hexadecane as an oil phase.

Figure B6 Phase behavior of 1:1 volume ratio of sodium dioctylsulfosuccinate (AOT) and internal olefins sulfonate (IOS C_{24-28}) using hexadecane as an oil phase.
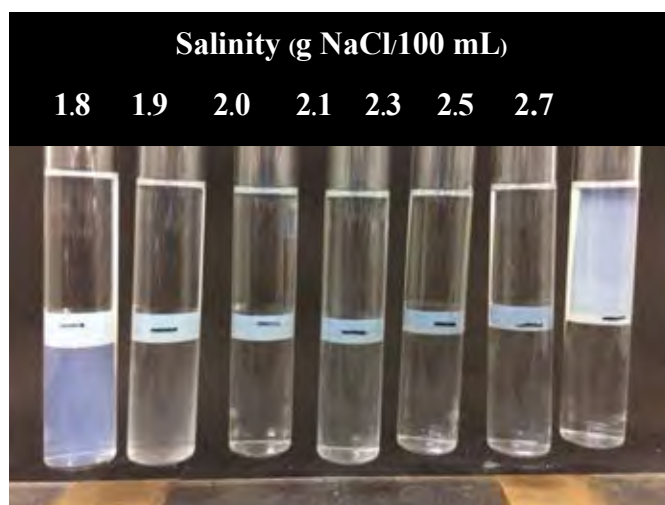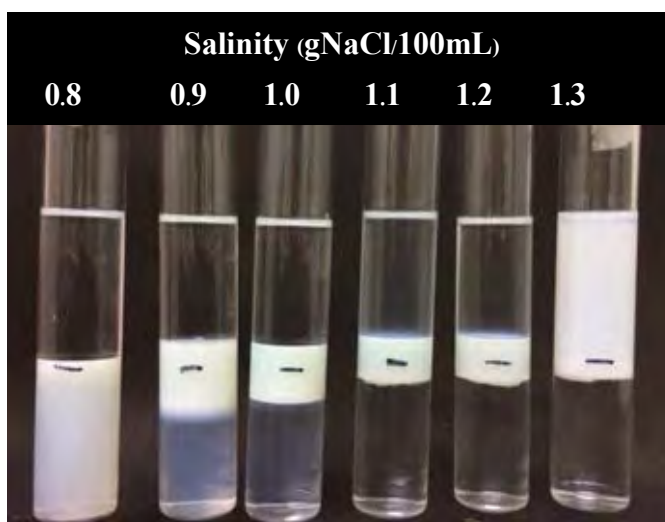
Figure B7 Phase behavior of 1:1 volume ratio of sodium dioctylsulfosuccinate (AOT) and internal olefins sulfonate (IOS C$_{15-18}$) using crude oil as an oil phase.

Figure B8 Phase behavior of 1:1 volume ratio of sodium dioctylsulfosuccinate (AOT) and internal olefins sulfonate (IOS C$_{19-23}$) using crude oil as an oil phase.
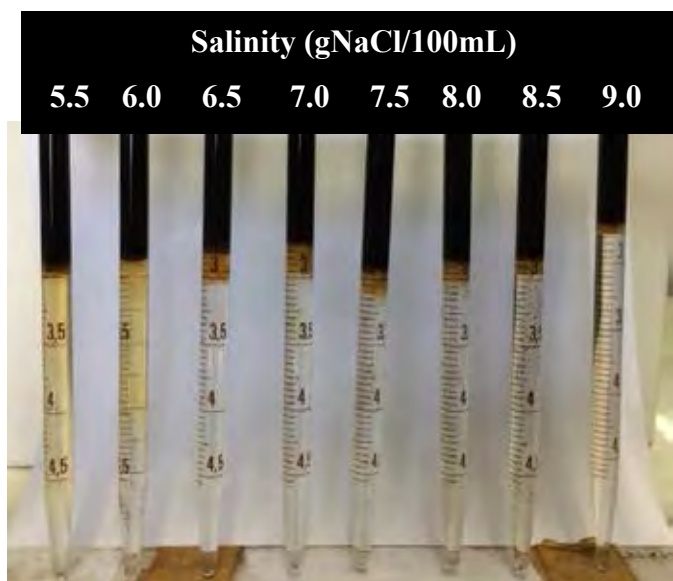
Figure B9 Phase behavior of 1:1 volume ratio of sodium dioctylsulfosuccinate (AOT) and internal olefins sulfonate (IOS C_{24-28}) using crude oil as an oil phase.
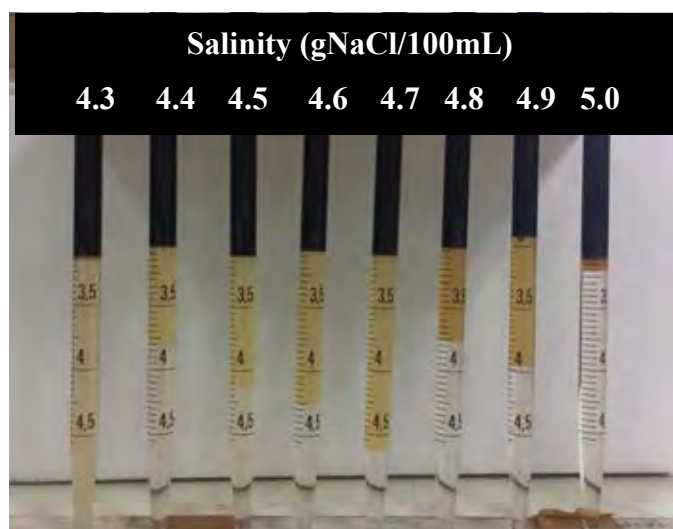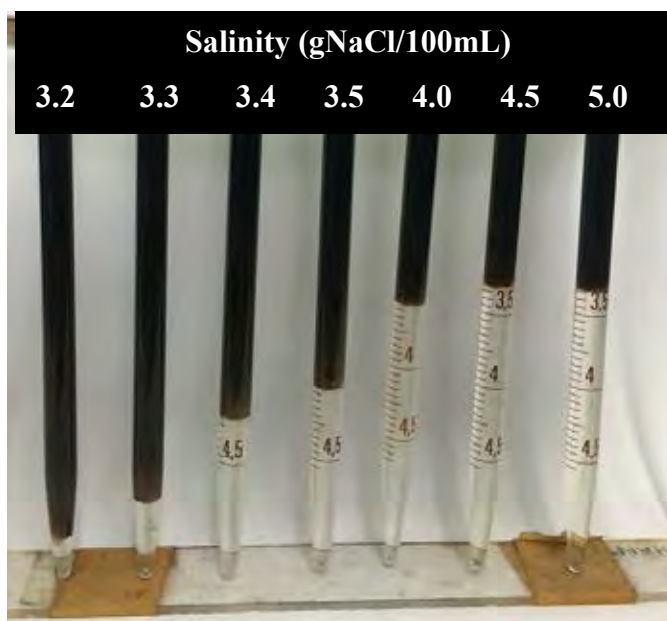
Appendix C Surfactant and Foam Flooding Results

C1. Surfactant and Foam Flooding Results

Table C1 Surfactant and Foam Flooding of AOT:IOS C_{15-18} using heptane as an oil phase at 25±2 °C and 1 atm

Column Results		AOT:IOS C_{15-18} (S*=1.6)							
Run		1	2	3	4	5	6	7	8
NaCl (g/100mL)		1.6	1.6	1.6	1.6	1.6	1.6	0.16	0.16
EOR		SFT	FOAM	SFT	FOAM	SFT	FOAM	SFT	FOAM
Surfactant slug size (PV)		1 PV	1PV	1 PV	1 PV	3 PV	3 PV	1 PV	1 PV
Operating condition		Normal	Normal	Shut in	Shut in	Normal	Normal	Normal	Normal
PV(mL)		17.05	17.37	15.95	16.29	16.55	15.90	17.27	17.65
Porosity(%)		41.99	42.77	40.61	40.11	40.75	39.15	42.53	43.46
Permeability(D)		0.68	0.67	0.48	0.61	0.62	0.69	0.74	0.65
OOIP(mL)		6.82	9.42	8.53	9.3	6.95	8.97	6.59	6.29
Initial Oil Saturation (%Soi)		40.00	54.23	53.48	57.09	41.99	56.42	38.16	35.64
Brine	Brine BT (PV)	0.42	0.32	0.39	0.48	0.43	0.56	0.40	0.17
Flooding	%OOIP	60.12	65.82	53.93	70.97	61.87	72.46	56.15	52.46
EOR	Oil BT (PV)	2.42	2.12	2.38	2.8	2.36	2.61	2.76	2.56
	%OOIP	14.66	10.62	19.93	11.83	11.51	11.15	3.03	9.54
Total %Oil recovery		74.78	76.43	73.86	82.8	73.38	83.61	59.18	62.00

Table C2 Surfactant and Foam Flooding of AOT:IOS C_{19-23} using heptane as an oil phase at 25±2 °C and 1 atm

Column Results		AOT:IOS C_{19-23} (S*=0.8)			
Run		9	10	11	12
NaCl (g/100mL)		0.8	0.8	0.8	0.8
EOR		SFT	FOAM	SFT	FOAM
Surfactant slug size (PV)		1 PV	1 PV	1 PV	1 PV
Operating condition		Normal	Normal	Shut in	Shut in
PV(mL)		17.98	17.18	17.64	15.21
Porosity(%)		44.28	42.31	43.44	37.46
Permeability(D)		0.59	0.59	0.48	0.37
OOIP(mL)		7.52	8.10	5.92	10.76
Initial Oil Saturation (%Soi)		41.82	47.15	33.56	70.74
Brine Flooding	Brine BT (PV)	0.32	0.44	0.31	0.4
	%OOIP	53.19	54.32	43.92	47.4
EOR	Oil BT (PV)	2.35	2.04	3.00	2.17
	%OOIP	23.94	27.16	20.27	25.09
Total %Oil recovery		77.13	81.48	64.19	72.49

Table C3 Surfactant and Foam Flooding of AOT:IOS C_{15-18} using hexadecane as an oil phase at 25±2 °C and 1 atm

Column Results		AOT:IOS C_{15-18} (S*=6.2)			
Run		13	14	15	16
NaCl (g/100mL)		5.4	5.4	5.4	5.4
EOR		SFT	FOAM	SFT	FOAM
Surfactant slug size (PV)		1 PV	1 PV	1 PV	1 PV
Operating condition		Normal	Normal	Shut in	Shut in
PV(mL)		15.41	15.46	16.86	15.77
Porosity(%)		37.95	38.07	41.52	38.83
Permeability(D)		0.49	0.50	0.49	0.61
OOIP(mL)		13.36	12.78	9.54	13.15
Initial Oil Saturation (%Soi)		86.70	82.66	56.58	83.39
Brine Flooding	Brine BT (PV)	0.35	0.55	0.39	0.5
	%OOIP	80.09	76.68	74.42	81.37
EOR	Oil BT (PV)	5.39	6.45	6.39	6.94
	%OOIP	2.25	1.56	6.29	3.04
Total %Oil recovery		82.34	78.25	80.71	84.41

Table C4 Surfactant and Foam Flooding of AOT:IOS C_{19-23} using hexadecane as an oil phase at 25±2 °C and 1 atm

Column Results		AOT:IOS C_{19-23} (S*=2.3)			
Run		17	18	19	20
NaCl (g/100mL)		2.3	2.3	2.3	2.3
EOR		SFT	FOAM	SFT	FOAM
Surfactant slug size (PV)		1 PV	1 PV	1 PV	1 PV
Operating condition		Normal	Normal	Shut in	Shut in
PV(mL)		16.94	16.67	17.26	16.2
Porosity(%)		41.72	41.05	42.5	39.94
Permeability(D)		0.61	0.61	0.5	0.58
OOIP(mL)		10.37	11.06	10.28	11.61
Initial Oil Saturation (%Soi)		61.22	66.35	59.56	71.58
Brine Flooding	Brine BT (PV)	0.46	0.44	0.42	0.49
	%OOIP	63.65	60.58	67.1	67.18
EOR	Oil BT (PV)	2.44	2.05	2.68	2.23
	%OOIP	14.46	16.27	13.62	11.2
Total %Oil recovery		78.11	76.85	80.74	78.38

Table C5 Surfactant and Foam Flooding of AOT:IOS C_{24-28} using hexadecane as an oil phase at 25±2 °C and 1 atm

Column Results		AOT:IOS C_{24-28} (S*=1.2)			
Run		21	22	23	24
NaCl (g/100mL)		1.2	1.2	1.2	1.2
EOR		SFT	FOAM	SFT	FOAM
Surfactant slug size (PV)		1 PV	1 PV	1 PV	1 PV
Operating condition		Normal	Normal	Shut in	Shut in
PV(mL)		16.61	16.47	16.17	16.30
Porosity(%)		40.90	40.56	39.82	40.14
Permeability(D)		0.80	0.61	0.80	0.57
OOIP(mL)		11.01	9.99	10.42	10.63
Initial Oil Saturation (%Soi)		66.29	60.66	64.44	65.21
Brine Flooding	Brine BT (PV)	0.46	0.47	0.47	0.45
	%OOIP	65.40	63.06	64.30	60.21
EOR	Oil BT (PV)	2.92	2.22	2.84	2.24
	%OOIP	11.81	11.01	13.44	16.93
Total %Oil recovery		77.20	74.07	77.74	77.14

C2. Calculation of properties in sand pack column flooding

The example of properties calculation in AOT:IOS C_{15-18} with heptane as oil phase as shown below

Pore volume = Injected volume – Outlet volume – other volume

= 25.95 – 5 -3.9

= 17.05 mL

Porosity = $\dfrac{\text{Pore Volume}}{\text{Bulk Volume}} \times 100$

= $\dfrac{17.05 \text{ mL}}{40.61 \text{ mL}} \times 100$

= 41.99 %

Permeability = $\dfrac{\Delta P}{L} = \dfrac{q\mu}{kA}$

Where μ = 0.089 cP (viscosity of water at 25ºC)

ΔP = $0.25 \text{ psi} \times \dfrac{1 \text{ atm}}{14.7 \text{ psi}}$

= 0.017 atm

q = $0.5 \dfrac{\text{mL}}{\text{min}} \times \dfrac{1 \text{ min}}{60 \text{ s}} \times \dfrac{1 \text{ cm}^3}{1 \text{ mL}}$

= $0.0083 \dfrac{\text{cm}^3}{\text{s}}$

L = $3 \text{ inch} \times \dfrac{2.54 \text{ cm}}{1 \text{ inch}}$

= 7.62 cm

A = πr^2

= $\pi \times \left(\dfrac{2.5}{2}\right)^2$

= 4.91 cm^2

Permeability $\quad$ = $\qquad \dfrac{\Delta P}{L} = \dfrac{q\mu}{kA}$

$\qquad\qquad$ = $\qquad$ $0.0083 \dfrac{cm^3}{s} \times 0.89\ cP \times 7.62\ cm \times \dfrac{1}{0.017\ atm} \times \dfrac{1}{4.91\ cm}$

$\qquad\qquad$ = $\qquad$ $0.68\ D$

OOIP $\qquad$ = $\qquad$ Injected oil volume – Oil outlet volume – other volume

$\qquad\qquad$ = $\qquad$ $17.22 - 6.5 - 3.9$

$\qquad\qquad$ = $\qquad$ $6.82\ mL$

%S_{oi} $\qquad$ = $\qquad$ $\dfrac{OOIP}{PV} \times 100$

$\qquad\qquad$ = $\qquad$ $\dfrac{6.82}{17.05} \times 100$

$\qquad\qquad$ = $\qquad$ $40.00\ \%$

Table C6 Recovered oil in each pore volume of AOT:IOS C_{15-18} with heptane as oil phase in surfactant and foam flooding

Column Results	AOT:IOS C_{15-18} (S*=1.6)							
Run	1		2		3		4	
NaCl (g/100mL)	1.6		1.6		1.6		1.6	
EOR process	SFT		FOAM		SFT		FOAM	
Surfactant slug size (PV)	1 PV		1 PV		1 PV		1 PV	
Operating condition	Normal		Normal		Shut in		Shut in	
	PV	%OOIP	PV	%OOIP	PV	%OOIP	PV	%OOIP
	0.00	0.00	0.00	0.00	0.00	0.00	0.00	0.00
	0.50	60.12	0.50	56.26	0.50	37.51	0.50	51.61
	1.00	60.12	1.00	62.63	1.00	49.24	1.00	70.97
	1.50	60.12	1.50	65.82	1.50	53.93	1.50	70.97
	2.09	60.12	2.08	65.82	2.00	53.93	2.00	70.97
	2.67	71.85	2.65	76.43	2.50	53.93	2.50	70.97
	3.26	71.85	3.23	76.43	3.00	73.86	3.00	82.80
	3.85	74.78	3.80	76.43	3.50	73.86	3.50	82.80
	4.43	74.78	4.38	76.43	4.00	73.86	4.00	82.80
	5.02	74.78	-	-	4.50	73.86	4.50	82.80
	-	-	-	-	5.00	73.86	5.00	82.80
	-	-	-	-	5.50	73.86	5.50	82.80
	-	-	-	-	6.00	73.85	6.00	82.80

Table C6 Recovered oil in each pore volume of AOT**:**IOS C$_{15-18}$ with heptane as oil phase in surfactant and foam flooding (continued)

Column Results	AOT:IOS C$_{15-18}$ (S*=1.6)							
Run	5		6		7		8	
NaCl (g/100mL)	1.6		1.6		0.16		0.16	
EOR process	SFT		FOAM		SFT		FOAM	
Surfactant slug size (PV)	3 PV		3 PV		1 PV		1 PV	
Operating condition	Normal		Normal		Normal		Normal	
	PV	%OOIP	PV	%OOIP	PV	%OOIP	PV	%OOIP
	0.00	0.00	0.00	0.00	0.00	0.00	0.00	0.00
	0.50	56.12	0.50	66.89	0.50	54.63	0.50	42.93
	1.00	61.87	1.00	71.35	1.00	56.15	1.00	46.10
	1.50	61.87	1.50	72.46	1.50	56.15	1.50	49.28
	2.10	61.87	2.00	72.46	2.08	56.15	2.00	52.46
	2.71	73.38	2.63	79.15	2.66	56.15	2.50	52.46
	3.31	73.38	3.26	83.61	3.24	59.18	3.07	58.82
	3.92	73.38	3.89	83.61	3.82	59.18	3.63	58.82
	4.52	73.38	4.52	83.61	4.40	59.18	4.20	60.41
	5.13	73.38	5.14	83.61	-	-	4.77	62.00
	-	-	5.77	83.61	-	-	5.33	62.00

Table C7 Recovered oil in each pore volume of AOT:IOS C_{19-23} with heptane as oil phase in surfactant and foam flooding

Column Results	AOT:IOS C_{19-23} (S*=0.8)							
Run	9		10		11		12	
NaCl (g/100mL)	0.8		0.8		0.8		0.8	
EOR process	SFT		FOAM		SFT		FOAM	
Surfactant slug size (PV)	1 PV		1 PV		1 PV		1 PV	
Operating condition	Normal		Normal		Shut in		Shut in	
	PV	%OOIP	PV	%OOIP	PV	%OOIP	PV	%OOIP
	0.00	0.00	0.00	0.00	0.00	0.00	0.00	0.00
	0.50	42.55	0.50	51.85	0.50	40.54	0.50	41.82
	1.00	50.53	1.00	54.32	1.00	43.92	1.00	45.54
	1.50	53.19	1.50	54.32	1.50	43.92	1.50	47.40
	2.00	53.19	2.00	54.32	2.00	43.92	2.00	47.40
	2.56	53.19	2.58	66.67	2.50	43.92	2.50	47.40
	3.11	77.13	3.16	81.48	3.00	54.05	3.00	65.99
	3.67	77.13	3.75	81.48	3.50	57.43	3.50	72.49
	4.22	77.13	4.33	81.48	4.00	57.43	4.00	72.49
	4.78	77.13	4.91	81.48	4.50	57.43	4.50	72.49
	5.34	77.13	5.49	81.48	5.00	60.81	5.00	72.49
	-	-	-	-	5.50	64.19	5.50	72.49
	-	-	-	-	6.00	64.19	6.00	72.49

Table C8 Recovered oil in each pore volume of AOT:IOS C_{15-18} with hexadecane as oil phase in surfactant and foam flooding

Column Results	AOT:IOS C_{15-18} (S*=6.2)							
Run	13		14		15		16	
NaCl (g/100mL)	5.4		5.4		5.4		5.4	
EOR process	SFT		FOAM		SFT		FOAM	
Surfactant slug size (PV)	1 PV		1 PV		1 PV		1 PV	
Operating condition	Normal		Normal		Shut in		Shut in	
	PV	%OOIP	PV	%OOIP	PV	%OOIP	PV	%OOIP
	0.00	0.00	0.00	0.00	0.00	0.00	0.00	0.00
	0.50	42.66	0.50	49.30	0.50	57.65	0.50	51.71
	1.00	65.12	1.00	68.08	1.00	68.13	1.00	69.96
	1.50	74.85	1.50	74.33	1.50	72.33	1.50	76.81
	2.00	78.59	2.00	76.68	2.00	74.42	2.00	81.37
	2.50	80.09	2.50	76.68	2.50	74.42	2.50	81.37
	3.00	80.09	3.00	76.68	3.00	74.42	3.00	81.37
	3.50	80.09	3.50	76.68	3.50	74.42	3.50	81.37
	4.00	80.09	4.00	76.68	4.00	74.42	4.00	81.37
	4.50	80.09	4.50	76.68	4.50	74.42	4.50	81.37
	5.00	80.09	5.00	76.68	5.00	74.42	5.00	81.37
	5.50	82.34	5.50	76.68	5.50	74.42	5.50	81.37
	6.00	82.34	6.00	76.68	6.00	78.62	6.00	81.37
	6.50	82.34	6.50	76.68	6.50	78.62	6.50	81.37
	7.00	82.34	7.00	76.68	7.00	80.71	7.00	81.37
	7.50	82.34	7.50	78.25	7.50	80.71	7.50	84.41
	8.00	82.34	8.00	78.25	8.00	80.71	8.00	84.41
	8.50	82.34	8.50	78.25	8.50	80.71	8.50	84.41
	9.00	82.34	9.00	78.25	9.00	80.71	9.00	84.41

Table C10 Recovered oil in each pore volume of AOT**:**IOS C$_{24-28}$ with hexadecane as oil phase in surfactant and foam flooding

| Column Results	AOT:IOS C$_{24-28}$ (S*=1.2)							
Run	21		22		23		24	
NaCl (g/100mL)	1.2		1.2		1.2		1.2	
EOR process	SFT		FOAM		SFT		FOAM	
Surfactant slug size (PV)	1 PV		1 PV		1 PV		1 PV	
Operating condition	Normal		Normal		Shut in		Shut in	
	PV	%OOIP	PV	%OOIP	PV	%OOIP	PV	%OOIP
	0.00	0.00	0.00	0.00	0.00	0.00	0.00	0.00
	0.50	51.77	0.50	50.05	0.50	53.74	0.50	48.92
	1.00	60.85	1.00	58.06	1.00	61.42	1.00	56.44
	1.50	65.40	1.50	63.06	1.50	64.30	1.50	60.21
	2.00	65.40	2.00	63.06	2.00	64.30	2.00	60.21
	2.60	65.40	2.61	70.07	2.62	64.30	2.61	67.73
	3.20	69.03	3.21	74.07	3.24	70.06	3.23	71.50
	3.81	69.03	3.82	74.07	3.86	70.06	3.84	71.50
	4.41	72.66	4.43	74.07	4.47	70.06	4.45	77.14
	5.01	77.20	5.04	74.07	5.09	77.74	5.07	77.14
	5.61	77.20	5.64	74.07	5.71	77.74	5.68	77.14
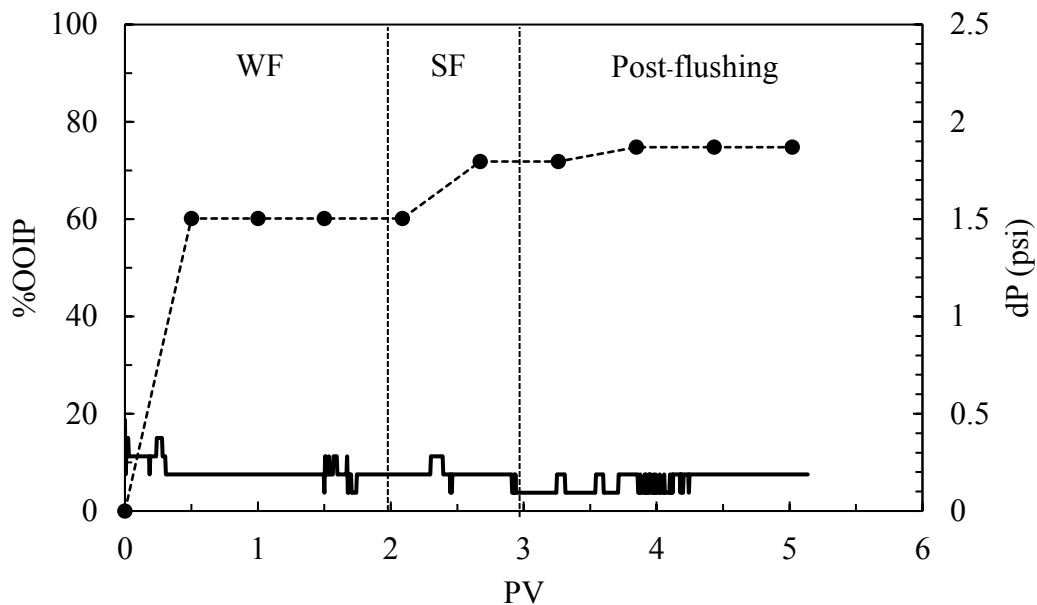
Figure C1 The accumulative oil recovery and pressure drop during water and surfactant flooding as a function of pore volume by AOT:IOS C_{15-18} at optimum salinity in heptane.
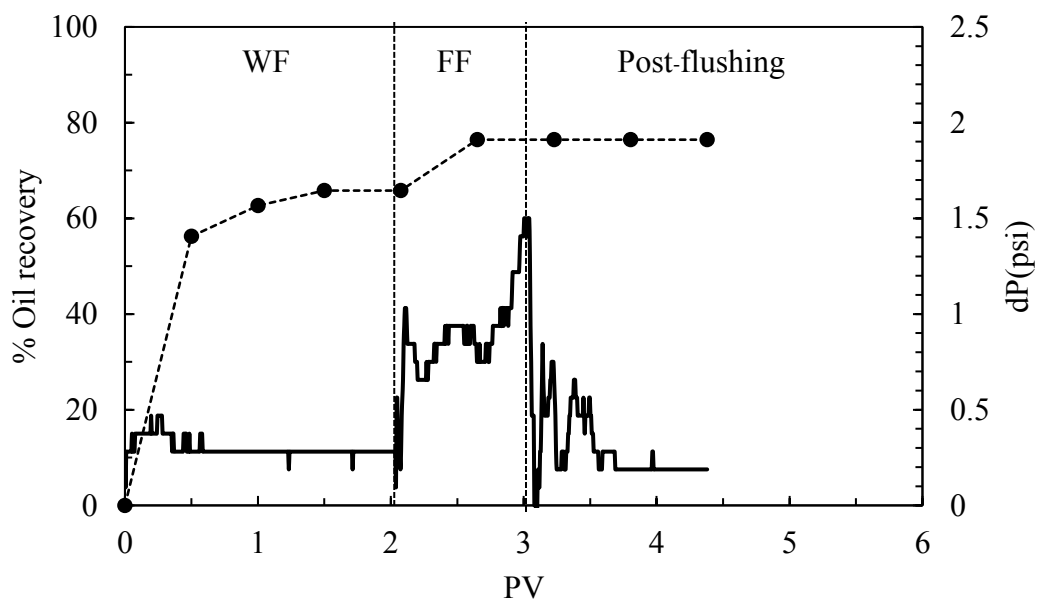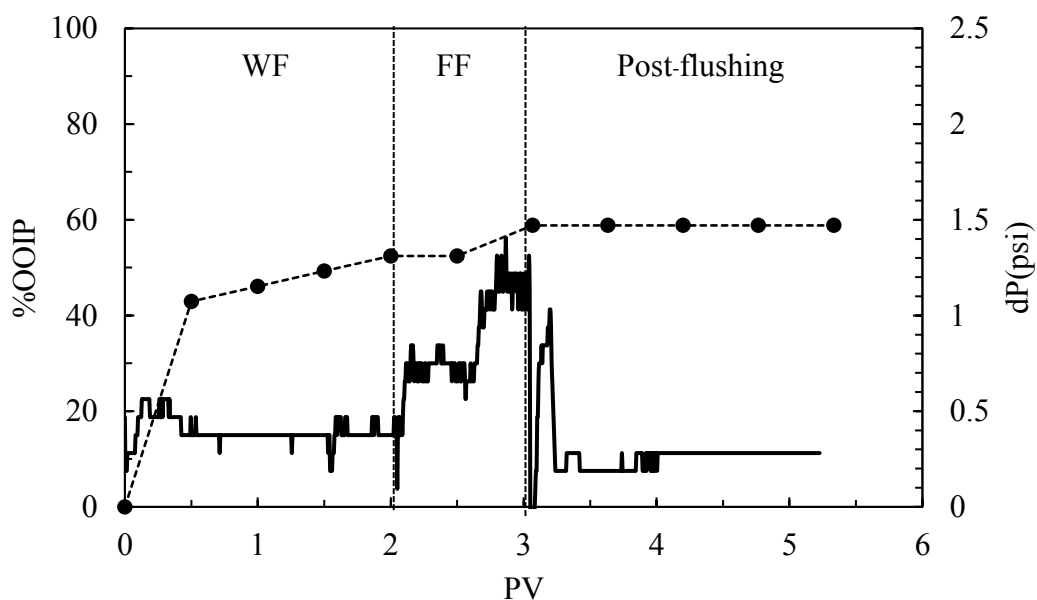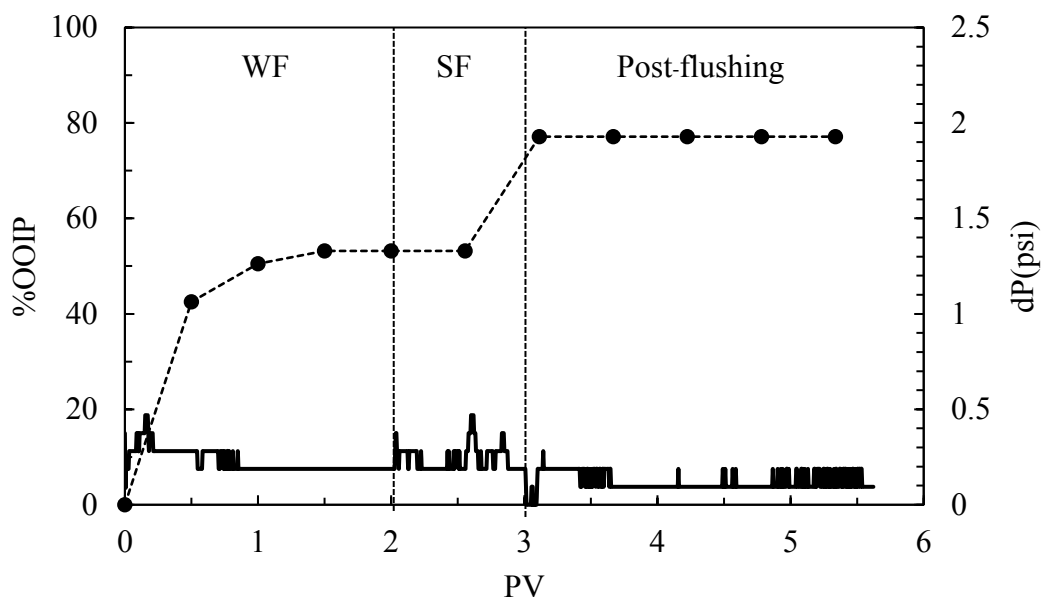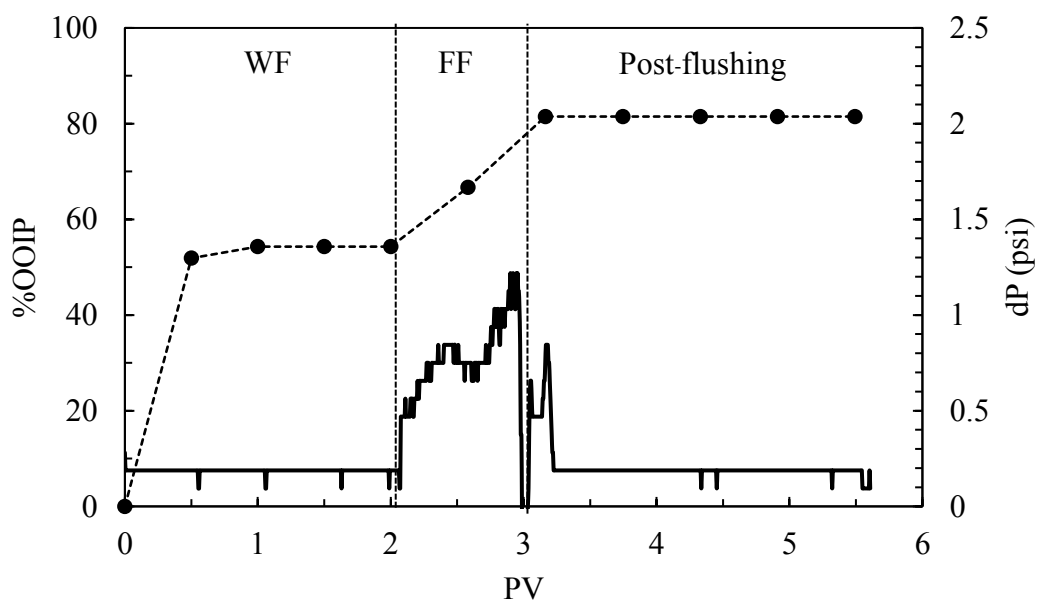

Figure C2 The accumulative oil recovery and pressure drop during water and foam flooding as a function of pore volume by AOT:IOS C_{15-18} at optimum salinity in heptane.
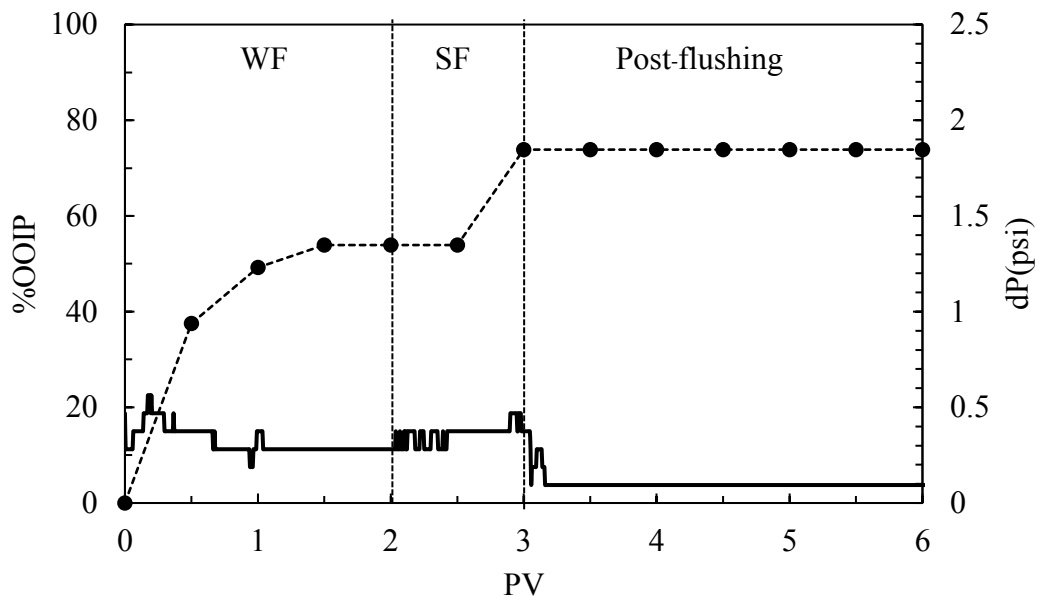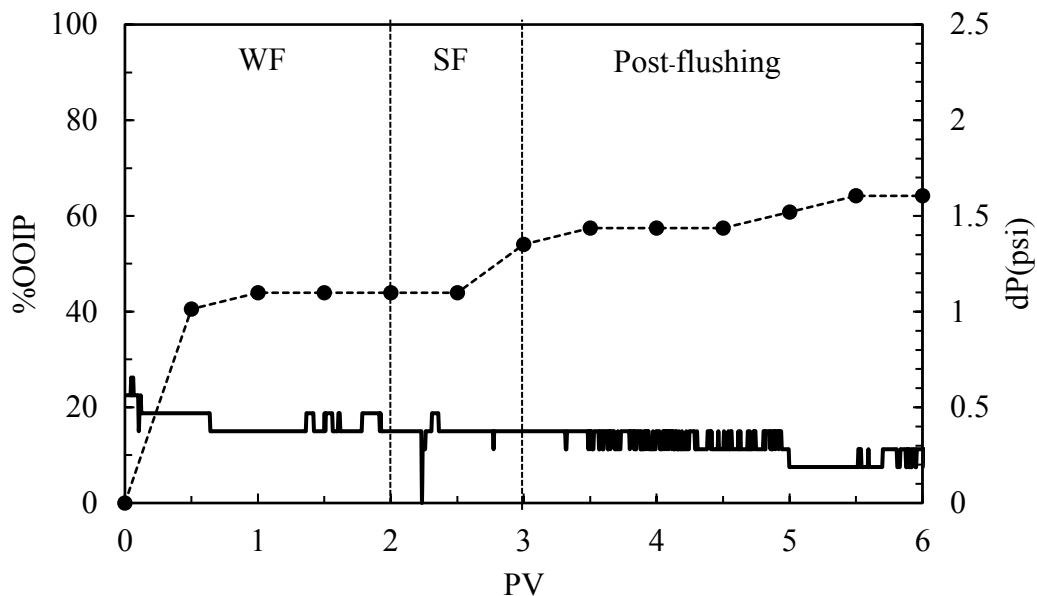
Figure C3 The accumulative oil recovery and pressure drop during water and surfactant flooding before 24 hours shutting in as a function of pore volume by AOT:IOS C_{15-18} at optimum salinity in heptane.
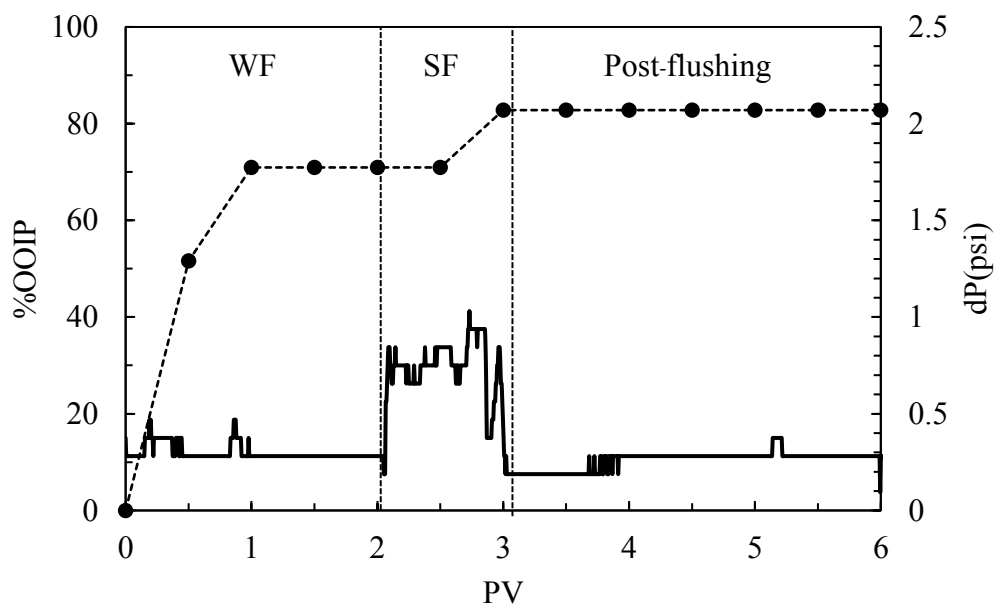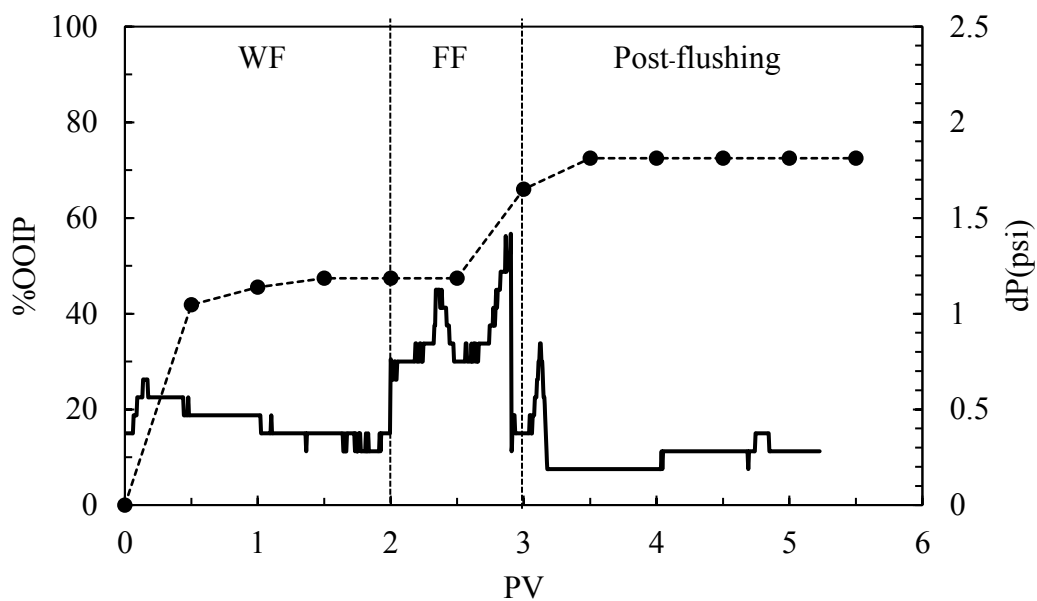

Figure C4 The accumulative oil recovery and pressure drop during water and foam flooding before 24 hours shutting in as a function of pore volume by AOT:IOS C_{15-18} at optimum salinity in heptane.
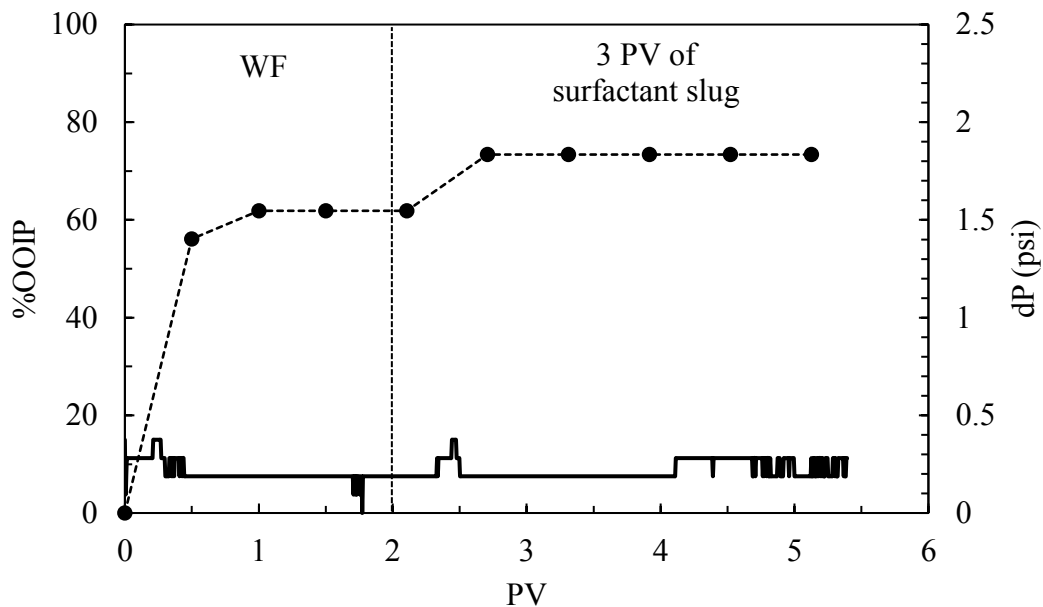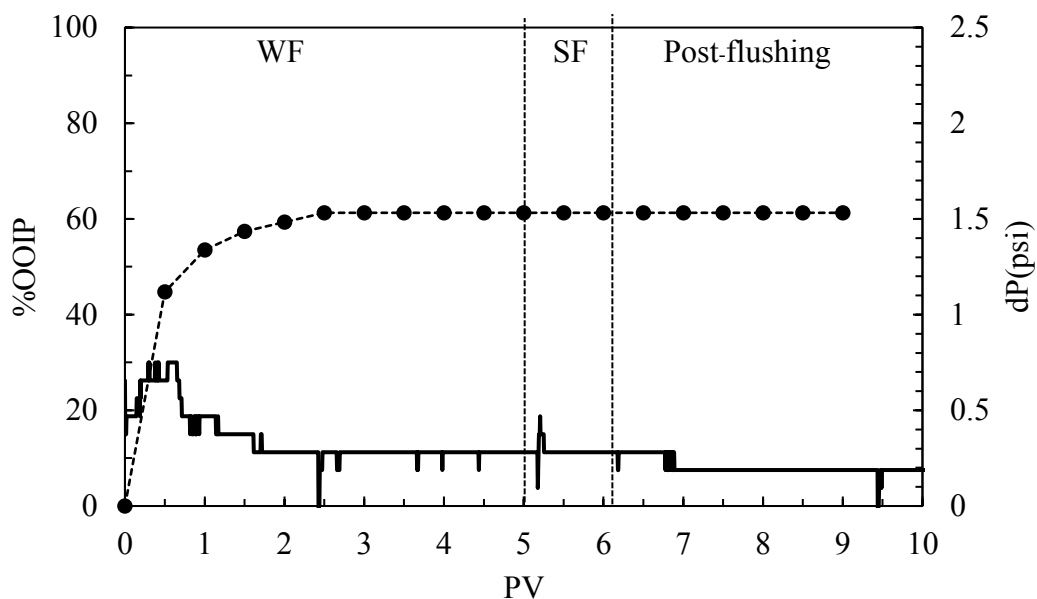
Figure C5 The accumulative oil recovery and pressure drop during water and surfactant flooding as a function of pore volume by AOT:IOS C_{15-18} at optimum salinity and 3 PV surfactant slug in heptane.
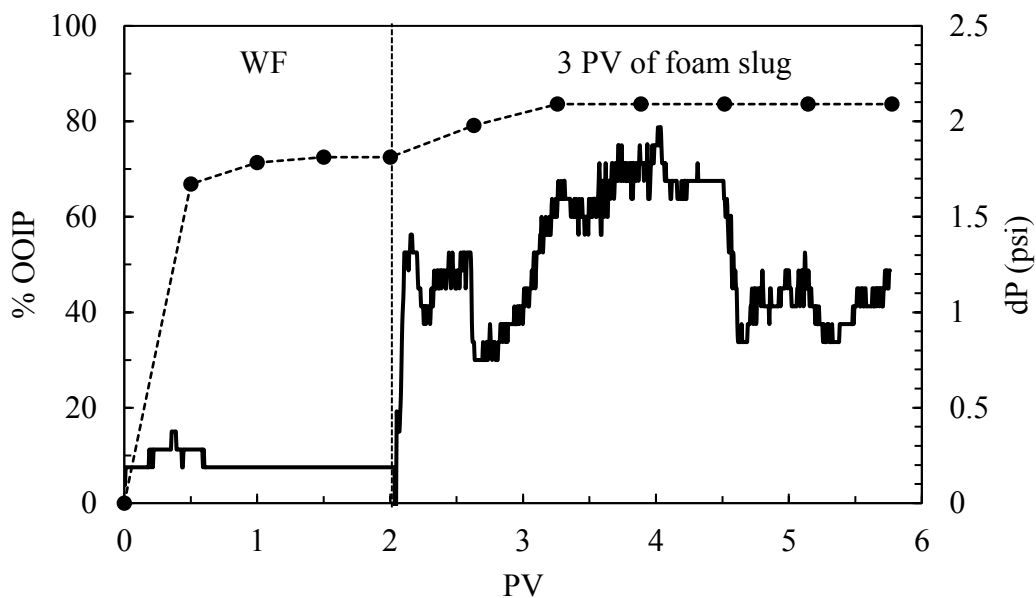
Figure C6 The accumulative oil recovery and pressure drop during water and foam flooding as a function of pore volume by AOT:IOS C_{15-18} at optimum salinity and 3 PV foam slug in heptane.
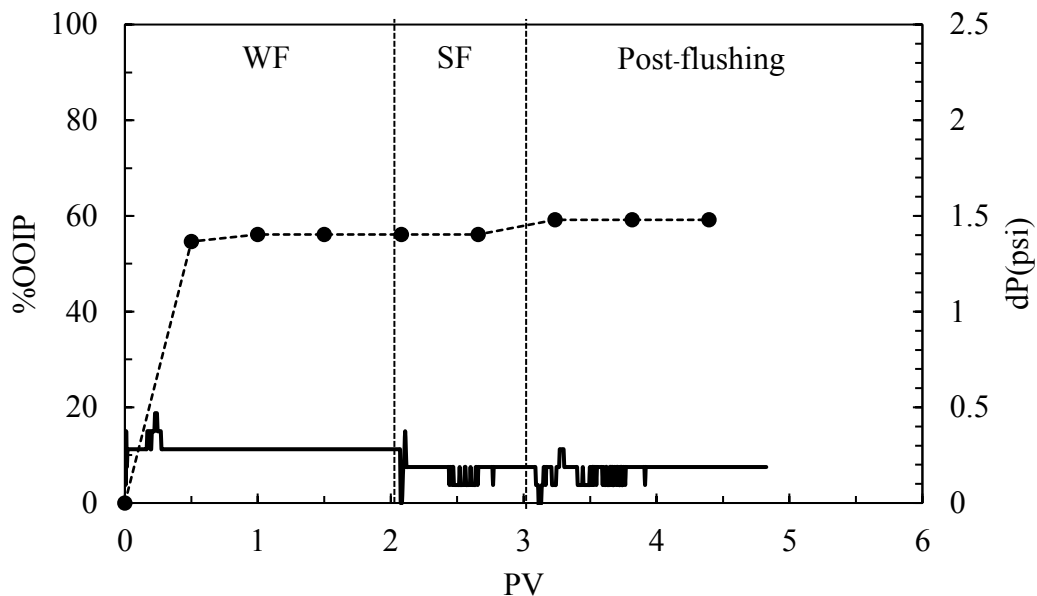
Figure C7 The accumulative oil recovery and pressure drop during water and surfactant flooding as a function of pore volume by AOT:IOS C_{15-18} at dilute salinity in heptane.
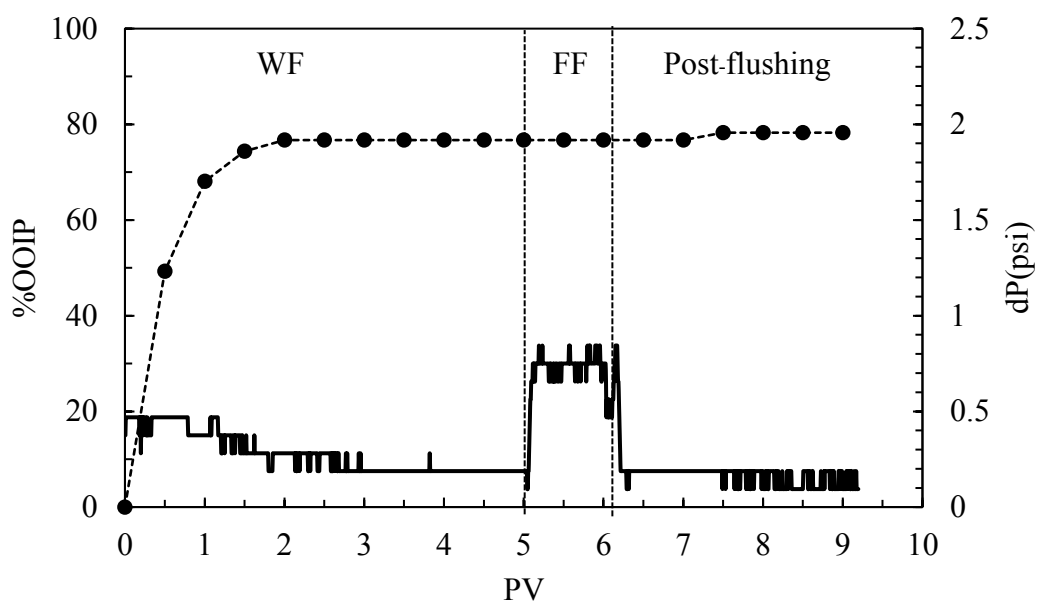

Figure C8 The accumulative oil recovery and pressure drop during water and foam flooding as a function of pore volume by AOT:IOS C_{15-18} at dilute salinity in heptane.
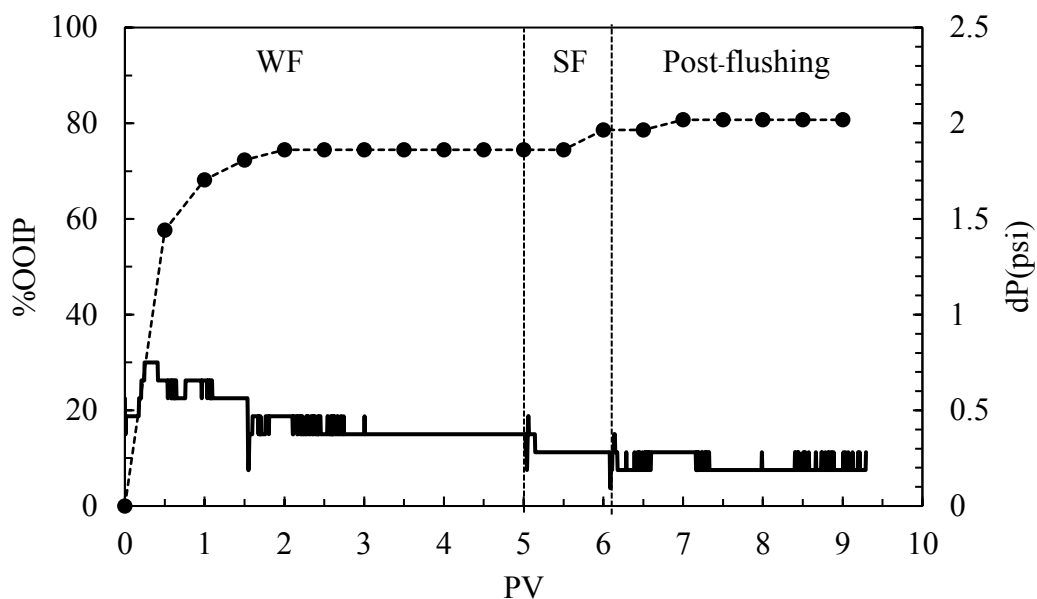
Figure C9 The accumulative oil recovery and pressure drop during water and surfactant flooding as a function of pore volume by AOT:IOS C_{19-23} at optimum salinity in heptane.

Figure C10 The accumulative oil recovery and pressure drop during water and foam flooding as a function of pore volume by AOT:IOS C_{19-23} at optimum salinity in heptane.

Figure C11 The accumulative oil recovery and pressure drop during water and surfactant flooding before 24 hours shutting in as a function of pore volume by AOT:IOS C$_{19\text{-}23}$ at optimum salinity in heptane.
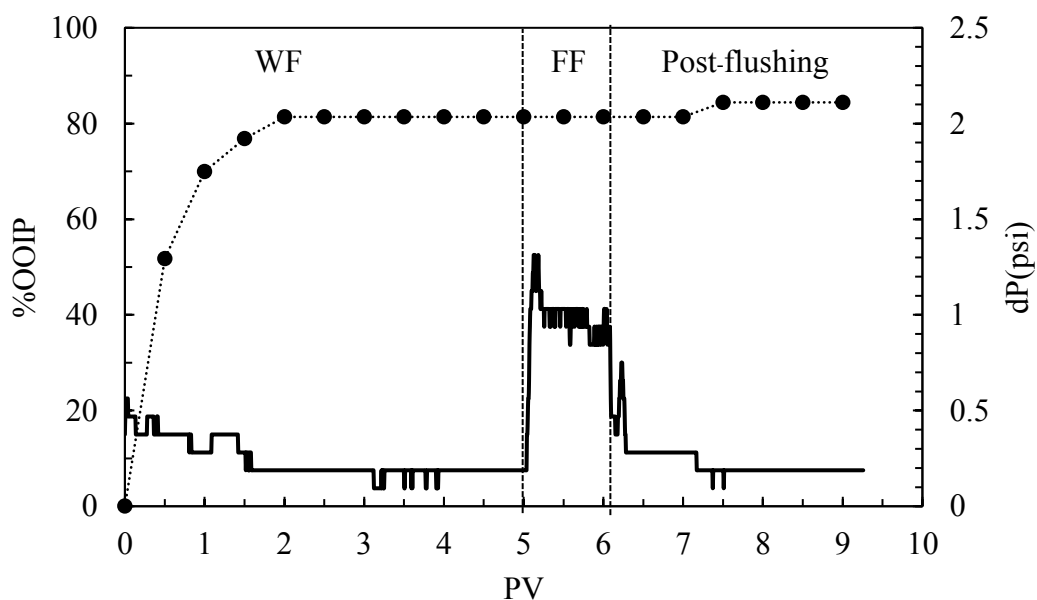

Figure C12 The accumulative oil recovery and pressure drop during water and foam flooding before 24 hours shutting in as a function of pore volume by AOT:IOS C$_{19\text{-}23}$ at optimum salinity in heptane.

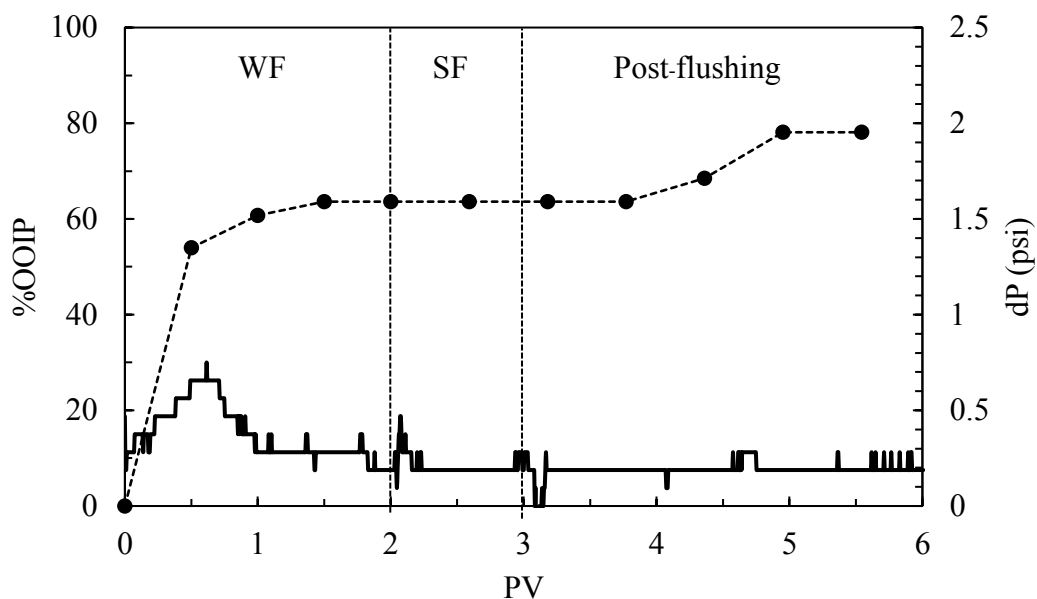**Figure C13** The accumulative oil recovery and pressure drop during water and surfactant flooding as a function of pore volume by AOT:IOS C_{15-18} at optimum salinity in hexadecane.

Figure C14 The accumulative oil recovery and pressure drop during water and foam flooding as a function of pore volume by AOT:IOS C_{15-18} at optimum salinity in hexadecane.

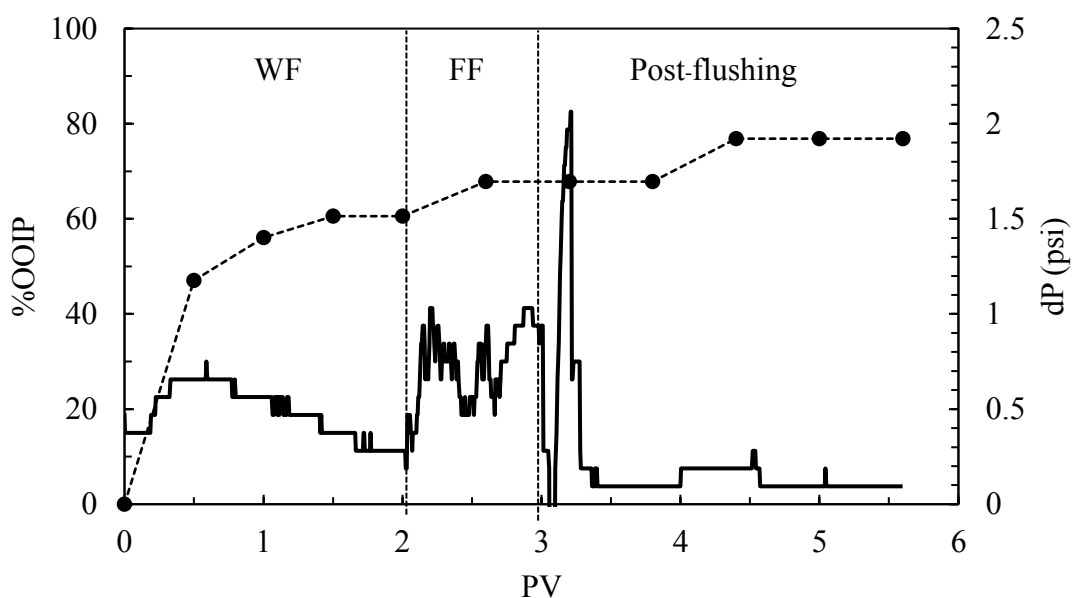**Figure C15** The accumulative oil recovery and pressure drop during water and surfactant flooding before 24 hours shutting in as a function of pore volume by AOT:IOS C_{15-18} at optimum salinity in hexadecane.
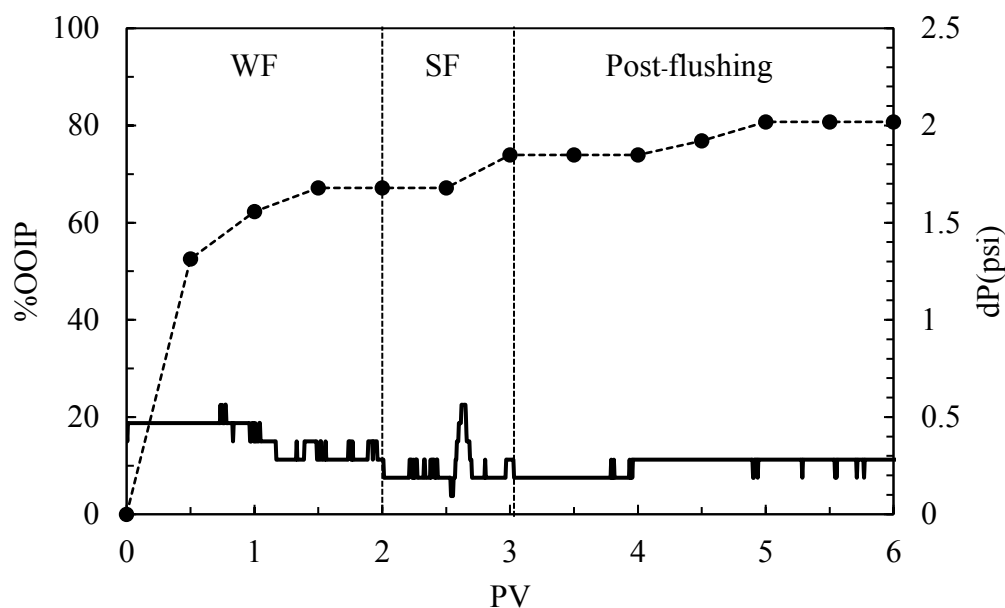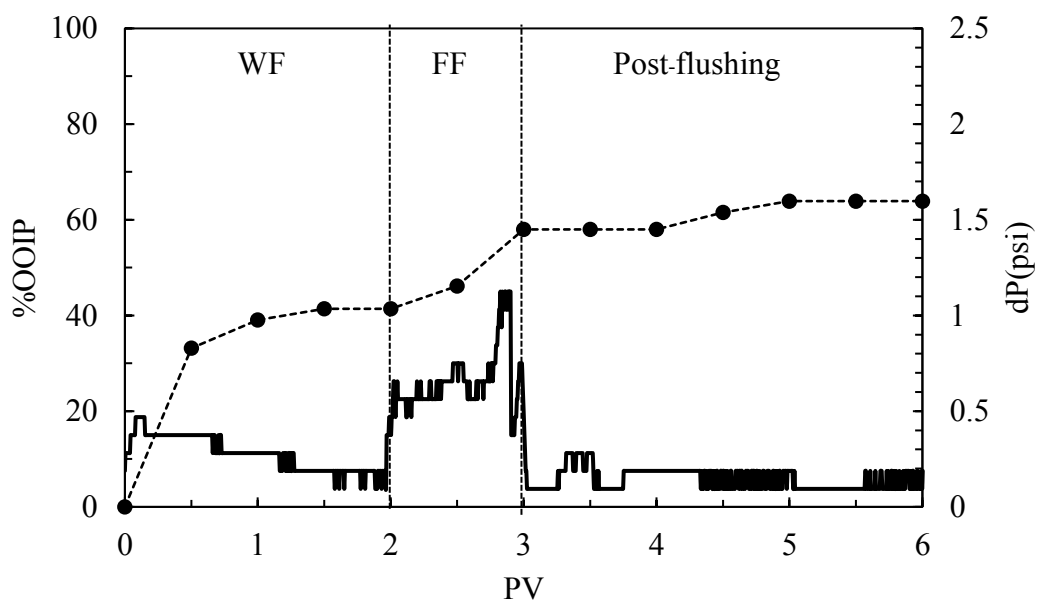

Figure C16 The accumulative oil recovery and pressure drop during water and foam flooding before 24 hours shutting in as a function of pore volume by AOT:IOS C_{15-18} at optimum salinity in hexadecane.

Figure C17 The accumulative oil recovery and pressure drop during water and surfactant flooding as a function of pore volume by AOT:IOS $C_{19\text{-}23}$ at optimum salinity in hexadecane.

Figure C18 The accumulative oil recovery and pressure drop during water and foam flooding as a function of pore volume by AOT:IOS $C_{19\text{-}23}$ at optimum salinity in hexadecane.

Figure C19 The accumulative oil recovery and pressure drop during water and surfactant flooding before 24 hours shutting in as a function of pore volume by AOT:IOS C_{19-23} at optimum salinity in hexadecane.

Figure C20 The accumulative oil recovery and pressure drop during water and foam flooding before 24 hours shutting in as a function of pore volume by AOT:IOS C_{19-23} at optimum salinity in hexadecane.
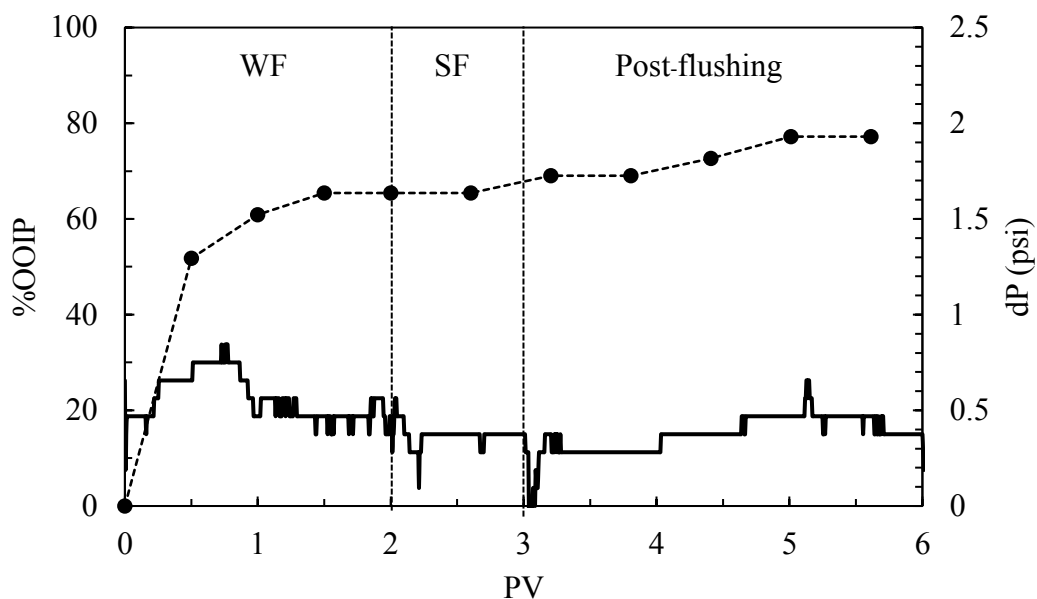
Figure C21 The accumulative oil recovery and pressure drop during water and surfactant flooding as a function of pore volume by AOT:IOS C_{24-28} at optimum salinity in hexadecane.
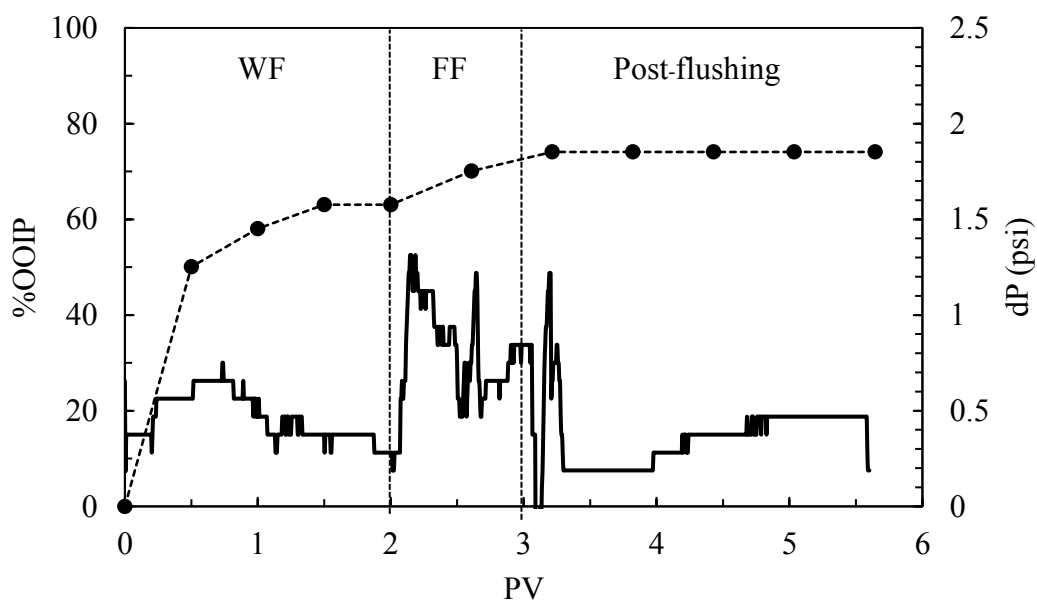
Figure C22 The accumulative oil recovery and pressure drop during water and foam flooding as a function of pore volume by AOT:IOS C_{24-28} at optimum salinity in hexadecane.
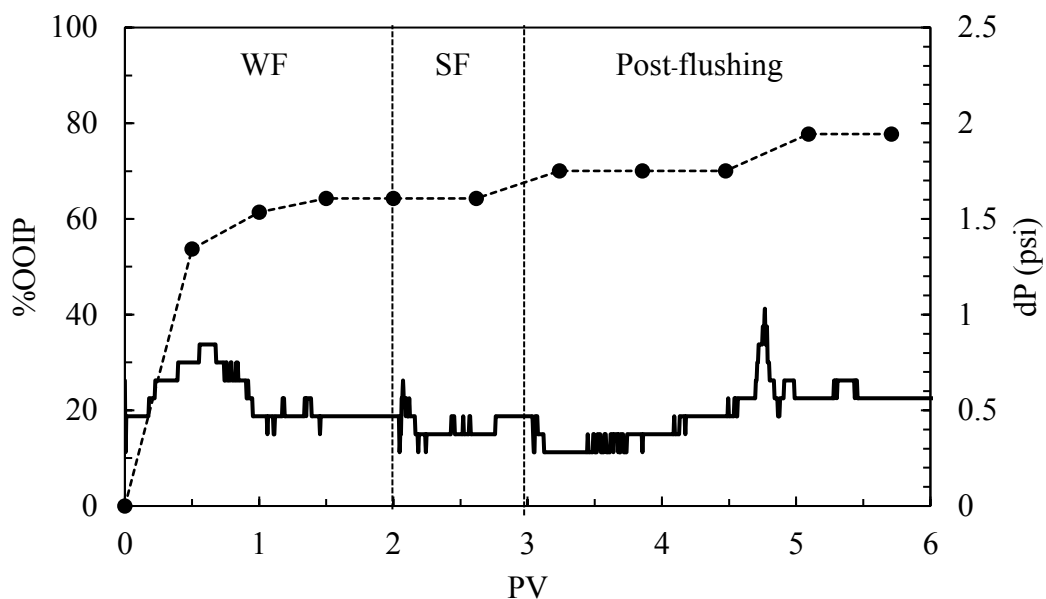
Figure C23 The accumulative oil recovery and pressure drop during water and surfactant flooding before 24 hours shutting in as a function of pore volume by AOT:IOS C_{24-28} at optimum salinity in hexadecane.
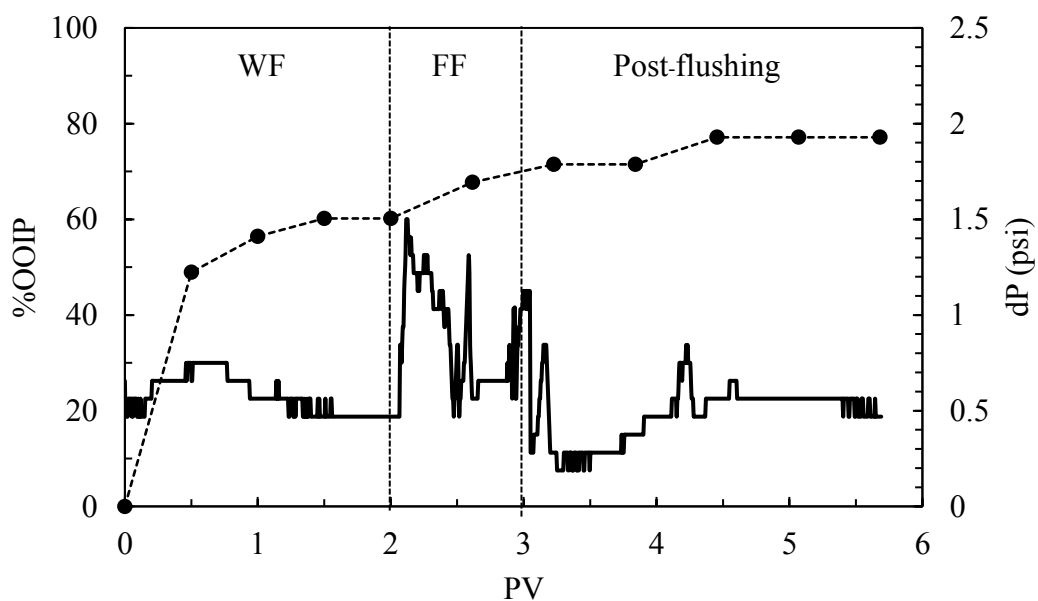

Figure C24 The accumulative oil recovery and pressure drop during water and foam flooding before 24 hours shutting in as a function of pore volume by AOT:IOS C_{24-28} at optimum salinity in hexadecane.

The shifted salinity condition from 6.2 to 5.4 gNaCl/100mL of AOT:IOS C_{15-18} with hexadecane was conducted in the sand pack column to investigate the incremental oil recovery by surfactant and foam flooding.
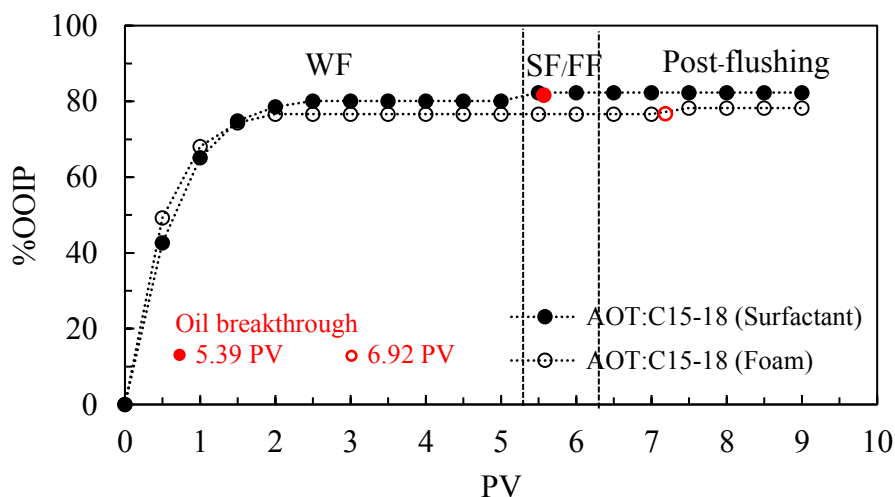

Figure C25 Accumulative oil recovery by surfactant and foam flooding of AOT:IOS C_{15-18} using hexadecane as an oil phase.

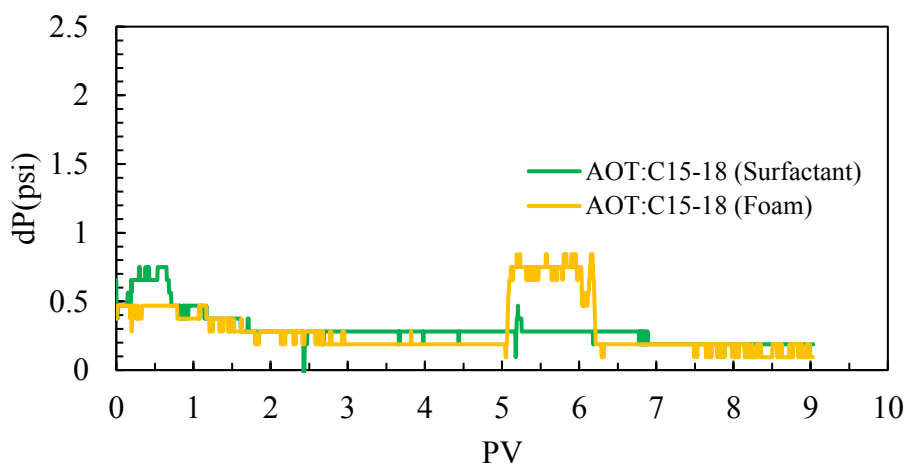**Figure C26** Variation of pressure drop across the sand pack column at different flooding conditions using an optimum formulation of of AOT:IOS C_{15-18} in hexadecane.

Figure C25 shows the amount of oil recovery of shifted condition of AOT:IOS C_{15-18} in hexadecane without surfactant precipitation. It is noted that the sand-pack experiment of the AOT:IOS C_{15-18} in hexadecane was not performed at the

optimal salinity condition due to the surfactant precipitation. The salinity was lowered to prevent surfactant precipitation. The additional oil recovery in AOT:IOS C_{15-18} was quite low or only 2 %OOIP. This may cause by a very high oil recovery by brine flooding (80 %OOIP).

In foam flooding, the additional oil recovery after the brine flooding of AOT:IOS C_{15-18} system was only 1.6 %OOIP because 76.7 %OOIP was recovered by brine flooding, giving very little room for the additional oil recovery in the tertiary step (see Figure C25).
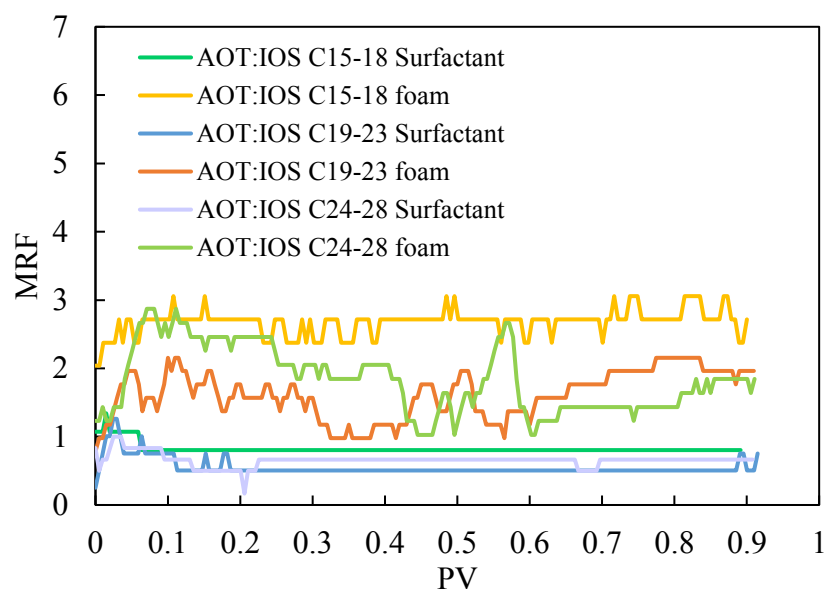

Figure C27 Plotting between the mobility reduction factor (MRF) versus pore volume of surfactant or foam slug injection in presence of heptane.

Although the MFR of AOT:IOS C_{15-18} was highest among three mixed surfactants, It is suggested that surfactant solution might be precipitated during injection. The differential pressure was increased because sand was blocked by precipitated particle instead of high foam stability.
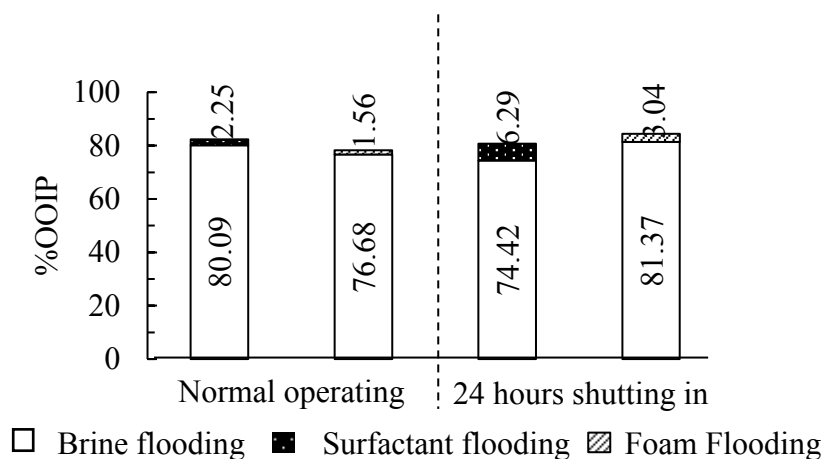
Figure C28 Summary total oil recovery of AOT and IOS C_{15-18} with hexadecane for different operating condition in surfactant and foam flooding**.**

The shut in operation has no significant difference when compared with the normal operations (see Figure C28). Although the contact time between surfactant or foam slug was increased during 24 hours shutting, precipitation might be occured and plugged in the porous media.

CURRICULUM VITAE

Name: Mr. Sorrawit Tantipalakul

Date of Birth: March 5, 1993

Nationality: Thai

University Education:

      2016-2018   Master Degree of Petroleum Technology, The Petroleum and Petrochemical College, Chulalongkorn University, Bangkok, Thailand

      2012-2015   Bachelor Degree of Chemical Technology, Faculty of Science, Chulalongkorn University, Bangkok, Thailand

Work Experience:

      2014   Position: Quality analysis traninee

                     Company name: PTT Public Company Limited, Phrakhanong, Bangkok

Proceedings:

1. Tantipalakul, S., Charoensaeng, A., Shiau, B.J., and Suriyapraphadilok, U., (2018, June 5) Microemulsion Mixtures From Mixed Surfactants in Enhanced Oil Recovery. Proceedings of The 24th PPC Symposium on Petroleum, Petrochemicals, and Polymers and The 9th Research Symposium on Petrochemicals and Materials Technology, Bangkok, Thailand.

2. Tantipalakul, S., Charoensaeng, A., Shiau, B.J., and Suriyapraphadilok, U., (2017, Oct 18-20) Low Interfacial Tension Mixtures from Microemulsion in Enhanced Oil Recovery. Proceedings of The 7th International Thai Institute of Chemical Engineering and Applied Chemistry Conference 2017 (ITChE 2017), Bangkok, Thailand.